Universidade do Porto
Faculdade de Engenharia
FEUP

Evaluation of Integration of Pumped Storage Units in an Isolated Network

Paul David Brown

B.S. Electrical Engineering from Iowa State University, USA (2004)

Submitted to the Department of Electrical and Computer Engineering
in partial fulfillment of the requirements for the degree of
Master of Science
in
Electrical Engineering
(Area of specialization in Power Systems)

Dissertation performed under the supervision of
Professor Doctor João Abel Peças Lopes
Associated Professor with Aggregation
Department of Electrical and Computer Engineering
Faculty of Engineering, University of Porto

Porto, May 2006

Abstract

This thesis considers the case of a small island system that has abundant renewable energy available but that at times cannot accept all of this power because of limits imposed by security criteria and difficulty in regulating frequency. The question of integrating pumped storage in an isolated network like this is considered from two directions. First, the problems with frequency regulation that can occur when large amounts of renewable energy resources are included are addressed. Pumped storage is considered as an option to alleviate these problems and allow larger integration of renewable resources without compromising system security. A modification to the security criteria generally used is developed and tested.

The second part of the work is an economic analysis of the inclusion of pumped storage. The question of whether or how much pumped storage to include is addressed by formulating a linear programming problem. The stochastic nature of load and renewable production in an isolated system is addressed using scenarios developed through fuzzy clustering. Both the unit capacity in MW and the reservoir storage capacity in MWh are optimized, and optimal operating strategies for the scenarios are produced.

Results showed that including pumped storage can be an effective means of allowing larger penetration of intermittent renewable energy sources, improving both the dynamic security and the economic operation of a test system. Including the dynamic security criteria in the economic question of dimensioning the pumped storage unit proved to make a significant difference in the optimal pumped storage capacity.

Resumo

Esta dissertação considera o caso de uma pequena ilha eléctrica que possui abundantes recursos de energia renovável mas que por vezes não pode integrar toda esta energia devido a limites impostos por critérios de segurança e a dificuldades na regulação de frequência. A problemática da integração de capacidade de bombagem numa rede eléctrica isolada como esta é vista em dois planos. Em primeiro lugar, analisam-se os problemas que podem surgir na regulação de frequência devido à ligação de grandes quantidades de fontes de energia renovável. Considera-se a inclusão de uma componente de bombagem como uma solução para superar estes problemas e permitir uma maior integração de fontes de energia renovável sem comprometer a segurança do sistema. É também desenvolvida e testada uma modificação ao critério de segurança normalmente utilizado.

A segunda parte do trabalho compreende uma análise económica da inclusão de capacidade de bombagem. Aborda-se a questão sobre a utilização de bombagem, ou sobre que capacidade de bombagem incluir, formulando um problema de programação linear. Considera-se também a natureza estocástica da carga e da geração de origem renovável num sistema eléctrico isolado utilizando cenários desenvolvidos a partir da aplicação de técnicas de *fuzzy clustering*. Optimiza-se tanto a capacidade da unidade (em MW) como a capacidade de armazenamento do reservatório e obtêm-se estratégias óptimas de operação para os cenários criados.

Os resultados obtidos mostraram que a inclusão de uma componente de bombagem pode ser um meio eficaz de permitir uma maior integração de fontes intermitentes de energia renovável, garantindo melhorias em termos de segurança dinâmica e de operação económica do sistema de teste. A inclusão do critério de segurança dinâmica no problema económico do dimensionamento das unidades de bombagem provou ter um impacto significativo na capacidade óptima de bombagem.

Résumé

Cette thèse considère le cas d'un système d'une petite 'île qui possède grand quantité de ressources d'énergie renouvable mais qui parfois ne peut pas faire l'intégration de la production à cause de limites imposées par des critères de sécurité et des difficultés de régulation de fréquence. La question de l'intégration de l'énergie hydraulique pompée stocké dans un réseau isolé comme ceci est considérée en deux directions. En premier, on considère les problèmes de régulation de fréquence qui peut devenir de l'intégration de l'énergie renouvable. Le stockage d'énergie est considéré comme une option pour réduire ces problèmes et permettre une plus grande intégration de ressources renouvelables sans compromettre la sécurité du système. Un changement des critères de sécurité habituellement utilisés est développé et testée.

La deuxième partie du travail contient une analyse économique de l'intégration du stockage d'énergie. La question de connaitre la quantité d'énergie a stocker qui ont peut intégrer est abordé par la simulation d'une programmation linéaire. La nature stochastique de la production renouvable dans un système isolé est adressée utilisant des scénarios différents identifies avec l'aide de *fuzzy clustering*. On optimise le volume du reservatoire d'énergie ainsi qu'on essaye d'optimiser la capacité de production à partir du reservatoire d'énergie.

Les résultats ont montré qu'inclure le stockage pompé peut être un moyen efficace de permettre une plus grande pénétration de sources d'énergie renouvelables intermittentes, en améliorant la sécurité dynamique et l'opération économique d'un système test. Inclure des critères de sécurité dynamiques dans la question économique à prouvé faire une différence considérable dans l'optimisation de la capacité du stockage d'énergie.

Acknowledgements

In the first place, I would like to thank the organizations that have made my study possible. This includes funding from the U.S. National Science Foundation International Programs as well as a scholarship from INESC Porto. The support of Dr. James McCalley at Iowa State and Prof. João Abel Peças Lopes at the Faculty of Engineering of the University of Porto/INESC Porto has been indispensable.

Thanks to Prof. Peças Lopes for orienting me in this endeavor. He balanced giving clear direction in the way to go and leaving the process open for me to find my own way. Additional thanks to Prof. Manuel Matos for his useful advice about the work in the area of fuzzy clustering.

I would also like to thank my colleagues in the Power Systems Unit of INESC Porto. Much is owed to the work of Luis Seca in the entering of the data of the test system. André Madureira and Ana Paula Castro helped in the translation of the abstract. Thanks are due to those whose daily question, "So... The thesis?? All done??" kept the work moving along. The value of being surrounded by capable minds for discussion, questions, corrections, and examples is immeasurable.

My parents have been unwavering in their support, always encouraging me in the pursuit of my dreams. It seems appropriate also to give a word of thanks to the members of the First Baptist Church of Porto. These have really been like family for me during these two years in Porto.

The last and biggest thanks goes to my heavenly Father, who opened the door to this opportunity, who has accompanied me along the way, and who I pray will be glorified in my work.

Contents

List of Tables

List of Figures

Chapter 1

Introduction

Rising fossil fuel costs and concerns about the environmental impact of burning fossil fuels has generated tremendous interest in the use of renewable energy sources to supply more and more of the electrical energy needs of society. The growth of renewable energy sources in the supply of electrical power is illustrated in the decrease in cost and increase in installed photo-voltaic and wind capacity as shown in Figures 1.1 and 1.2.

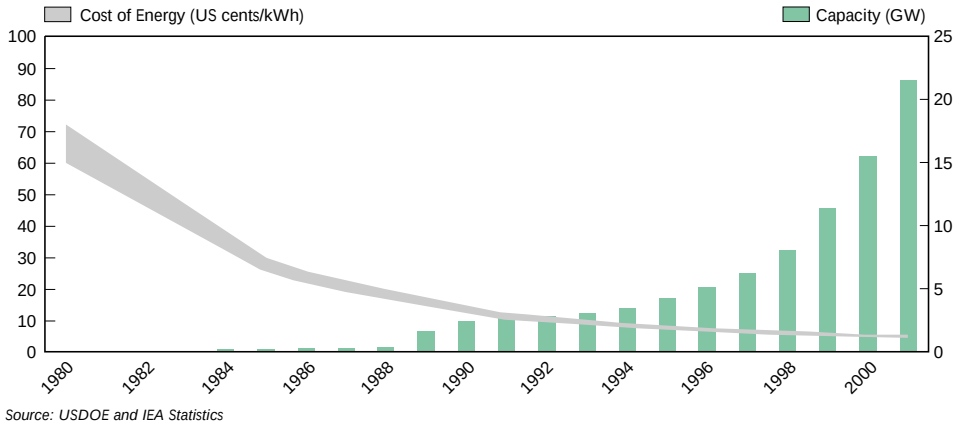

Figure 1.1: Cost and Capacity Trends in Wind Power [1]

The strong growth in renewable generation is expected to continue to grow, and as its role increases, it will bring new challenges. These are principally related to the intermittency of renewable resources. The primary energy sources for technologies like wind and solar power are not controllable and can be, at best, forecast.

Energy storage used in conjunction with renewable energy has been suggested as a means to increase the use of renewable energy while maintaining a high quality of service reliability [2, 3, 4]. The use of storage devices can help offset the effects of the inclusion of renewable energy sources and allow them to gain a larger penetration in the electrical energy supply. Storage may also be used to transfer energy from peak-use periods to low-use periods, allowing the system to operate at a more constant level and

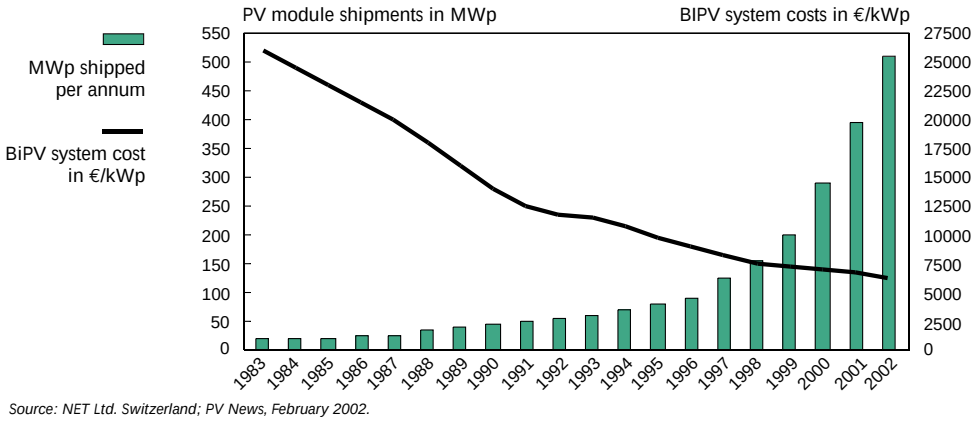

Figure 1.2: Annual World PV Module Production and Building-integrated System Costs [1]

reducing energy supply costs.

Isolated island systems have felt these pressures even more strongly since they often face exaggerated fuel costs due to extra costs of shipment and small overall system size. They also frequently have substantial renewable energy resources available. However, the use of these renewable resources, such as wind and hydro generation, is often limited by dynamic security concerns. The network must be operated within tight margins of frequency and voltage and wind parks and other renewable sources are generally unable to assist in maintaining the system at the necessary operating point – and in fact may have a negative effect due to their intermittency.

This thesis considers the case of a small island system that has abundant renewable energy available but that at times cannot accept all of this power because of limits imposed by security criteria and difficulty in regulating frequency. The question of integrating pumped storage in an isolated network like this is considered from two directions. First, the problems with frequency regulation that can occur when large amounts of renewable energy resources are included are addressed. Pumped storage is considered as an option alleviate these problems and allow larger integration of renewable resources without compromising system security. A modification to the security criteria generally used is developed and tested.

The second part of the work is an economic analysis of the inclusion of pumped storage. The question of whether or how much pumped storage to include is addressed by formulating a linear programming problem that addresses the stochastic nature of load and renewable production in an isolated system. Both the unit capacity in MW and the reservoir storage capacity in MWh are considered.

1.1 Structure of Document

In Chapter 2, an introduction to energy storage is given, with emphasis on the electric power system applications of energy storage and the technologies that are available for energy storage. Since this work focuses on pumped storage, some additional information is given on this topic.

In Chapter 3, the approach to the dynamic studies done in this work is described. Some background information about frequency regulation is given first, followed by the development of how pumped storage may be used to address some of the difficulties in frequency regulation in an island system. The technical approach that is adopted is described as well as the dynamic models chosen.

Chapter 4 describes the capacity optimization problem that has been formulated in this work. The developments from Chapter 3 referring to the security constraints are included in this formulation. The linear program is presented and the values of the necessary parameters chosen. A scenario-selection approach based on fuzzy clustering is described.

In Chapter 5, an overview of the test system that was used for this work is given. Special attention is given to the renewable energy resources that are available and the challenges that the system faces in regulating frequency under certain circumstances.

Chapter 6 presents the results of the dynamic simulation studies that are described in Chapter 3. The adequacy of the tools used is evaluated.

In Chapter 7 the results of the capacity optimization are given. The scenarios produced using the fuzzy clustering technique presented in Chapter 4 are shown. Then the results of the optimization problem itself are presented. An evaluation is made of the tools used in this part of the study.

Chapter 8 the general conclusions of the work done in this thesis are presented. Some suggestions for future work are made.

Chapter 2

State of Art

In this chapter an overview is given for the use of storage in the electric power system, including reasons why storage may be used and technologies that are available for energy storage devices. Additional attention is given to pumped hydro storage since this is the area of focus for the studies of this thesis.

2.1 Motivation (Why Storage?)

In its simplest conceptual terms, energy storage is a way to transfer energy in time, moving it from one moment to another moment. Historically, the bulk electric energy system has not included much capacity for storage. In the U.S., storage, mostly in the form of pumped hydro, comprises 3% of the national generation capacity [5]. However, with rising fuel costs, increasing public concern about the environmental impact of continued use of fossil fuels, and continually advancing capabilities in semiconductor devices, the role of energy storage is growing, both in old and new applications.

Electrical engineering technical societies have accompanied the development of new technologies that offer improved efficiency, higher storage density, and lower costs. IEE Power Engineering Journal published an edition in 1999 focusing on energy storage [6]. In 2005 IEEE Power & Energy Magazine focused on the subject as well [7, 8, 9].

Additionally, there are entire professional associations and lobbies devoted to the discussion and promotion of storage technology, including Energy Storage Association and the Energy Storage Council. In the United States, the Department of Energy supports energy storage through the Energy Storage Systems Program [10] as well as the initiatives of individual states and utilities.

In the European Union, the vision for the future of the electric grid is being cast using the Smart Grid concept [11]. The vision document presents a trans-European network in which a telecommunications infrastructure enables flexibility at every level and allows loads and generators of all sizes to “plug and play”, both providing and having access to energy and ancillary services through competitive market structures. Renewable energy sources and distributed generation play key roles in energy supply, with

storage devices able to enter the network and compete to provide services.

Energy storage in the electric power network has a wide range of applications depending on the amount of energy that can be stored and the length of time for which it is able to be stored. In [2], applications of storage are given for durations ranging from 20 seconds to 4 months, and [9] shows a chart of utility applications on axes of storage time and available power for times ranging from fractions of a second up to tens of hours and 10 kW to 100 MW. This chart is reproduced in Figure 2.1. The following subsections explain some of the applications of energy storage in the short, medium and long-term.

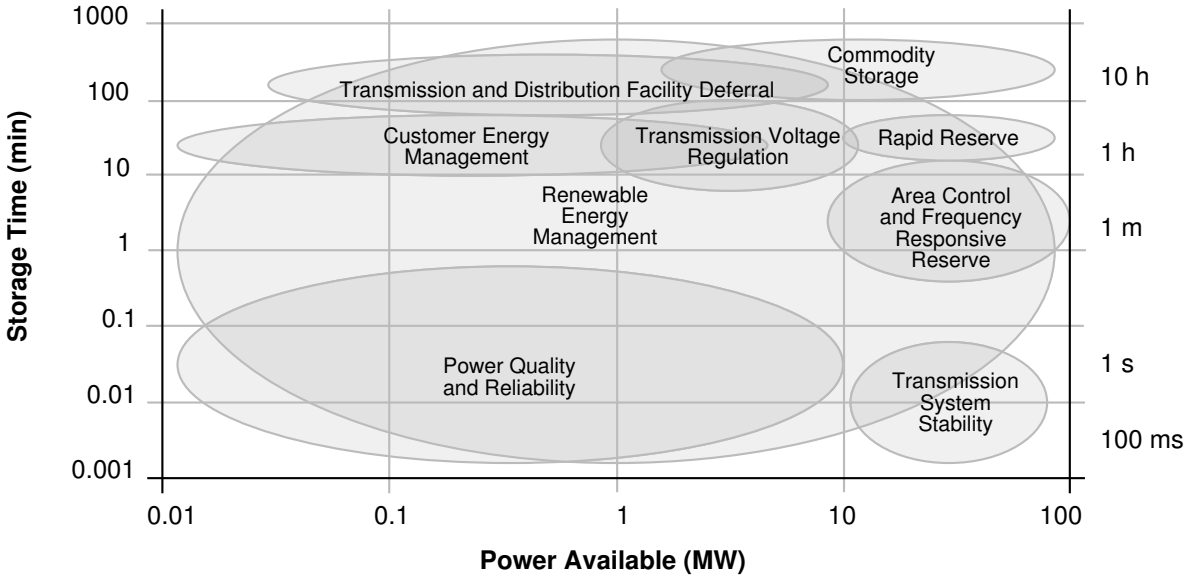

Figure 2.1: Utility Applications of Electric Energy Storage [9]

2.1.1 Short-term Storage

Short-term storage is storage that maintains energy reserves sufficient to provide rated power for a few seconds up to a minute. The two basic applications are as uninterruptible power supply (UPS) or for power system stabilization.

UPS devices are used in situations where sensitive equipment or industrial operations require a high level of power quality. Most electrical service interruptions are caused by temporary faults and last only a short time. The flexibility and quick response of the power electronic interfaces used in many storage technologies makes them well-suited to these applications since they are able begin providing power within a fraction of a cycle of main service failure or a voltage depression.

The use of storage for power system stabilization requires large amounts of power to be available momentarily in order to damp system oscillations. Installations of this type are particularly useful in remote areas or in locations where the grid is weak and prone to instability. Reinforcement of the network may be delayed or avoided through the use of stabilizing storage devices. Since they are generally based on power electronics interfaces, voltage support/reactive power control can be provided continuously in addition to short-time active power supply.

Short-term storage also plays a critical role operating in cooperation with microgeneration within the microgrids concept. When in islanded operation, storage devices are responsible for primary load-frequency control [12]. Likewise, similar capabilities may be required for small island systems with very large integration of wind power.

Most of the new technologies described in Section 2.2 are finding their first applications in short-term storage. These include especially flywheels, super-capacitors, and SMES devices.

2.1.2 Medium-term Storage

Medium-term storage is storage that maintains energy reserves sufficient to provide rated power for a few minutes up to a few hours. Applications for this type of storage capability include renewable energy management, customer energy management, area control/frequency regulation, and rapid reserve.

Renewable energy sources such as wind and photovoltaic are variable and non-dispatchable and for these reasons are devalued in energy markets. Their value can be greatly increased when coupled with storage devices that allow their operators to make firm energy offers.

Medium-term storage can also be useful for energy customer peak-shaving. Electric energy service rates typically contain a component that is based on the maximum power demand that the customer draws from the grid. In many cases, this maximum demand lasts only a short time, and by using stored energy to provide this power, the customer is able to reduce costs. Peak-shaving is often done in conjunction with energy storage used for UPS [13]. Peak-shaving by the utility at locations where equipment loading is approaching its limits may also be an attractive alternative to making costly network reinforcements.

Using storage devices for area control, frequency regulation, and rapid reserve can reduce the amount of generation capacity that is required to be online, free the online generators to operate at more economic loading levels, and reduce the mechanical stress caused by changing output.

2.1.3 Long-term Storage

Long-term storage is able to hold energy for times ranging from a few hours to weeks and months. This is typically bulk energy storage and is generally used to take advantage of the energy price difference between peak and off-peak periods. A typical daily cycle would include energy storage during off-peak nighttime hours and generation during peak daytime hours.

Long-term storage can also be useful in reducing daily peaks and allowing deferral of generation capacity expansion. Furthermore, by leveling the system load profile, costs of operation of thermal units can be reduced by reducing the frequency that unit startup and shutdown needs to be done. According to [14], the reducing cycling of thermal units can be up to 50% of the benefit of pumped storage.

When considering storage purely from the perspective of moving energy from a low cost period to

a high cost period, the necessary price difference can be found in terms of the efficiency of the storage cycle. Defining the following variables:

η – cycle efficiency

E_s – energy to be stored (taken from grid)

P_s – price paid for energy to be stored

P_g – price received for energy recovered

The cost then to store some unit of energy is then

$$E_s \cdot P_s$$

Given the efficiency η of the storage cycle, the energy that can be recovered is

$$E_s \cdot \eta$$

which has the value

$$E_s \cdot \eta \cdot P_g$$

At the break-even point, the value of energy consumed or purchased is equal to the value of energy recovered:

$$E_s \cdot P_s = E_s \cdot \eta \cdot P_g$$

$$\frac{P_g}{P_s} = \frac{1}{\eta}$$

For example, if the round-trip efficiency η is 0.8, the price ratio P_g/P_s should be at least 1.25 to attain profit. One of the methods of short-term scheduling of pumped storage units is to match energy blocks pairwise between high-price (or high-marginal-cost) and low-price (or low-marginal-cost) periods in an iterative procedure that in [15] is called the “gradient method”.

2.1.4 Special conditions of small/isolated systems

Small, isolated systems have some characteristics that make the use of storage especially interesting:

- Fuel costs in isolated systems are often much higher than in large interconnected systems.
- Isolated systems often include high penetration of renewable resources.
- Small systems do not have strong frequency and voltage regulation capabilities.

Elevated fuel costs provide strong motivation for the use of renewable energy sources and for the most efficient use possible of necessary thermal generation resources. The energy output from renewable

resources is variable over both short and long time periods. This increases the difficulty in maintaining system reliability and quality of service. The Power Systems Unit of INESC Porto has prepared a number of studies of island power systems in which the introduction of renewable resources becomes limited because of lower limits imposed by diesel generating sets and because of frequency regulation problems during low-loading, high-renewable-production conditions. Energy storage can serve to relax both of these restrictions.

2.2 Types of storage

In Section 2.1, an overview of the applications of storage devices is given. In the current section, some of the technologies available for storage devices are presented. The technologies for storing energy are divided into three basic groups: mechanical, electrical, and electrochemical [16]. Many new technologies for energy storage are emerging and beginning to find commercial application. The Energy Storage Association provides basic information and principles of operation for a variety of storage technologies on its website [17]. Other good overviews can be found in [3] and [18].

2.2.1 Pumped hydro

Pumped hydro storage stations store energy by using motors to pump water from a reservoir to a reservoir at a higher elevation. The energy is recovered by driving a turbine and generator as the water flows back down to the lower reservoir. Pumped hydro storage is the most mature of the storage technologies and has a large number of utility-scale installations in service around the world. Pumped hydro storage depends on appropriate geographical features, and according to [3], most of the workable sites are already in use. Nonetheless some very large new stations have been built recently in the UK (6 x 300 MW [19]), in Japan (2 x 400 MW [20]), and in China (6 x 300 MW [21, 22]. Round-trip efficiency is generally about 70 - 80% [3, 14, 23]. Section 2.3 contains additional information about pumped-hydro storage.

2.2.2 Batteries

The battery is perhaps the energy storage device most commonly thought of. There are several advantages to the use of batteries in power system load-leveling applications. According to [24], battery systems offer the advantages of quick manufacturing, modularity (i.e. able to install in groups, add, relocate), and flexibility in siting.

The lead-acid or “lead-lead oxide” battery is the most mature of available batteries [25]. A number of utility-scale installations have already been done, including a 10 MW/40 MWh plant in Chino, California [26] and a 20 MW/14.1 MWh installation in Puerto Rico [27]. For smaller installations, valve-regulated lead-acid (VRLA) batteries (see [25]) have been developed that use starved electrolyte

technology to avoid free acid and reduce size. One such example can be found in [13].

Nickel-cadmium is another battery alternative for power system applications. Nickel-cadmium batteries have the advantage that the positive and negative electrode plates and support structures do not participate in the electrochemical process and therefore do not suffer from corrosion as do the materials in a lead-acid battery. Ni-Ca batteries operate at normal ambient temperatures and are more tolerant of warmer and colder conditions than lead-acid batteries [28]. A 46 MW battery storage system using Ni-Ca cells was installed in 2003 for Golden Valley Electric Association (GVEA) in Alaska [7], principally for use as spinning reserve.

Other battery chemistries have been developed and are reaching maturity for commercialization. High temperature cells have been developed that are able to achieve high efficiencies and do not require rare materials in their construction [29]. These batteries are not as mature as lead-acid batteries, but they are reaching the point of commercialization and have utility-scale demonstration projects in service. One such type of high-temperature battery is based on sodium and sulfur electrodes. A 6 MW/48 MWh NaS battery station is in service for the Tokyo Electric Power Company [30]. In load-leveling operation, this site attains about 90% efficiency.

Some additional battery types that are not discussed here but which may be of interest to the reader include zinc/bromide [31] and lithium ion.

2.2.3 Compressed air

Compressed-air energy storage (CAES) devices store energy by compressing air into underground caverns or into pipe/tube systems. Energy is recovered by using it in expansion turbines to drive electric generators. It is often necessary to heat the air in the expansion process by burning natural gas, though new designs minimize the fuel needed in the generation cycle [3]. Large installations have been made in Germany (290 MW/1160 MWh) and in the United States (110 MW/2860 MWh for Alabama Electric Cooperative).

2.2.4 Flow batteries

“Regenerative flow cells”, also known as “redox fuel cells”, or “flow batteries” are secondary batteries in which liquid electrolytes are stored in external tanks and pumped through a fuel cell where ion exchange takes place [32]. Because the electrolyte is stored in external tanks, the energy storage capacity of the flow cell may be increased independently from the power input/output rating of the unit.

The first utility-scale regenerative flow cell to be commercialized was that of Regenesys systems [33, 16]. This system uses solutions of sodium bromide and sodium polysulphide. A utility-scale demonstration of a 100 MWh/10MW unit was planned for installation at Didcot in the UK [33] to be completed in 2000. However, an article from 2001 [16] indicates a 120 MWh plant planned for black start and energy

arbitrage at Little Barford Power Station in the UK with no mention of any trial at Didcot. A 120 MWh facility for the Tennessee Valley Authority [34] was planned to be the first installation in the U.S., but the parent company of Regenesys decided to discontinue production of the system [35, 36].

The Vanadium Redox Battery (VRB) is another regenerative flow battery that has been commercialized. It was originally developed at the University of New South Wales [37] and is now developed commercially by VRB Power Systems Inc. [38]. They present several case studies on the order of 1000 kWh of storage capacity installed for use in remote systems and in conjunction with wind power [39].

2.2.5 Flywheel

Flywheel batteries operate by storing energy as kinetic energy in a mass rotating at high speeds. They are smaller and lighter than an equivalent lead-acid system and are able to make both short but frequent as well as long discharges while still having a longer expected useful life [40]. Modern flywheel storage units are designed to fail with the rotor intact [41]. Flywheels have been principally applied for UPS and power quality and in vehicles where size and weight are important factors [7]. Round-trip efficiency of 80 - 85% is typical [3].

2.2.6 Super-capacitor

Super-capacitors are electrolytic capacitors designed to store large amounts of charge and deliver it in a short amount of time. They are typically integrated in systems along with other storage devices such as batteries, where the super-capacitor is used to meet large-power, short-time demand which would strain the battery system while allowing the batteries to carry average power needs [42].

2.2.7 Superconducting magnetic energy storage

Superconducting magnetic energy storage (SMES) devices store energy in the magnetic field produced by current flowing in a superconducting coil. To maintain the material in a superconductive state, the coil is immersed in a coolant such as liquid helium or liquid nitrogen [43, 3]. Because the superconductor has no resistance, only a small voltage is necessary to maintain a constant current in the coil. The system applications described in [43] are for protection against voltage dips. A 30 MW/ 0.5 MWh installation in Alaska is described in [44]. This SMES system was designed to offer short-time spinning reserve as well as provide reactive power support, AGC, and power system stabilization functions.

2.2.8 Hydrogen

The storage medium perhaps most expected to have a dramatic impact in the energy industry is hydrogen. Much discussion has been devoted to the so-called “hydrogen economy” of the future. In 2003 the International Partnership for the Hydrogen Economy was formed, and it now counts as members

most of the world's leading nations [45]. *IEEE Power & Energy* magazine devoted an issue to discussion of they hydrogen economy [46] as has *Energy Policy* [47]. Further, there is the International Association for Hydrogen Energy (IAHE) and its scientific journal *International Journal of Hydrogen Energy* and international conferences such as the World Hydrogen Energy Conference.

For energy storage, hydrogen is produced through the electrolysis of water. The hydrogen can then be stored at high pressure and later recovered through the use of fuel cells. Unlike the other storage technologies mentioned in this section, hydrogen offers the possibility of being transported. The vision for a hydrogen economy imagines hydrogen being used to supply energy to fuel-cell-powered vehicles.

There are several locations where hydrogen is being produced and distributed for use in fuel-cell-powered vehicles. Two examples of such tests include BC HydroGEN, a venture of BC Hydro in Canada [48], and an initiative of HEW, the electricity supplier in Hamburg, Germany [49].

Hydrogen is also proposed as the storage medium for hybrid wind-fuel cell-diesel systems, especially for locations where there are abundant renewable energy resources available and either a weak or non-existent connection to the main power system. An optimization procedure for the operation of such a system is presented in [50], and several field trials of systems of this type are described in [51].

2.3 Details about pumped hydro storage

Pumped hydro storage systems operate by transferring water between reservoirs at two different elevations. To store energy, water is pumped from from the lower reservoir to the upper reservoir. To recover the energy, water is released from the upper reservoir and used to turn a turbine as it flows to the lower reservoir. A diagram of a typical pumped storage station is shown in Figure 2.2.

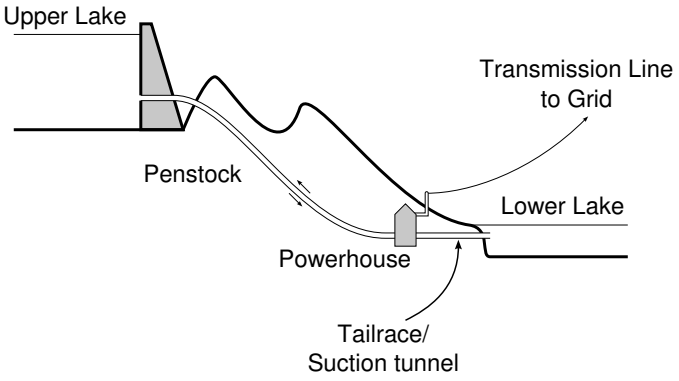

Figure 2.2: Typical Pumped Storage Plant Layout [52]

A pumped storage plant is not much different from a typical hydropower station and includes many of the same components. The only differences are the requirement of the lower lake and extra machinery in the powerhouse for pumping [52]. The machinery required for a pumped hydro station may take three possible configurations [53]:

- Four units: A pump coupled to a motor and a turbine coupled to a generator. This configuration occupies a large amount of space and is no longer used.
- Three units: A pump and turbine are both coupled to a single reversible motor/generator. The efficiencies of the pump and turbine can be optimized and multi-stage pumps can be used for very high heads.
- Two units: A reversible pump/turbine is coupled to a reversible motor/generator. This configuration takes up a smaller space compared to the other two and has a lower installation cost. The disadvantage is a decrease in the efficiency. More than 95% of pumped storage power plants are of this type [53].

According to [52] and [54] the efficiency of each of the components of the pumped hydro storage system can be estimated by the value shown in Table 2.1.

Table 2.1: Efficiency of Pumped Storage Components

Component	Efficiency (%)
Motor-generator	96 – 97
Turbine-pump	88 – 92
Penstocks	92 – 98
Overall Efficiency	65 – 80

Pumped storage units have typically been used for load transfer from peak to off-peak hours, reducing the amount of generation from expensive thermal peaking units. They are also commonly used for spinning reserve to allow base-load units to operate at higher, more efficient load levels. With the recent interest in renewable generation, pumped storage has also been proposed to be used in conjunction with wind parks to smooth the overall output, allow larger penetration of renewable energy in the network, and take advantage of the financial signals provided by the electric energy market [55, 50, 56, 4, 57].

Numerous pumped storage stations are in operation around the world. In [54], a list has been compiled on installations as of 1987. Since then, there have no doubt been many more. In the United States, 3% of generation capacity in in the form of pumped hydro, and in Japan it is 10% [5]. In Portugal, 560 MW of reversible hydro capacity was in service in 2000 and 1113 MW is projected for 2010 [58], which will represent more than 10% of the peak load.

Chapter 3

Dynamic Behavior Analysis

The system under study is a small, isolated system typical of the network of an island. Electrical energy is supplied by a thermal station made up of several diesel-powered generators as well as a large number of hydroelectric stations of varying sizes and a number of wind parks. Owing to this generation mix, under some conditions, the system has some problems with dynamic performance, namely difficulty in frequency regulation. In this chapter the problem is characterized and a solution incorporating the use of pumped hydro storage is proposed. The effectiveness of the proposed solution is explored through the use of dynamic simulation.

3.1 About Frequency Regulation

In order to understand the problem and the solution presented in this chapter, it is necessary to understand some basic principles of operation of modern power systems. A balance between power generated and power consumed must be maintained at all times. An overwhelming majority of the energy supply in modern power systems is provided by generators based on synchronous machines. These machines rotate at the same speed as the voltage they produce, and through the electrical network they are all coupled together to operate at the same speed.

The load in the power system is always changing: household lights are turned on and off, motors start and stop, and appliances vary their demand. When the electrical power output from the generator does not equal the mechanical power that is put into it, the machine accelerates, rotating faster if more mechanical power is applied, and slowing if more electrical power is applied.

In order to maintain a nearly constant rotating speed and thereby a nearly constant frequency, the mechanical power must be constantly adjusted to react to the changes in load that occur. If centralized secondary frequency control is not used, frequency regulation is generally done through a feedback control loop such as the one shown in Figure 3.1.

The feedback control loop has two components: one is a proportional gain ($1/r$), and the other is an

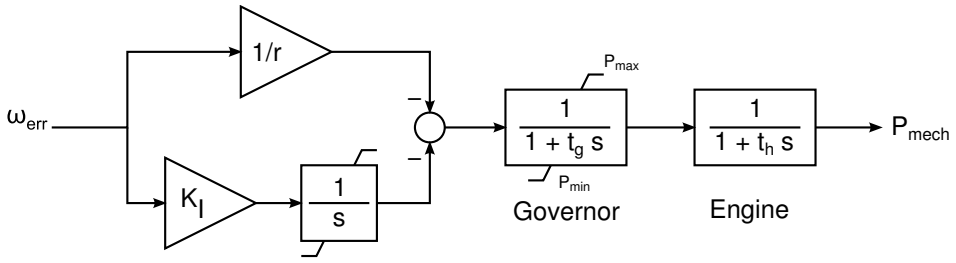

Figure 3.1: Diesel generator speed controller

integral gain (K_I). The proportional gain gives what is known as a speed-droop characteristic. Suppose a load increase occurs. The electrical power output from the generators now exceeds the mechanical power input and the frequency begins to fall. As the frequency falls, the control system notes the frequency error and responds by increasing mechanical power proportionally to the error. At some point the additional mechanical power will equal the additional load that was applied and the system will reach equilibrium at some new operating point of power and frequency. (The speed-droop characteristic is more fully explained in many introductory texts to electrical power systems, such as [59].)

The integral control loop serves to correct the steady state error that would occur if only the droop characteristic were used. In the case of the hypothetical load increase introduced above, the integrator will continue to increase the mechanical power supplied to the generator until the frequency recovers to the nominal value for the system.

In order to guarantee that the system will have generation capacity available to be able to respond to a disturbance, spinning reserve criteria are applied to the unit commitment. The criteria specify that there must be sufficient generation capacity online but unused to be able to cover the most severe power imbalance that is expected. This imbalance is usually loss of the largest generating unit in the system.

If for some reason a disturbance occurs that is beyond the capability of the generation system to respond adequately, the system frequency may continue to fall. In order to prevent total system collapse, some loads are selected to be disconnected when the frequency falls to specified points. This reduces and can even reverse the imbalance between load and generation, allowing the system to recover without total loss of load. Load shedding results in loss of service for some customers and so is used only as a last resort.

Isolated systems can have difficulties with frequency regulation. For large interconnected systems, even the loss of a very large generating unit will not produce a very large drop in frequency. This is because the total number of generators in the system is quite large, and they can respond with little burden falling to each one. In a smaller system, however, there are not so many generators, and the frequency variations caused by the loss of one of them will be much more significant. In fact, according to [60], frequency stability may be the most urgent stability issue facing a small system.

This difficulty in isolated systems becomes even more pronounced when large amounts of renewable resources are introduced that do not participate in frequency regulation. These resources displace

generating units that would normally perform frequency regulation and leave the system with even less frequency regulating capability. It is clear that there are strong economic and environmental reasons to increase the use of renewable resources; however, solutions must be found that do not compromise the security of the network.

3.2 Including Pumped Storage in Spinning Reserve

A pumped hydro storage station may be able to play a significant role in improving the performance of the system in the face of the difficulties described above. It has three helpful effects:

- Increases system load to allow more renewable generation to be connected
- May be disconnected while in pumping mode as a “quick-shed” load
- May be ramped up in generating mode quickly after a system event to cover for the loss of other generation

This section describes how these items may be incorporated into the system dispatch criteria to improve system security without resorting large safety margins that would result in unnecessary curtailing of renewable production.

In an island system with large integration of wind and small hydro production, system collapse almost always is a result of cascading generation loss. Reserve is often available to cover the generation deficit of the original disturbance, but when frequency falls to below the point at which hydro and wind units begin to trip, the deficit quickly grows until the system is able to recover only through underfrequency load shedding, and even then recovery is not always possible.

The spinning reserve criteria guarantees that the system has generation capacity sufficient to cover the loss of the largest thermal unit. This criterion may be formulated as the following:

$$P_{reserve} = \sum_i P_i^{max} + P_{renewable} - P_{load} > 1.5 \cdot \Delta P_{max} \tag{3.1}$$

where $P_{reserve}$ is the spinning reserve that is required, P_i^{max} are the power capacities of the thermal units that have been committed, $P_{renewable}$ is the sum of wind and hydro production, and P_{load} is the sum of system load that must be met. Spinning reserve must be at least $1.5 \cdot \Delta P_{max}$ where ΔP_{max} is the loss of power that would occur if the largest thermal unit tripped.

Although the spinning reserve criterion requires that enough capacity be available to cover the largest loss of generation that can be expected, this criterion does not specify at what frequency the system will stabilize. If the amount of generation online is small, as it is during off-peak periods with high penetration of renewable sources that do not participate in frequency regulation, this minimum frequency is often low enough that cascading generation loss begins. In this research, a new criterion is proposed that

attempts to guarantee that the minimum frequency for the largest covered disturbance will not be below a specified frequency. In this way, tripping of generation on underfrequency/underspeed protection is avoided and system security is maintained.

This new criterion uses an approach similar to that found in [61] and is based on the frequency droop characteristic that is the basis of frequency regulation in the electrical power system. As the frequency deviates from its nominal value, the speed control system of all regulating machines responds by applying more or less mechanical power input in proportion to the speed deviation that is observed. Without the action of secondary control (an integral component in the control system), the frequency will settle to a new steady-state at a frequency different from the nominal frequency. How far this new frequency is from the nominal frequency depends on the droop of the generators participating in frequency regulation and is given by the following expression:

$$\frac{\Delta f}{f_{base}} = r \cdot \frac{\Delta P}{P_{base}} \tag{3.2}$$

where r is the per-unit droop, Δf is the frequency deviation, ΔP is the original active power imbalance, and f_{base} and P_{base} are the bases for the droop.

It is likely that not all generators will have equal droop settings. The single-machine equivalent power rating and droop are given by

$$\frac{P_{eq}}{r_{eq}} = \sum_i \frac{P_i}{r_i} \tag{3.3}$$

The values of P_{eq} and r_{eq} may be chosen in whatever manner is deemed most convenient as long as they are consistent with (3.3). The approach used for this part of the work is to choose a typical value $r_{typical}$ for the droop and choose P_{eq} to be a sum of the power capacities adjusted by their droop relative to the chosen typical value, as shown in (3.4). This has the advantage that generating units with droops equal to the typical value do not need any adjustment and can be summed directly. Only "non-typical" units need to be adjusted, and all adjustments may be calculated independently of which other machines may be online. This adjusted value can be thought of as the "frequency-regulating strength" of the unit.

$$\begin{aligned} r_{eq} &= r_{typical} \\ P_{eq} &= \sum_i P_i \cdot \frac{r_i}{r_{eq}} \end{aligned} \tag{3.4}$$

The expression in (3.2) will overestimate the maximum frequency deviation that occurs as a result of a power imbalance because it considers only the action of proportional control. The speed control systems also include an integral control loop which serves to bring the steady state error back to zero. At the time that the system reaches minimum frequency, the effect of integral control is not very large and can be approximately accounted for by introducing another parameter to the equation. The value of this parameter will depend on factors such as the response speed of the speed regulators and the machine

inertia, but for sets of similar machines as exist in the test system, it is not difficult to find a value that gives a good approximation. The expression with the new parameter a then becomes:

$$\frac{\Delta f}{f_{base}} = a \cdot r \cdot \frac{\Delta P}{P_{base}} \tag{3.5}$$

where a is a factor to account for integral control action at the point that the largest frequency excursion is reached. This factor a should be between 0 and 1, with the actual value to be determined either by dynamic simulation or by analysis of data collected during system disturbances.

In order to use this expression as a criterion for the system unit commitment and dispatch, it must be rearranged to place a lower limit on the sum of frequency-regulating machines committed. The objective is to limit the frequency deviation to less than a specified value, so the equation can be turned into the following inequality:

$$\frac{\Delta f_{max}}{f_{base}} > a \cdot r \cdot \frac{\Delta P_{max}}{P_{base}}$$

where Δf_{max} is the maximum frequency deviation that is to be allowed and ΔP_{max} is the maximum active power imbalance that is expected.

Rearranging gives

$$P_{base} > \frac{f_{base}}{\Delta f_{max}} \cdot a \cdot r \cdot \Delta P_{max}$$

The shedding of pumped storage load can be included by subtracting it from the power imbalance. This is only valid in the case that the frequency variation is negative; however, this is the direction in which problems are in fact encountered. This modification gives the following:

$$P_{base} > \frac{f_{base}}{\Delta f_{max}} \cdot a \cdot r \cdot (\Delta P_{max} - P_{shed})$$

where P_{shed} is the pumping load that is to be shed before reaching Δf_{max}.

In this formulation, the criterion does not necessarily protect against the loss of a unit. This is because not only is the power provided by the unit lost, but so is its frequency regulation capacity. To include this effect in the criterion, this capacity should be added on the right-hand side of the inequality:

$$P_{base} > \frac{f_{base}}{\Delta f_{max}} \cdot a \cdot r \cdot (\Delta P_{max} - P_{shed}) + P_{genlost} \tag{3.6}$$

where $P_{genlost}$ is the generation capacity lost in the case that ΔP_{max} the the loss of a unit.

This criterion could offer the ability to integrate large amounts of renewable resources while still assuring that the system will have the frequency-regulating capability necessary to avoid excessive frequency deviations. It should be verified that the expression is adequate and a value for the parameter a estimated.

3.3 Solution Approach: Dynamic Modeling

In order to evaluate the effectiveness of the shedding strategies and security criteria including the new pumped storage, it is necessary to perform dynamic simulations. This means adopting dynamic models for all of the elements of the system: generators, loads, lines, transformers, and wind parks. These models provide a large set of differential and algebraic equations that approximately describe the behavior of the system for the phenomena that are of interest.

For this study, the phenomena of interest are the evolution of system frequency after a system disturbance for a time of ten seconds to one minute following the disturbance. Voltage regulation and stability can also be studied on this time frame, but the primary focus is on the balance of active power in the network and the interaction that pumped storage can have in this aspect.

3.3.1 Platform of choice: EuroSTAG

Dynamic models for major power system components are already well-established and software has been developed specifically for this type of study. The platform chosen for the project is EuroSTAG, software produced by Tractabel EDF (*Electricité de France*). EuroSTAG is a dynamic simulation package for electrical power systems. It contains models for electric machines and major system components such as lines and transformers. Several standard control systems and turbine models are also included. For applications that require models that are not included in the package, a modeling module is available in which new models can be built from simple building blocks such as time constants, integrators, limiters, summation, and so on.

EuroSTAG includes a power flow module that is especially useful for initializing the dynamic simulation. The modeling module encourages the calculation of steady-state initial conditions by requiring that the model initialize itself and throwing warnings if the dynamic simulation does not begin reasonably close to steady state. This is a tremendous advantage over the other platforms that do not provide for initialization that therefore require a significant amount of simulation time for the system to settle numerically to a steady state.

Another advantage of the EuroSTAG platform for this study is its use of an intelligent variable-step-size numeric integration algorithm. The solver is able to take quite large time steps when there is nothing of interest happening in the system and reduce the integration step as necessary when disturbances occur to appropriately capture the desired phenomena. It should be noted that EuroSTAG is not an electromagnetic transients simulation program and fast transients are neither modeled nor captured in simulation.

The workflow for the EuroSTAG platform is shown in Figure 3.2. Each simulation is the result of the contents of three files:

- Load flow data file

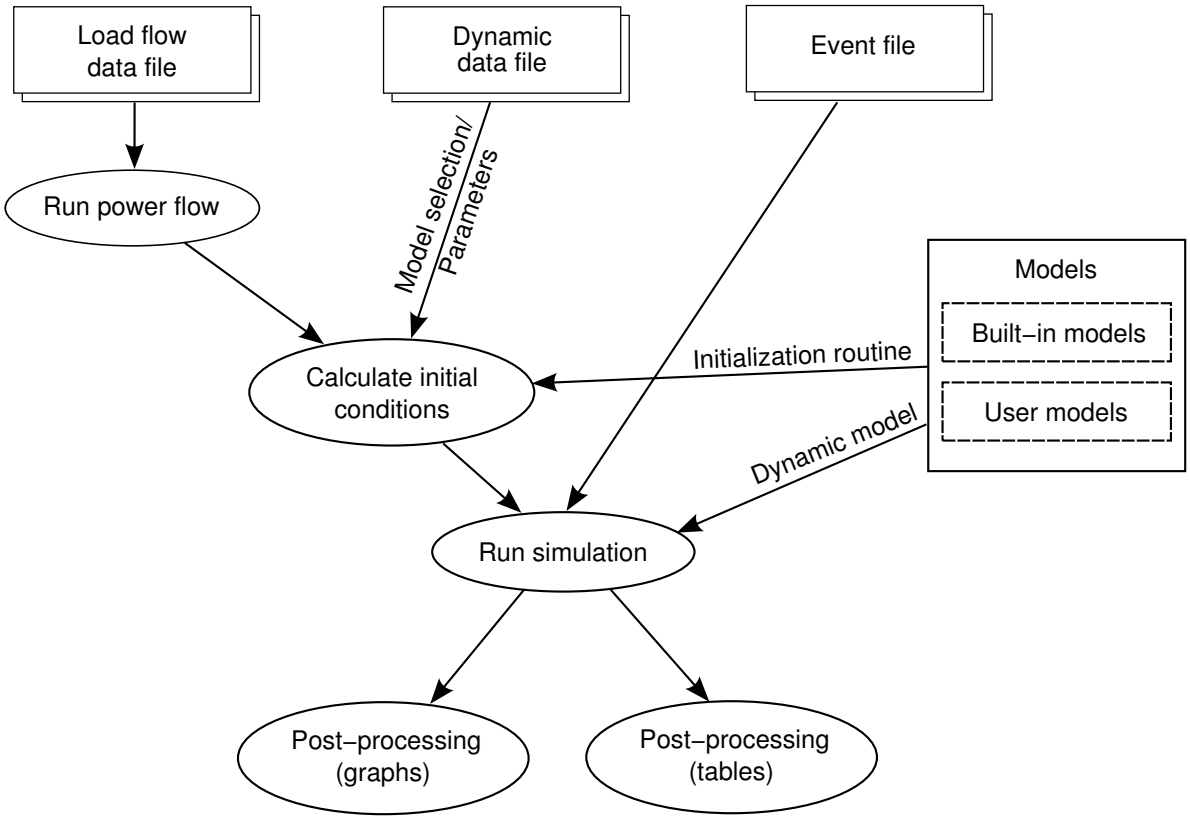

Figure 3.2: EuroSTAG Work Process

- Dynamic data file
- Event file

The load flow module determines the steady-state voltages and power flows in the network. The data about system elements needed to run the power flow is included in the *load flow data file*.

The results of the load flow are used to determine the initial conditions for the dynamic simulation. The *dynamic data file* specifies the models to be used for each of the system elements with dynamic behavior, such as machines and other injectors, as well as system protection devices. All models include an initialization routine. This routine uses the results of the power flow together with the models' parameters to calculate initial values for all internal blocks that must be initialized. (See Section 3.3.3 for additional information about EuroSTAG macroblock modeling.)

Before beginning numerical integration, the dynamic simulation module verifies that all state variables are in steady-state. If no critical error is found, numerical integration begins. The events that are scheduled to occur during the simulation as well as the parameters of the numeric integration process are included in the *event file*. This includes simulation start and stop time, minimum and maximum integration steps allowed, and error tolerances in the numeric process as well as events such as short-circuit faults, machine disconnections, branch openings, and set-point changes, among others.

The dynamic simulation module uses an advanced algorithm to adjust step size and solution algorithm order throughout the simulation and is able to simulate long time periods without missing phenomena

that may appear after the occurrence of a system event. The algorithm does not work by magic, so it still is necessary for the user to have some care in setting up the simulation and designing models so as to avoid numerical problems.

The following subsections describe the most important steps and the data needed for them in more detail.

3.3.2 Load flow

The load flow definition file describes the network including its nodes and branches. The EuroSTAG power flow module uses the usual power flow formulation, so nodes are specified in one of three ways: by active and reactive power injections; by active power injection and voltage magnitude; or by voltage magnitude and angle. Only one node is specified with the voltage magnitude and angle. This node serves as the reference node for the power flow calculation and is also known as the *slack node*.

Branches may be defined as lines, fixed-ratio transformers, or variable-ratio (tap-changing) transformers. Transformers may have two or three windings. The impedance and shunt admittance should be specified for all these elements, and in the case of tap-changing transformers, the maximum and minimum available ratios should be given as well as the voltage target settings.

Shunt capacitor or reactor banks may also be included in the load flow definition.

3.3.3 Macroblock modeling

In order to allow the use of models beyond the standard models included with the platform, EuroSTAG includes the possibility of creating macroblock models. These models can be used to to implement custom control systems or to develop power, current, or admittance injector models to represent new system devices. A screenshot of the EuroSTAG macroblock model graphical design interface is shown in Figure 3.3.

A macroblock can receive input signals of three basic types:

- System quantities, such as bus voltage magnitude, injected power, and reference frequency
- Machine quantities, such as rotation speed, field current, and winding fluxes, in the case that the macroblock is associated with a machine
- State variables or named signals output from another macroblock associated with the same machine or injector

The necessary outputs depend on what the macroblock is being used for. A synchronous machine will require excitation field voltage and mechanical torque. An asynchronous (induction) machine requires only mechanical torque. Injectors may require real and reactive power or injected current real and imaginary components.

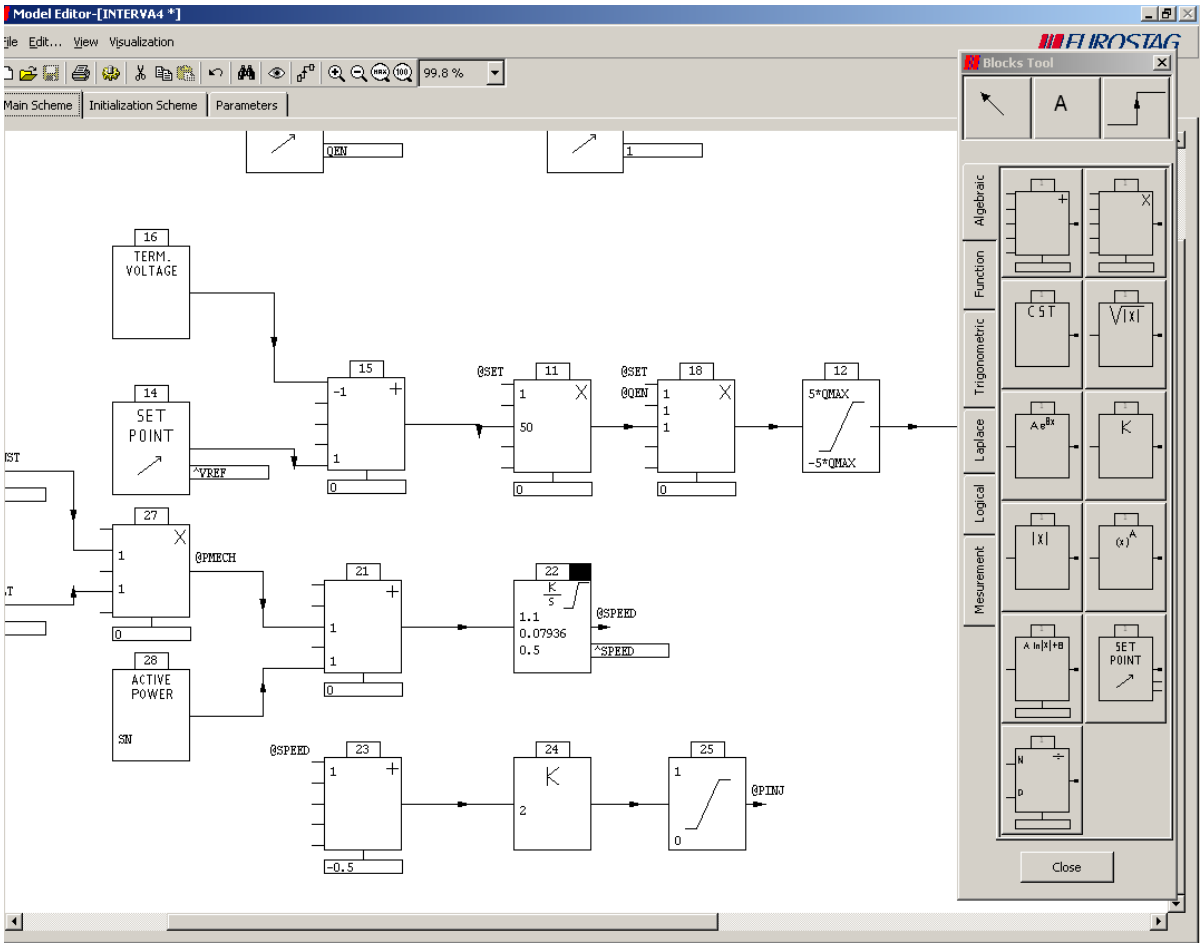

Figure 3.3: Macroblock Modeling

Between the input and the output, the signal may be manipulated by any of a number of operation blocks. Most of the blocks typically used in a control system are available. Some commonly used examples include summation, multiplication, division, single time constant delay, integrators, polynomial Laplace (s-domain) transfer functions, limiters, and so forth. These blocks are laid out and connected using a visual editor. The platform resolves feedback loops algebraicly. Block parameters may be specified with literal values or using parameter names.

Many of the blocks available require initial values as do all interface variables. The initial values are calculated by the initialization routine which is specified along with the model. Inputs available to the initialization routine are values resulting from the load flow, such as bus voltage or injected powers, or machine values such as field voltage, speed, or torque as determined by automatic initialization of the EuroSTAG machine model. The same control blocks and visual layout editor are used to design the initialization routine as are used for the main model.

The third part of the macroblock definition are the parameter sets. These are sets of parameters that can be substituted in the control blocks of the model. Multiple sets of parameters may be defined, and the specific set to be used for a given machine is indicated by an entry in the dynamic data file. Individual parameters may be overridden in the dynamic data file as well.

3.3.4 Dynamic simulation

In order to carry out the dynamic simulation of the test system, models must be specified for all important system components. In most cases specifying a model means choosing the appropriate standard model from the library of the simulation platform and determining the appropriate parameters for this model. In some cases, new models may need to be created or adapted to represent certain devices.

Models and parameters are needed for the following system elements:

- Generating units
  - Electrical machine
  - Turbine/mechanical system
  - Speed control system
  - Excitation/voltage control system
- Wind parks
- Lines and transformers
- Loads

In addition to models for the system elements, it is necessary to model the protection devices used in the system. Information about the following protection equipment is needed:

- Generator over/under-speed protection
- Generator over/under-voltage protection
- System load-shedding steps
- Operation times for line protection

In some cases, data may not be available for certain parameters and it may be necessary to resort to the use of “typical data”. It should be verified that these parameters are not decisive in the results of the analysis and that another model that does not require this data is not better suited to the application.

3.4 Scenarios to simulate

Performing a dynamic simulation results in a set of time-series events and values for system quantities for a given set of pre-conditions and stimulus. In this aspect, dynamic simulation does not provide general results; it provides a specific set of consequences a a result of a specific set of system conditions. In order to draw general conclusions, many simulations must be made for various carefully chosen system conditions. It is not feasible to describe the system in all possible configurations for all possible disturbances.

Some knowledge of the system must be used in combination with understanding of the problem that is to be solved in order to produce a reasonable number of scenarios.

This part of the study focuses on the impact of a pumped storage station on the dynamic performance of the system. Specifically, validation and refinement of pumped load shedding strategies as a method for reducing the likelihood of system load shedding and increasing system robustness is desired. Since the problem that is to be addressed is the difficulty of frequency regulation/active power control, the scenarios must be chosen when this problem is worst and the system is most exposed in this respect. This occurs when load is lightest and renewable energy production is highest.

The disturbances to be simulated should be chosen to be of severity appropriate to highlight the behavior that is under study. In this case, the use of the pumped storage station as a sheddable load to avoid system load shedding is of concern. Therefore the disturbances should be chosen to cause active power imbalance and lead to frequency deviations, especially underfrequency. If the disturbance is too strong, the system will collapse regardless of the effect of shedding the pumped storage load, and the simulation will not provide useful information. On the other extreme, if the disturbance is too light, the system will recover without difficulty and will not need the shedding of pumped storage to recover. It cannot be known beforehand what the result of a simulation will be, so it is necessary to simulate a variety of disturbances, and then analyze in more detail the ones that provide interesting results.

In order to determine the impact that pumped storage and the modification to the spinning reserve criteria may have, it is necessary to consider scenarios that show system behavior both with and without pumped storage, and with and without the proposed addition to the spinning reserve criteria. The scenarios are chosen for conditions in which these criteria are limiting; that is, it is considered that there is sufficient wind and hydro resource available to be able to use as much of the renewable resource as the system is able to accept. Given the characteristics of the test system, this is a situation that is likely to occur at times and which is of highest interest to investigate.

Off-peak hours are period in which frequency regulation is most difficult and in which the spinning reserve criteria limit the use of wind and hydro power. It is in this period that the most severe problems occur and it is in this period that the greatest improvement from adopting the strategies proposed in this paper will be seen.

Given these considerations, the following scenarios are proposed:

- Dispatch according to the old spinning reserve criteria only; no pumped storage considered
- Dispatch according to modified spinning reserve criteria; no pumped storage included
- Dispatch according to modified spinning reserve criteria; include pumped storage units

For each of these scenarios, a unit commitment and dispatch must be created that respects the spinning reserve criteria that are being used, as expressed in (3.1) and (3.6). The unit commitment in each

case may be determined by finding the smallest amount of thermal generation that can be committed while still meeting the requirements of these criteria.

The old criterion, which only requires a minimum amount of unused capacity in the committed generators, does not directly specify a minimum amount of total generation capacity. However, since it is known that the generators will operate at their technical minimums, the total capacity may be determined once the required quantity of spinning reserve is known. First, it is known that the largest unit in the test system is 16.5 MW and that the technical minimum is 0.7. (See the test system description in Chapter 5. Therefore, the power carried by the largest unit will be $16.5 \cdot 0.7 = 11.6$ MW. Using the safety factor of 1.5 that is required, $P_{reserve}$ must be at least 17.3 MW. Since the diesel units are going to operate at their technical minimums of 0.7 pu, the spinning reserve must be provided by the remaining 0.3 pu of capacity. Therefore, the total amount of thermal generating capacity online must be at least $17.3/0.3 = 57.75$ MW.

The new additional criterion depends on the amount of pumping being done. The parameters required have been determined by experimentation in simulations, and after substituting the values that are found (see Section 6.1), the criterion as expressed in (3.6) can be given as

$$\begin{aligned} P_{base} &> \frac{50}{0.5} \cdot 0.85 \cdot 0.06 \cdot (\Delta P_{max} - P_{shed}) + P_{genlost} \\ &> 5.1 \cdot (\Delta P_{max} - P_{shed}) + P_{genlost} \end{aligned} \tag{3.7}$$

For the loss of a 16.5 MW unit carrying 11.6 MW, with no pumped storage that can be shed, the minimum frequency-regulating generation required to be online is 75.7 MW. This requirement is higher than that which is imposed by the old spinning reserve criterion, so when the new criterion is included in the unit commitment procedure, the number of units committed will increase and the amount of power from renewable sources will have to be reduced. If 5 MW of storage is available, the minimum becomes 50.2 MW. At this point the old criterion is more restrictive than the new one, so including the new criterion does not result in modification to the unit commitment and dispatch.

The system load for the scenarios is chosen as the system's typical off-peak load of 80 MW. When pumped storage is included, a single unit of 5 MW is used. This may not be the optimal value (see the problem presented in Chapter 4), but it will serve to illustrate the effects of using pumped storage to improve the frequency regulating capability of the system. The maximum renewable production permitted by the system has been added in each case. Table 3.1 summarizes the scenarios that are to be simulated, indicating the amount of thermal generation that is committed, the spinning reserve available, and the amount of renewable generation that is allowed. Details of the scenarios may be found in Appendix E.

The disturbances to be used must also be chosen. As discussed earlier, the disturbances should be chosen to be strong enough to cause frequency deviations without being so strong as to bring the system down completely regardless of what measures are taken. For the test system as described in Chapter 5,

Table 3.1: Summary of Simulation Scenarios

New Criterion Met (Y/N)	Thermal Capacity (MW)	Spinning Reserve (MW)	Pumping Load (MW)	Renewable Generation (MW)
N	56.1	19.1	0	44.0
Y	76.6	25.7	0	30.0
Y	56.1	18.8	5	48.7

seven disturbances are considered:

- Fault on the 30 kV line from Lincoln to Brighton.
- Fault on the 60 kV line from Curtis to Lincoln
- Loss of the largest unit at the Manning Thermal Station
- Load step increases of 5%, 10%, 15%, and 20%

The two faults are applied in the area of the wind parks and are intended to see if the wind parks and hydro units in that area will be lost due to the fault, and how the system will respond to this. The loss of the largest thermal unit at Manning is the most severe disturbance that the security criteria consider. This disturbance, then, is a good test to see if the criteria function correctly. The load step increases are artificial disturbances; in practice the load does not make such changes. However, they introduce a series of power imbalances from medium to large size, and so help to more systematically illustrate the behavior of the system for a range of disturbances.

3.5 Models

In order to do dynamic simulation, it is necessary to specify models for all system components. In this section, the models chosen for the various elements of the test system are described. Throughout the section, reference is made to specific elements of the test system. An overview of the system can be found in Chapter 5.

3.5.1 Diesel Generator

The diesel generating sets at the thermal stations at Manning and Aurora are synchronous machines driven by motors fueled by diesel or fuel oil. They are the primary energy source for the test system and are responsible for frequency regulation. Diesel generators generally show fast response in frequency regulation but do not usually have very large inertia. The parameters of the machines in the test system may be found in Appendix B.

In order to reduce the burden of data entry and the computational load of representing many machines, machines that have the same parameters and ratings have been modeled as a single equivalent

machine. This occurs principally for the older machines that are used only for peaking and therefore are not used during the off-peak scenarios that are being simulated in this work.

Electrical Machine The diesel generating sets are based on synchronous machines. EuroSTAG has both a full synchronous machine model and a simplified synchronous machine model. For the data available for the test system and the purposes of the study, the simplified model is best suited. The details of the simplified synchronous machine model may be found in Appendix C.

Speed Regulation The frequency regulation done by the diesel units is of such importance that it has already been presented in Section 3.1 of this chapter to give some background in order to better present the study being done. in Figure 3.1 is somewhat simplified. The block diagram for a commercial diesel generator speed governor [62] is shown in Figure 3.4.

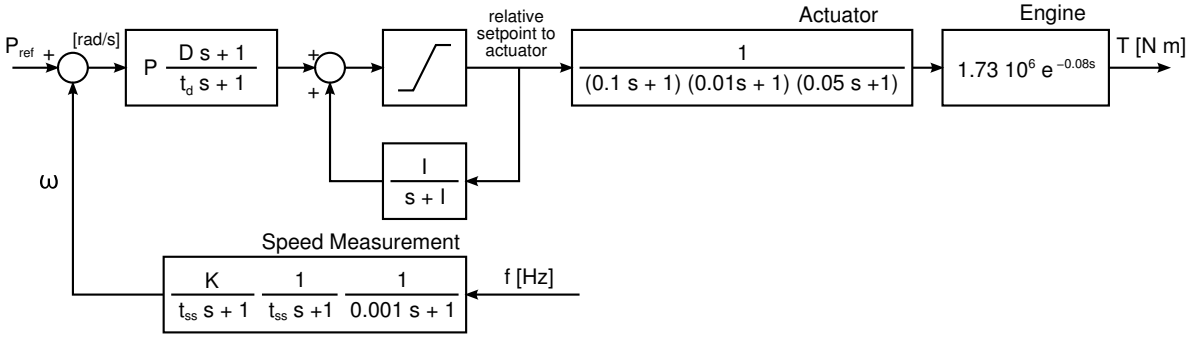

Figure 3.4: Block Diagram for Commercial Diesel Generator Speed Governor [62]

The constants for the model presented in Figure 3.4, as indicated by the manufacturer of units similar to those used in this research are the following:

f	=	Pickup frequency [Hz]
K	=	2 π / number of teeth on the flywheel
t_{ss}	=	Speed filter time constant. Set for 0.01 sec. when generator breaker is closed.
D	=	Differential gain (adjustable)
t_d	=	D x 0.2
P	=	Proportional gain [relative unit/(rad/s)] (adjustable)
I	=	Integral gain (adjustable)
T	=	Engine Torque [N m]
$EnginePower$	=	27720 kW
$EngineRPM$	=	150.0 r/min

The delay in frequency response due to the system's inertia is much larger than the delays in the speed control system, so for the purposes of this study, there is no reason to use such a detailed model. The model presented in Figure 3.4 has been simplified by ignoring the fast transients in the actuator, engine

and speed measurement blocks. A single time constant has been used for the engine delay rather than the exponential. The large constant ($1.76 \cdot 10^6$) in the engine block converts from per-unit on base of the machines rated power and speed to N-m, a conversion that is not necessary in the EuroSTAG platform since the torque is output in per-unit. Finally, the controller adopted for the study does not include any differential component and only has the proportional and integral parts.

The only initialization that is necessary is to set the initial output of the integrator and time constant blocks to the steady-state power as determined by the power-flow module.

Voltage Regulation The voltage regulator used for the diesel generating sets is modeled using the IEEE Type 1 exciter model as shown in Figure 3.5 [63]. Magnetic saturation has been neglected.

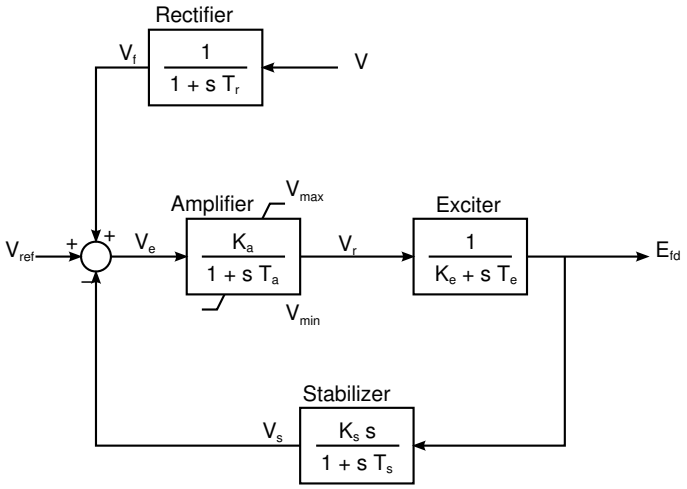

Figure 3.5: Block diagram of IEEE Type 1 Exciter and AVR

The parameters of the model are the following:

K_a	=	Amplifier gain
K_e	=	Exciter gain
K_s	=	Stabilizer gain
T_a	=	Amplifier time constant (in seconds)
T_e	=	Exciter time constant (in seconds)
T_r	=	Rectifier time constant (in seconds)
T_s	=	Stabilizer time constant (in seconds)
V_{min}, V_{max}	=	Amplifier lower and upper limits (in p.u.)

Initialization of the exciter and voltage regulator model is done based on the results of the load flow, which calculates the initial terminal voltage V and excitation E_{fd}^0. Figure 3.6 shows a block diagram of the initialization scheme.

Protection Since the diesel generators are the principal energy source for the system, they have been designed to stay online through system disturbances, only being tripped in the event that mechanical

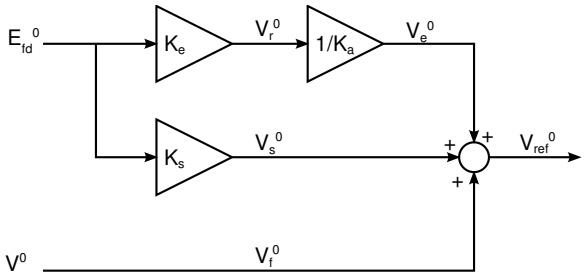

Figure 3.6: Initialization scheme of IEEE Type 1 Exciter and AVR

damage would otherwise be suffered. Over-heating protection operates if the temperature of the cooling system rises to excessive levels.

For simulation purposes, the diesel generators are protected by over/under-speed relays that trip the unit when its speed violates an upper or lower threshold for specified time intervals. These thresholds are set for the unit to trip only for very large, prolonged speed deviations for which it is apparent that the system is collapsing and will certainly not be able to recover. In these conditions, the numerical integration process often slows down considerably, so it is desirable to remove all machines from service so that the simulation will terminate.

Minimum power relays have also been used to streamline the simulation process. The dynamic data file includes data for all of the generators in the system. Because some of them are not in operation for a given scenario, either these machines must be removed from the file, or they must be tripped at the beginning of the simulation. The initialization, based on the results of the power flow, will initialize the machines that are not being used to a power set point of zero. A minimum power relay can detect this condition and remove these machines from service in the first few seconds of the simulation.

The minimum power relay has been implemented using the EuroSTAG power protection relay. The purpose of the power protection relay is to trip out lines when the active power flow is too high. The relay has separate settings for power import and export mode, as shown in the logic diagram in Figure 3.7. To get the relay to function as a minimum power relay instead of a maximum power relay, a negative value is used for the limit of the power flow in the opposite direction. If the directions of positive power flow for export and import are as shown Figure 3.8, then tripping for exportation of less than 0.1 MW may be done by setting $SIMP$ and $SDIMP$ so that the relay trips for importation greater than -0.1 MW. The exportation limits $SEXP$ and $SDEXP$ can then be set to large values so that the relay does not trip the unit under normal loading.

3.5.2 Hydro Generator: Cherry Hills

The three hydro units at Cherry Hills are the only hydro units in the test system that participate in frequency regulation.

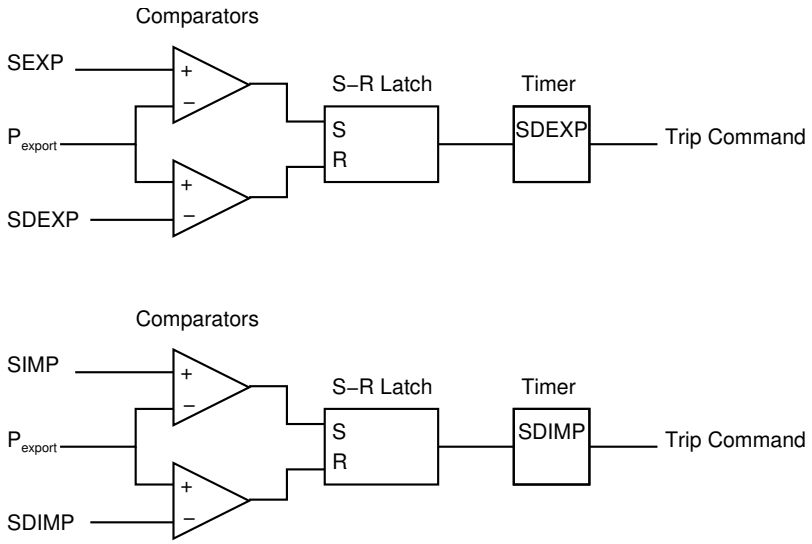

Figure 3.7: EuroSTAG Power protection relay

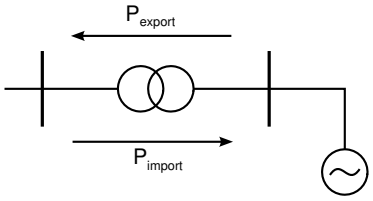

Figure 3.8: Definition of positive power flow direction

Electrical Machine The same simplified model for the synchronous machine is used as was presented for the diesel units. The details of this model may be found in Appendix C.

Speed Regulation Like the diesel units, the Cherry Hills unit regulates speed using a speed droop characteristic together with an integral component. The only difference is in the response of the turbine, which in the case of the hydro unit must include the water starting time t_w. The block diagram of the hydro unit speed regulation model is shown in Figure 3.9.

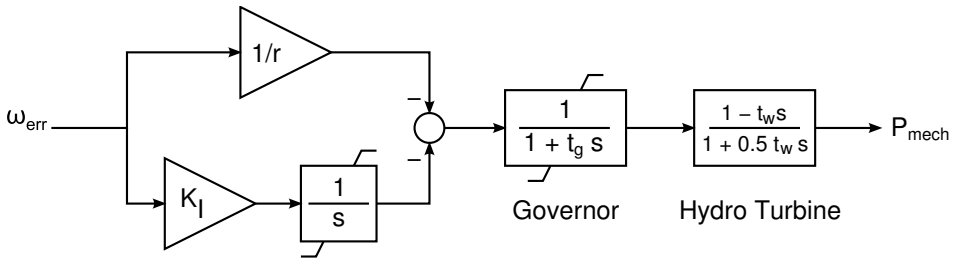

Figure 3.9: Block Diagram for Hydro Generator Speed Governor

Voltage Regulation The same IEEE Type 1 voltage regulator model is used for the Cherry Hills units as was presented for the diesel generators (see Figure 3.5).

Protection Like the diesel generators, the Cherry Hills units are designed to be able to ride through most system disturbances and only be tripped in absolute necessity. They are protected by over/under-voltage relays as well as the same speed protection and minimum power protection schemes that were used for the diesel generators so simplify the simulation process.

A logic diagram of the voltage relay available in EuroSTAG is shown in Figure 3.10. The logic of the voltage relay is somewhat non-intuitive in that the time interval during which the voltage must violate the threshold and return to a reset value is equal to the tripping time $TINF$ or $TSUP$ minus the reset time $TRINF$ or $TRSUP$.

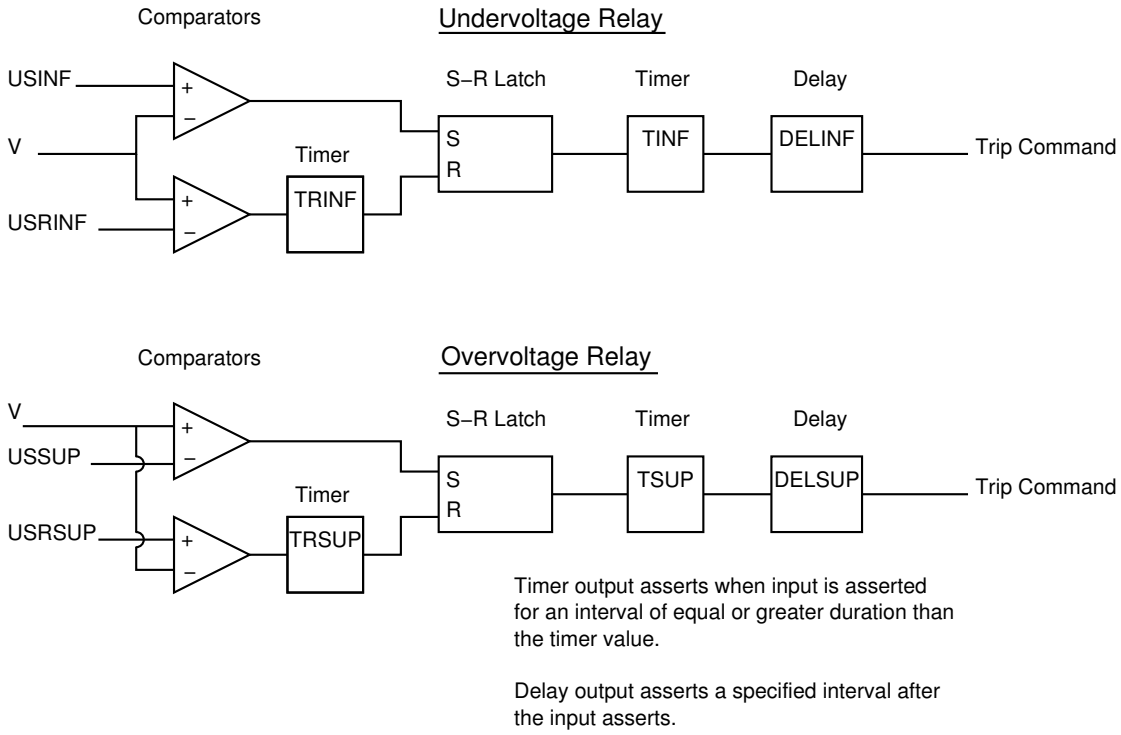

Figure 3.10: EuroSTAG voltage relay logic diagram

3.5.3 Hydro Generator: Run-of-river

Electrical Machine The same simplified model for the synchronous machine is used as was presented for the diesel units. The details of this model may be found in Appendix C.

Speed Regulation The run-of-river hydro units do not have any speed regulation. They have a constant torque input that is initialized such that the output of the unit equals that which was specified in the power flow.

Voltage Regulation The same IEEE Type 1 voltage regulator model that was presented for the diesel generators is again used, as shown in Figure 3.5.

Protection The run-of-river hydro units have relays with much more sensitive settings than those of the diesel units or Cherry Hills, however, the same EuroSTAG devices are used. Over- and under-speed relays are used with settings to trip for frequency variations greater than 0.5 Hz. Over- and under-voltage relays are also used. Finally, the same minimum power export scheme has been used to disconnect machines that have not been dispatched in the scenario being simulated.

3.5.4 Wind Park: Standard Asynchronous Machines

There is a small part of the wind parks in the system that is based on older standard asynchronous machine technology. These units are sensitive to system frequency and voltage and trip easily during faults.

Mechanical Power As shown in the diagram in Figure 3.11, the aerodynamic part of the wind turbine has been neglected and the mechanical power is provided directly as a set point in the model. Another set point is included that is input to an integrator. This allows the mechanical power to be ramped up or down at a constant rate, a variation that may be used to approximate the response to a change in wind speed. Except in cases where a variation in wind is specified as the disturbance to be investigated, the mechanical power of the wind park is maintained constant.

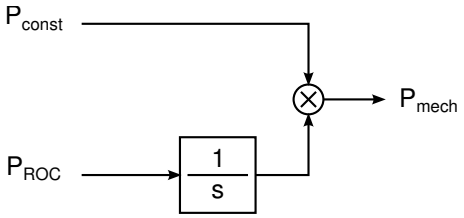

Figure 3.11: Mechanical Power for Wind Parks

Induction Machine For these older wind parks, the electrical machine that interfaces to the electrical network is a standard induction machine with a squirrel-cage rotor. The EuroSTAG model for an induction machine with macroblock input has been adopted for the wind park model. EuroSTAG has both a full and a simplified induction machine model. The full model includes dynamics of rotor fluxes for a double rotor cage while the simplified model, intended primarily to represent network loads, neglects rotor transients, the only dynamic equation being that of the rotating mass.

Although the simplified model does represent the inertia of rotating masses and is responsive to system frequency changes, it behaves only as a passive load and thus does not contribute fault current during short circuits [64]. Since the study will include investigation of system behavior following faults in the area where most of the wind parks are connected, it is most appropriate to use the full model so as to be able to include the contribution of the wind parks to the fault. The full induction machine model is presented in detail in Appendix D.

Protection The older wind parks based on simple induction machines are sensitive to frequency and voltage variations and easily trip during disturbances. Protection is provided by over/under-voltage relays as well as over/under-speed relays on the induction machine. In addition to this, a minimum power relay has been implemented using the macroblock threshold relay set to trip when the opposite of mechanical power exceeds a specified (negative) value. This is used for the same purpose as the minimum power logic for diesel and hydro generators: when the scenario as specified in the load flow case does not assign any output to the wind park, disconnect the machine from the system in the first few seconds of simulation.

3.5.5 Wind Park: Double-fed Induction Machines

The newer wind parks to be installed in the system are supposed to be based on newer technology and to have been required include fault-ride-through and voltage control capabilities. These requirements can be met most economically through the use of a double-fed induction machine as the electrical power conversion device. A simplified diagram of such a system is shown in Figure 3.12. Since the double-fed induction machine has the rotor voltages injected by a power electronic AC/DC/AC converter, the terminal output is quite controllable. The wind parks based on double-fed induction machines are modeled completely in macroblocks using a user-defined model. Each of the parts of the model are described in the following paragraphs.

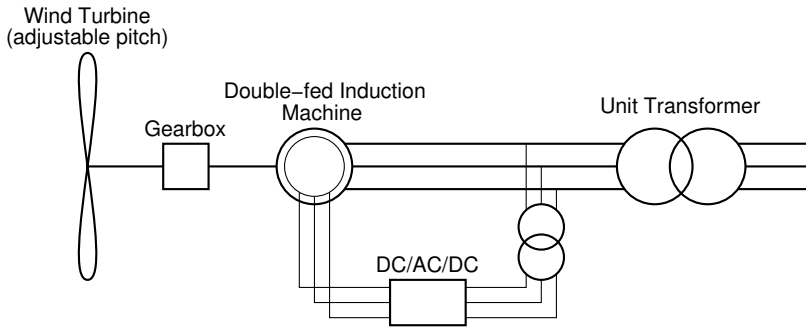

Figure 3.12: Wind Plant with Double-fed Induction Machine

Mechanical Power As had been done for wind parks based on asynchronous induction machines, mechanical power supplied to the wind park is considered as a direct input; the aerodynamic system is not modeled. There is a set-point for constant power as well as a set-point that allows constant-rate ramping of the mechanical power. A block diagram can be found in Figure 3.11.

Voltage Control The wind parks based on double-fed induction machines can include voltage/reactive power control. A simple proportional control loop has been used for this study, as proposed in [65] and shown in Figure 3.13. The limiter has been added before the time constant to help with numerical

stability during the sudden voltage change when a fault occurs near the wind park. Q_{max} has been set to 0.4 for all parks.

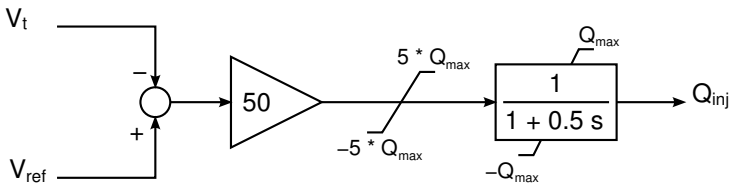

Figure 3.13: DFIM-Base Wind Park Voltage Control

Simplified Machine Model The details of the double-fed machine and the associated voltage source converter and controls are not included in this model. As proposed by Slootweg in [66], a simplified model has been used for the double-fed machine and AC/DC/AD converter in the variable speed wind turbine. This model is based on the fact that the controls for the power electronic converter operate quite quickly and are able to maintain the the rotor speed at its optimum value. A block diagram of the simplified model is shown in Figure 3.14.

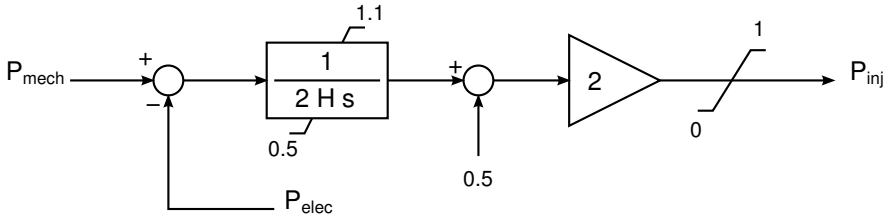

Figure 3.14: Simplified Variable Speed Wind Turbine Model

The P_{inj} and Q_{inj} provided by the machine model and the voltage control loop are transformed to real and imaginary components of current. A small time-constant delay is applied to the current signals to help with numerical stability during discontinuities such as faults. The transformation from (P_{inj}, Q_{inj}) to (I_R,I_I) is done using the following matrix multiplication, where U_R and U_I are the real and imaginary components of the terminal voltage, as provided to the model by the EuroSTAG platform during simulation:

$$\begin{pmatrix} I_R \\ I_I \end{pmatrix} = \frac{1}{U_R^2 + U_I^2} \begin{pmatrix} U_R & U_I \\ U_I & -U_R \end{pmatrix} \begin{pmatrix} P_{inj} \\ Q_{inj} \end{pmatrix} \tag{3.8}$$

The macroblock implementation of this transformation, including the delay on the output is as shown in Figure 3.15. Note that V_t is the terminal voltage, so $V_t^2 = U_R^2 + U_I^2$.

Protection The wind parks have both frequency and voltage protection. Frequency protection allows for frequency deviations of up to 0.5 Hz for 1 sec with instantaneous tripping for deviations greater than 1 Hz. This is consistent with the protection system settings of the general variable speed wind turbine

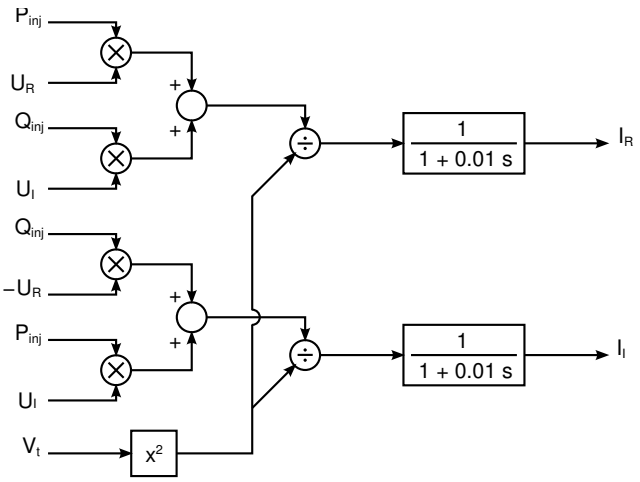

Figure 3.15: Transform from P,Q to Current

model presented in [66].

Undervoltage protection is assumed to conform to ride-through-fault capabilities as required by a typical grid code such as [67]. The voltage-time characteristic required by EON in is shown in Figure 3.16. Any interconnected generator is required to continue connected for voltages above the line. The characteristic modeled for this study is that the machines trip instantaneously for voltages less than 0.20 pu. For voltages between 0.20 and 0.80 pu it allows 700 ms, and above 0.80 pu it doesn't trip.

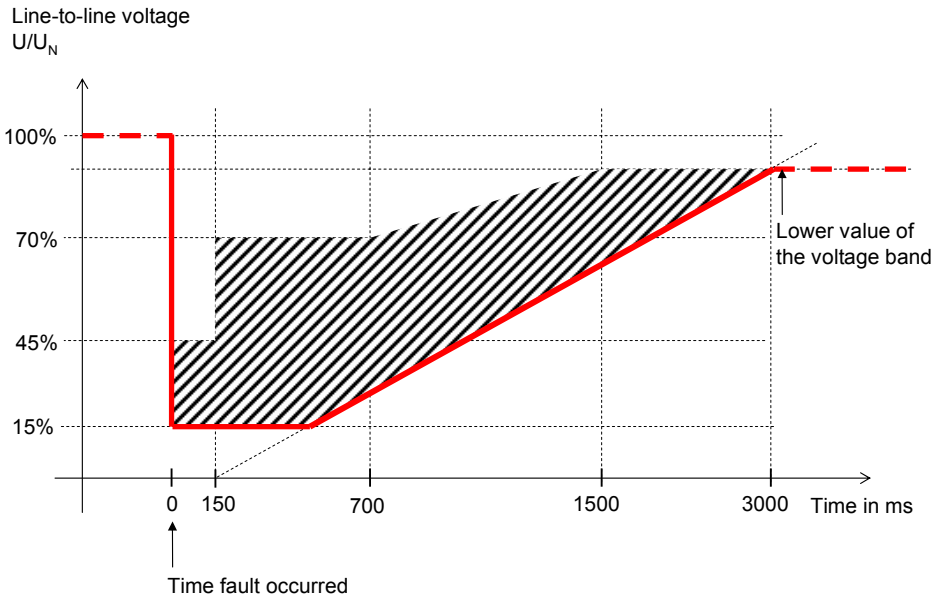

Figure 3.16: Voltage limit curve of network fault [67]

3.5.6 Pumped Storage Station

Since the pumped storage station may operate in both pumping and generating modes, separate models would be needed to represent the station in both cases. For the study done in this work, only pumping

mode is needed since the scenarios have been chosen for off-peak hours. When in generating mode, the pumped storage station could be treated in the same way that the other hydro generating stations have been treated.

Mechanical Power in Pumping Mode When in pumping mode, the mechanical power presented to the electrical machine is constant. In this way it is exactly the same as run-of-river hydro plants, with only a reversal of sign in the power.

Voltage Regulation Voltage regulation is done using an IEEE Type 1 voltage regulator and exciter as previously presented in Figure 3.5.

Electrical Machine The electrical machine is represented with the same simplified synchronous machine model that has been used for all other generation units. The details of this model can be found in Appendix C.

Underfrequency Shedding While in pumping mode, the pumped storage station is included in the load shedding strategy of the system. It is intended that the pumping load will be shed early to try to restore system frequency without the frequency falling to the point at which hydro plants and wind parks start to trip offline. The plant is tripped if a system frequency of less than 49.8 Hz is detected for more than 300 ms or if the system frequency falls below 49.6 Hz.

Protection Protection is provided by over/under-voltage relays as well as over/under-speed relays on the synchronous machine. In addition to this, a minimum power relay has been implemented using the macroblock threshold relay set to trip when the opposite of mechanical power exceeds a specified (negative) value. This is used for the same purpose as the minimum power logic for diesel and hydro generators: when the scenario as specified in the load flow case does not assign any load to the pumped storage station, disconnect the machine from the system in the first few seconds of simulation.

3.5.7 Loads

No specific data is known about the composition of the loads in the test system, so a standard load model has been used. For dynamic simulations, EuroSTAG allows multiple load models to be defined according to the general form shown in (3.9) and (3.10). In the model, P and Q are the active and reactive power of the load at a given moment in time, P_0 and Q_0 are the nominal active and reactive power of the load as resulting from the power flow, ω and U are the momentary system frequency and load bus voltage, and ω_0 and U_0 are the nominal system frequency and bus voltage as resulting from the power flow calculation. The parameters α, γ, β, and δ characterize the behavior of the load.

$$P = P_0 \left(\frac{|U|}{|U_0|} \right)^{\alpha} \left(\frac{|\omega|}{|\omega_0|} \right)^{\gamma} \tag{3.9}$$

$$Q = Q_0 \left(\frac{|U|}{|U_0|} \right)^{\beta} \left(\frac{|\omega|}{|\omega_0|} \right)^{\delta} \tag{3.10}$$

According to [68], the most common static load model is to represent active power as constant current and reactive power as constant impedance. In the EuroSTAG formulation of the static load model, this gives $\alpha = 1$ and $\beta = 2$. The parameters of frequency dependency are taken as $\gamma = 1$ and $\delta = 0$.

Load shedding is performed in three steps at the Cherokee and Santa Fe substations. The first step occurs at 49 Hz if the rate of change of frequency is -2.5 Hz or greater, otherwise it occurs at 48 Hz. In the first step, 25% of the load at these two substations is cut. The second load shedding step occurs at 47.5 Hz with the cutting of an additional 13% of load. The third and final step occurs at 47.0 Hz and removes 13% more.

3.5.8 Faults

Some of the disturbances require that a fault be applied to specified transmission lines in the system. The system is only represented by balanced elements, so the fault applied must be three-phase-to-ground. Some small impedance must be chosen for the fault to avoid numerical problems. Faults are cleared at both ends of the line after 300 ms.

3.6 Summary of Methodology

The methodology that has been presented to evaluate the effectiveness of the strategy of including pumped storage is the following:

1. Mount test system in dynamic simulation platform
2. Verify the minimum frequency expression in (3.5) and determine the value of a
3. Evaluate the effectiveness of the pumped load shedding strategy using the chosen disturbances
4. Compare system response with and without the proposed security criteria and pumped storage

Results may be found in Chapter 6.

Chapter 4

Capacity Optimization

One of the major tasks undertaken in this thesis is the optimization of the capacity of a pumped storage station. In this chapter, the problem will be explained in greater detail and an overview of the data needed to solve the problem given. Then a mathematical formulation of the problem will be presented followed by the concrete approach taken to resolve it. Results are presented in Chapter 7.

4.1 Explanation of the problem

In choosing to install a storage station, in this specific case a pumped storage station, there are two important economic questions to consider: 1) Is it worthwhile to install any storage units? 2) If so, how much should we install? "How much?" means both the amount of energy that will be able to be stored as well as the limit of power that will be able to be put into or taken out of storage at any given time. In the context of a pumped storage station, storage capacity will be related to the size of the reservoirs used to store the water. The amount of power available corresponds to the dimensioning of the electrical machines, mechanical housings, waterways, etc. In this thesis, these two ratings are considered to be independent of one another.

In the case of a large network, a storage unit of small or medium size will not change the price of energy. The answer to the questions proposed above will depend upon the expected prices of energy, the costs of the storage unit, and the round-trip efficiency of the storage technology. Examples of such analysis can be found in [69] and [50]. Prices may be considered fixed or treated stochastically but in any case are not affected by the presence or dimension of the storage unit being considered.

When optimizing a storage station for a small network, the approach must be different. The storage station will likely have a significant impact on the operation of the network. In a small network, the number of thermal generators used to meet load is relatively small. For the example system used, twenty-three diesel units are available, and during off-peak hours, the number of online units may be low enough to be counted on the fingers of one hand. Under these conditions, even a relatively small storage station

may significantly change the unit commitment and accordingly the marginal costs of generation during off-peak and peak hours. Since it is expected that the marginal costs will be modified by the inclusion of a storage station, the optimization problem should consider the entire energy supply system and not merely accept fixed energy prices for peak and off-peak hours.

Additionally, the test case under study (see Chapter 5) includes large components of wind and hydropower production. This is particularly significant because, during low loading periods in which a large amount of wind and hydro power is available, the technical limits and security concerns related to frequency regulation may require a minimum amount of thermal generation to be left online. The use of pumped storage can increase the system load during these off-peak periods and allow larger penetration of renewable energy sources.

Whatever optimization is done must be done in such a way as to take into account the amount of wind and hydro power available throughout the year. Hydropower production in particular demonstrates very strong seasonality (see Figure 5.6). Wind park production also shows some seasonality, and system load exhibits weekly and seasonal variations. A stochastic model is used and scenarios are generated to approximate the distribution of wind and hydro power and load throughout the year.

The approach used considers the benefits of a pumped storage unit in terms of energy storage on a daily cycle, storing energy during off-peak hours to be used during peak hours, as well as in terms of providing additional load during off-peak hours that can allow greater penetration of renewable energy sources without compromising system security. These are not the only benefits of pumped storage. Using the pumped storage unit to supply peak loads and allow greater utilization of renewable sources may play an important part in the expansion of the energy supply system in addition to or instead of investment in thermal generators [70]. The operation of a storage station will also help level the loading on the diesel groups, allowing them to operate more constantly and avoid some start-up and shut-down costs [14]. It is important to keep in mind that these effects are not included in the present study and will serve to increase the value of the pumped storage station.

4.2 Data required

In order to resolve the problem, several data items are necessary. First, the cost characteristics of installing a pumped storage station must be known. Because the energy and power capacities are being considered independently, the cost must be determined as a function of these two values.

Second, data must be available about the cost characteristics of generation in the system into which the pumping station will be integrated. This includes data about the limits and costs of the diesel groups. The security criteria, such as spinning reserve, must also be known and either incorporated into a single cost function to represent the aggregate cost of thermal generation or mathematically formulated and added as a set of additional problem constraints.

Third, we must have sufficient data about the wind and hydropower production and system load to be able to generate scenarios. Either we must know or be able to extract the parameters necessary to generate synthetic time-series values, or we must have historical time-series data directly available.

4.3 Problem formulation

The problem is formulated as a single-objective constrained linear programming optimization problem. The primary problem variables are the energy capacity (E_{max}) and the power capacity (P_{max}) of the pumped hydro station. The objective is to minimize the sum of operating costs and appropriately annualized installation costs. Operating costs are the expected operating costs over all scenarios of wind and hydropower production and load. In each scenario the operating costs are independently minimized in a sub-problem that considers as problem variables the pumping/generating use of the pumped storage station, constrained by E_{max} and P_{max}.

By formulating the problem in the way, the solution provides not only an answer to the question of how much pumped storage to install, but also provides insight into operating strategies for various wind/hydro/load scenarios. The problem of the uncertainty of the future wind or hydropower production is not considered in the subproblem optimization. In this respect it will be optimistic. Optimizing the operation of a pumped storage unit in conjunction with uncertain wind production has been treated in other works [56].

In this formulation the energy capacity and power capacity (E_{max} and P_{max}) are treated as continuous variables. Likewise, in the subproblems, the generation and pumping of the storage station (P_g and P_p) are treated as continuous variables. The cost of thermal generation is represented by a single piecewise linear function.

Objective function The objective function to be minimized is the expected daily cost of operation and amortization:

$$\begin{aligned} \text{minimize } t \cdot \sum_{i,j,k} p_i \cdot C_{T,k} \cdot P_{i,j,k} + \\ a \cdot C_{E_{max}} \cdot E_{max} + \\ a \cdot C_{P_{max}} \cdot Pg_{max} \end{aligned} \tag{4.1}$$

In the objective function (4.1), the last two lines are from the master problem and are the annualized install costs of energy and power capacity. The sum in the first line is the expected operation cost over all scenarios. The subscript i indexes scenarios, j indexes periods during the day, and k indexes parcels of power for thermal generation.

Constraints The following are the equality and inequality constraints of the problem.

$$0 \leq E_{i,j} \leq E_{max} \; \forall \; i, j \tag{4.2}$$

$$0 \leq Pg_{i,j} \leq Pg_{max} \; \forall \; i, j \tag{4.3}$$

$$0 \leq Pp_{i,j} \leq Pp_{max} \; \forall \; i, j \tag{4.4}$$

$$0 \leq Edump_{i,j} \; \forall \; i, j \tag{4.5}$$

$$0 \leq Pcurtail_{i,j} \; \forall \; i, j \tag{4.6}$$

$$E_{i,j+1} = E_{i,j} + t \cdot \eta_p \cdot Pp_{i,j} - t \cdot \frac{Pg_{i,j}}{\eta_g} - Edump_{i,j} \; \forall \; i, j \tag{4.7}$$

$$E_{i,0} = E_{i,n} \tag{4.8}$$

$$\sum_k P_{i,j,k} + Pg_{i,k} - Pp_{i,j} = Pload_{i,j} - (Phydro_{i,j} + Pwind_{i,j} - Pcurtailed_{i,j}) \; \forall \; i, j \tag{4.9}$$

$$\sum_k P_{i,j,k} \geq \frac{1.5 \cdot UnitSize \cdot TechMin}{1 - TechMin} \; \forall \; i, j \tag{4.10}$$

$$\sum_k P_{i,j,k} \geq TechMin \cdot (RegFactor\,(TechMin \cdot UnitSize - Pp_{i,j} + Pg_{i,j}) + ThermUnitSize) \; \forall \; i, j \tag{4.11}$$

$$0 \leq P_{i,j,k} \leq PParcelMax_k \; \forall \; i, j, k \tag{4.12}$$

$$Pg_{max} = Pp_{max} \tag{4.13}$$

Problem Variables (Master problem) The master problem includes the following variables:

E_{max} (MWh) is the maximum amount of energy that the system can store. It corresponds to the capacity of the reservoirs of the pumped hydro station.

Pg_{max} (MW) is the active power rating of the storage station while in generating mode. It can also be thought of as the maximum rate at which energy may be taken out of storage and injected into the power system. It corresponds to the rating of the electric generating machine that is to be used.

Pp_{max} (MW) is the active power rating of the storage station while in pumping mode. As in the case of Pg_{max}, it can also be thought of as the maximum rate at which energy may be taken out of the power system and injected into storage. It corresponds to the rating of the electric pump that is to be used. In the case that a single reversible machine is used, Pg_{max} and Pp_{max} are equal. This condition is enforced by a constraint in this problem formulation.

Problem Variables (Sub-problems) The sub-problems contain the following variables. The subscript i is used to index over scenarios and the subscript j is used to subscript over time periods within the scenario.

$Pg_{i,j}$ (MW) is the amount of power generated by the pumped storage station in generating mode.

$Pp_{i,j}$ (MW) is the amount of power consumed by the pumped storage station in pumping mode.

$P_{i,j,k}$ (MW) is the amount of power produced by block k of thermal generation. The sum $\sum_k P_{i,j,k}$ gives the total of thermal generation during time period j of scenario i.

$Pcurtail_{i,j}$ (MW) is the amount of renewable power that could be produced but has been curtailed. It could be wind power or hydro power or some combination of the two.

$E_{i,j}$ (MWh) is the energy balance of storage. This represents the reservoir's level at the beginning of time period j of scenario i.

$Edump_{i,j}$ (MWh) is energy in the storage device that is dumped. This represents water that is allowed to flow from the upper reservoir to the lower one without turning the generator.

Parameters (Master problem) The following parameters are associated with the master problem:

$C_{E_{max}}$ (EUR/MWh) is the constant incremental cost of installing reservoir capacity.

$C_{P_{max}}$ (EUR/MW) is the constant incremental cost of installing pumping station power capacity.

a is a dimensionless annualization parameter used to express the cost of the pumped storage station on a daily basis.

Parameters (Sub-problems) The following parameters are associated with the sub-problems:

p_i is the relative frequency of the i^{th} scenario.

$Pload_{i,j} - Phydro_{i,j} - Pwind_{i,j}$ (MW) defines the net load that must be met by the thermal generators and the pumped storage station together. Each scenario is defined by this series of values.

η_p is the efficiency of the pumping cycle of the pumped storage station. The value is dimensionless and should be the ratio of energy put into storage to energy taken from the network.

η_g is the efficiency of the generating cycle of the pumped storage station. The value is dimensionless and should be the ratio of energy injected into the network to the energy drawn from storage.

$UnitSize$ (MW) is the active power capacity of the first diesel machines to be committed. It is assumed that three of similar size are committed first and that no less than three may be committed.

$TechMin$ is the per-unit technical minimum of the diesel generating sets, below which the generators are not to be operated.

$RegFactor$ is the regulating factor for frequency regulation. This value is equal to the product $f_{base}/\Delta f_{max} \cdot a \cdot r$ as used in (3.6).

$C_{T,k}$ (EUR/MWh) are the marginal costs of the blocks of the cost curve for thermal generation. Figure 4.1 illustrates how C_T and $PParcelMax$ define the cost curve.

$PParcelMax_k$ (MW) are the sizes of the blocks of the cost curve for the thermal generation.

n is the number of time periods in each scenario that will be considered.

t (h) is the length of each time period in the scenarios.

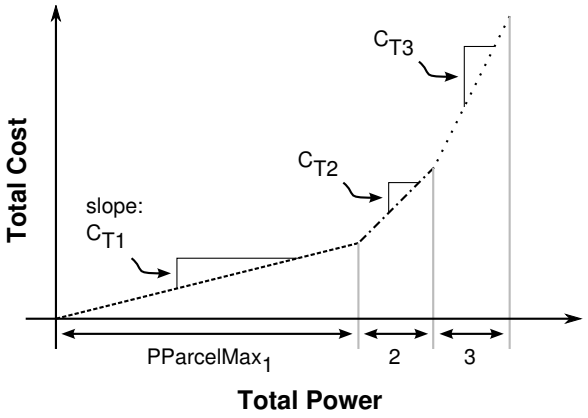

Figure 4.1: Thermal Cost Function

Description of Constraints The problem constraints presented in (4.2) to (4.13) are explained as the following:

The constraint in (4.2) limits the reservoir level in every time period of every scenario to the maximum of E_{max}. Likewise, (4.3) and (4.4) limit the generation or pumping power of the pumped storage station to a maximum of Pg_{max} and Pp_{max}, respectively, for all time periods of all scenarios.

Constraint (4.7) couples the reservoir level between subsequent time periods and takes into account the efficiencies of pumping and generating (η_p and η_g). The possibility of dumping water without using it to turn the generator is allowed by the inclusion of $Edump$. This could arise if pumping is done in order to raise system load in order to meet spinning reserve reserve requirements or frequency regulation unit commitment requirements as expressed in (4.10) and (4.11).

In (4.8) the boundary conditions of the reservoir level are set. Since the pumping/generating cycle is supposed to be repeatable on a daily basis, the beginning and ending balance of each scenario have been fixed as equal. This allows the storage cycle to start and end at any balance as long as the beginning and ending balances are equal.

In (4.9) the power balance between generation and load is enforced for every time period of every scenario. To allow for cases in which of the power from renewable sources cannot be accepted, the term $Pcurtailed$ has been included. No upper limit is needed for $Pcurtailed$ as long as the limits imposed by (4.10) and (4.11) are always below system load.

The constraint in (4.10) requires that the spinning reserve requirement be able to be met. It assumes that at the limit, the committed generators will be operating at their technical minimums $TechMin$ leaving $1 - TechMin$ as spinning reserve. The spinning reserve requirement is 1.5 times the load carried by the largest unit.

In (4.11), the thermal dispatch is constrained by a minimum unit commitment as determined by the criteria expressed in (3.6) as explained in Section 3.2. The Pg term does not properly belong in this constraint, however, it must be included to keep the solution from giving Pp and Pg both positive in the same time period. The inclusion of Pg has no effect as long as this constraint is not active during periods

in which the solution shows the pumped storage unit in generating mode.

The constraint (4.12) sets the power limits for the blocks of power at each marginal cost level in the piecewise linear thermal cost function.

Finally, in (4.13), the power limits for generation and pumping are fixed equal. This corresponds to the use of a reversible machine. In the case that separate machines are used for pumping and generating, this constraint could be removed and two separate cost elements used in the cost function.

4.4 Solution Approach

The solution approach adopted to deal with this problem includes three basic steps. The first is to determine values for the parameters that appear in the linear program. The second is to characterize the scenarios to be used in the stochastic formulation of the problem. The third is to code the linear program in a format that can be read by a solver and solve the problem. These steps are described in the following subsections.

4.4.1 Determining values for parameters

The formulation of the optimization problem as described in Section 4.3 includes several constants that must be defined.

Approximate costs for installing pumped storage can be found in [23] and [70]. These reference costs have been converted to Euros to give the $C_{E_{max}}$ = 13776 EUR/MWh and $C_{P_{max}}$ = 377200 EUR/MW.

The constant a is an annualization factor. This takes into account the time value of money and converts the one-time installation cost to a stream of daily costs. The value can be found by choosing a time period over which the installation cost will be spread out and the interest rate to be used and then applying the appropriate engineering economics formula (4.14), which equates a present value P to a series of future cash flows A.

$$(A/P, i, N) = \frac{i \cdot (1+i)^N}{(1+i)^N - 1} \tag{4.14}$$

A 30-year life with an annual discount rate of 5% is used, consistent with [23]. The annual discount rate of 5% is equivalent to a daily discount rate of $i = e^{\frac{\ln(1.05)}{365}} - 1 = 0.000134$. Applying (4.14) gives a = 0.000174.

The constants η_p and η_g are the efficiencies of pumping and generating respectively. These are each given values of 0.9. This gives a round-trip efficiency of 0.8, which is in the usual range for pumped storage facilities [70, 23, 14].

The value for $UnitSize$ is the capacity of the first diesel units to be committed. For the test system, this is 16.5 MW. $TechMin$ is the per-unit technical minimum of these machines and is chosen to be 0.7.

The test system operator does not operate below this point because efficiency of the diesel generating set decreases quickly at lower operating points.

The constant $RegFactor$ must be evaluated based on the frequency regulation characteristics of the test system and the security requirements being used. The following values were verified, as explained in detail in Section 6.1:

$$\begin{aligned} f_{base} &= 50\ Hz \\ \Delta f_{max} &= 0.5\ Hz \\ a &= 0.85 \\ r &= 0.06 \end{aligned}$$

These results give a value for $RegFactor$ of $f_{base}/\Delta f_{max} \cdot a \cdot r = 50/0.5 \cdot 0.85 \cdot 0.06 = 5.1$.

The sections of the thermal power cost function are shown in Table 4.1 and illustrated in Figure 4.2. The diesel units of the test system are divided into two groups: new units and old units. The approximate fuel consumption of the newer generating sets is 0.215 kg/kWh while the approximate consumption of the older units is approximately 0.273 kg/kWh. The fuel price is estimated at 70 USD/barrel or 0.41 EUR/kg. This is consistent with current prices, including cost of shipment.

Table 4.1: Cost of Thermal Generation

n	Power (MW)	Marginal Cost (EUR/MWh)
1	60	87.0
2	30	88.0
3	10	111.0
4	10	111.2
5	10	111.4
6	5	111.6
7	5	111.8
8	5	112.0
9	5	112.2
10	5	112.4
11	5	112.6
12	5	112.8
13	80	113.0

The constant n is the number of number of time periods over which to optimize each scenario. A daily cycle composed of 24 one-hour periods is chosen, so $n = 24$ and $t = 1$.

4.4.2 Stochastic scenarios

The optimization problem formulated in this work seeks to maximize the benefit obtained from the use of pumped storage in a system that includes significant power contributions from wind parks and hydropower stations. The solution should take into account the variations in the primary resources of

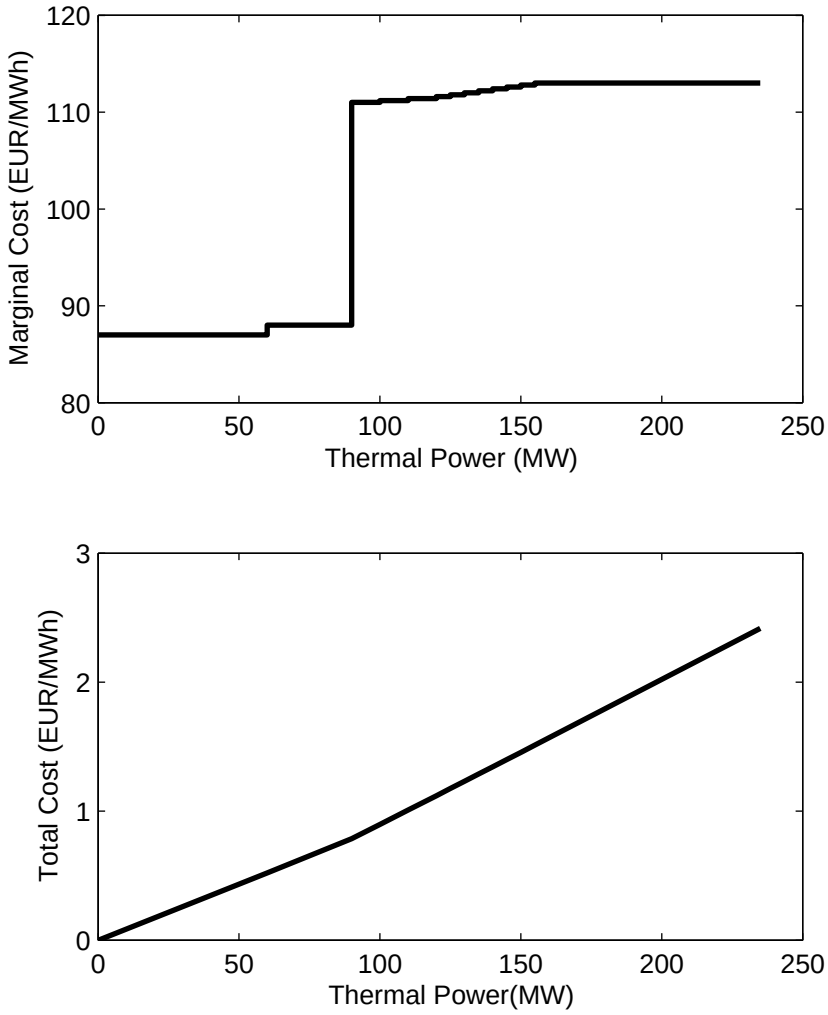

Figure 4.2: Cost of Thermal Generation

these power sources. In order to deal with these variations, a stochastic programming approach has been adopted. Several scenarios are developed with probabilities assigned that correspond to the relative frequency of occurrence of these scenarios.

The real variation of wind and hydropower production has a continuous distribution, but the use of stochastic scenarios can provide an approximation. Each scenario must represent a range of values for wind and hydro power. The data available conditions which techniques may be used to choose scenarios. If measured data is not available, expert information may be the best option available. If measured data is available for a significant time period, data analysis techniques may give better results.

For the test system used in this study, five years of hourly or semi-hourly power production data were available for thermal, hydro and wind power sources. With this amount of detailed data available, the most reasonable approach is to use data analysis to determine scenarios. Fuzzy clustering algorithms were chosen as a good means to determining good prototypes to use for scenarios.

Partitioning analysis such as that performed in fuzzy clustering seeks to discover natural groupings that exist in the data set. For example, in Figure 4.3, it is easy to identify three clearly separated clusters marked A, B, and C.

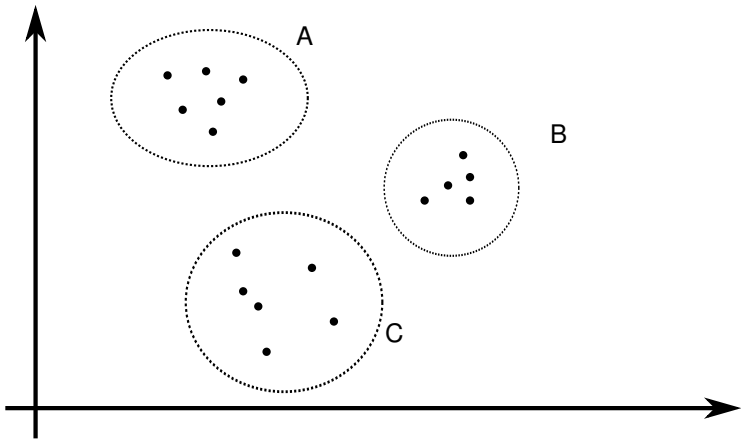

Figure 4.3: Example of Clusters

For a small data set like this, with few points and only two dimensions, it is not difficult to spot the clusters by looking at a plot. However, systematic, mathematic approaches have been developed that are able to identify clusters that may not be obvious and which may be done automatically. Clustering has found interesting application in all fields of investigation. Figure 4.4 shows the procedure that is followed when using clustering analysis.

Fuzzy clustering algorithms assign each data point to a cluster with a degree of membership that ranges between 0 and 1. Each cluster is represented by a prototype, most typically a point, though more advanced algorithms may use other shapes such as lines, circles, or ovals. The fuzzy clusters are produced by solving an optimization problem that seeks to adjust the membership values and cluster prototypes in such a way as to minimize some objective function that typically represents the distance between the

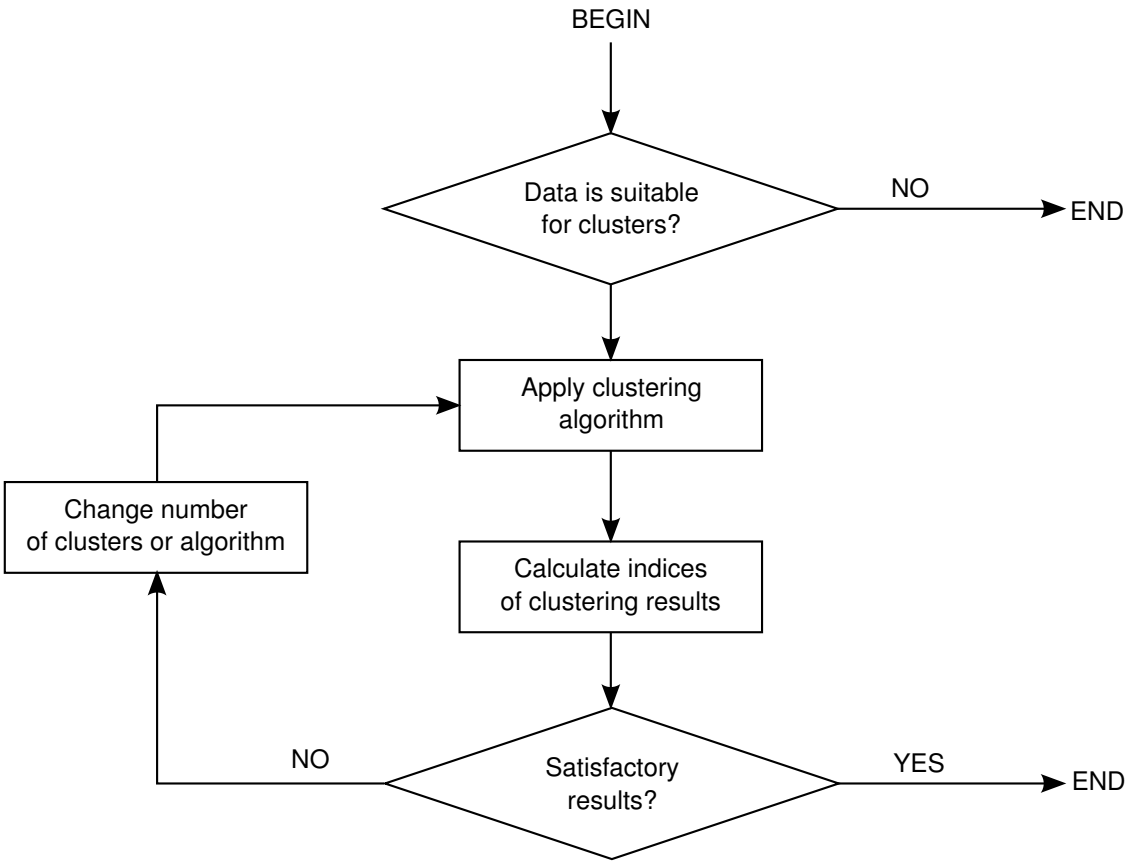

Figure 4.4: Clustering Procedure [71]

points assigned to a cluster and the cluster prototype.

The most basic fuzzy clustering algorithm is fuzzy c-means (FCM) as developed by Dunn [71, 72]. The objective function of FCM is the following:

$$J(X;U,V) = \sum_{i=1}^{c}\sum_{k=1}^{N} (\mu_{ik})^m \left\|x_k - v_i\right\|_A^2 \tag{4.15}$$

where X is a vector of N data points and U and V are the resulting degrees of membership and prototype vectors for c clusters.

The objective function in (4.15) may be minimized by a large number of optimization routines, however, the most popular for this problem is simple Picard iteration through the stationary points of (4.15) [71]. When this solution algorithm is used for this objective function, it is fuzzy c-means.

The norm usually used used in FCM is a standard Euclidean distance of the form

$$D_{ikA}^2 = (x_k - v_i)^T A (x_k - v_i) \tag{4.16}$$

The norm-inducing matrix A serves to scale the distances in each of the dimensions, and without any scaling at all it is simply the identity matrix. In any case, it is fixed for all clusters, which means that all clusters will take the same hyperspherical shape. This may not match the true form of the data clusters.

The Gustavson-Kessel fuzzy clustering method modifies the FCM algorithm by additionally allowing the optimization procedure to adjust the norm-inducing matrix A for each cluster [71, 72]. The objective function to be minimized now has the form

$$J(X;U,V,A) = \sum_{i=1}^{c}\sum_{k=1}^{N} (\mu_{ik})^m \, D_{ikA}^2 \tag{4.17}$$

where the new problem variable A is a c-tuple of the norm-inducing matrices $A = (A_1, A_2, \ldots)$. This allows each cluster to have a different hyperspherical shape as best fits the data. It also eliminates problems arising from scaling differences between the attributes of the data points.

An important step in the use of any clustering method is validation of the clusters. This is done by calculating any of several indices that have been developed for this purpose. These indices can be used to chose the appropriate number of clusters to use and indicate the quality of the partitioning produced by the clustering algorithm. In general, the validation indices seek to indicate compactness of individual clusters and separation of the clusters from each other. Each index has advantages and disadvantages, so it is good to check several indices. Some of the best-known indices available include Classification Entropy (CE), Partition Index (SC), Separation Index (S), Xie and Beni's Index (XB), and others [73, 72, 74].

MATLAB includes a fuzzy clustering function `fcm` in its Fuzzy Logic Toolbox. This function implements fuzzy c-means (FCM). Additionally, a Fuzzy Clustering and Data Analysis toolbox [72] has been contributed for MATLAB that includes functions that implement FCM and Gustavson-Kessel fuzzy clustering algorithms as well as the validation indices mentioned above. MATLAB with the Fuzzy Clustering and Data Analysis tool box was chosen to perform the fuzzy clustering analysis for the work described in this thesis.

One difficult decision that must be made before beginning clustering analysis is which attributes to use to produce the clusters. Without any data analysis, this type of problem is generally approached by producing scenarios for each of the seasons, known in advance to have certain typical characteristics. In the case of the test system, there is a strong summer-winter seasonality, especially in rainfall and hydro production, but also in wind and load profiles. From this knowledge a number of scenarios could be created, for example "summer windy weekday", "summer calm weekday", "sumer windy weekend", etc. The number of days expected to fall into each group could be estimated and probabilities assigned according to the relative frequencies of occurrence.

Approaching the choice of attributes in this way leads to an attempt to characterize scenarios based on wind park production, hydropower output, and system load profile; however, this may not be the best choice. None of these values is used directly in the optimization problem. Rather, in the formulation given in Section 4.3, the scenario for load, wind, and hydro production appears merely as a net load to be met by some combination of thermal generation and pumped storage, as appear on the left- and right-hand sides of (4.9).

What will therefore be most important to identify in creating scenarios is the shape of this net demand and its overall level. By defining the scenarios in this way, each scenario will no longer have the intuitive meaning that scenarios like "winter calm weekday" had. Instead they will represent something like "low offpeak load rising early to strong peak load" or "fairly even moderate load all day", without any indication of whether these are owing to any cause in particular.

Since the present problem deals with the economic benefits possible from shifting energy from offpeak to peak periods, the values in these two time periods is of special interest. Looking at the load diagrams in Figures 5.2 and 5.3, three daily time periods present themselves:

- Off-peak, the period in which load reaches a minimum, between 3 and 5 AM.
- Peak, the period at which load generally reaches a maximum, between 8 and 10 PM.
- Intermediate, the mid-day period in which load rises to an intermediate peak, between 12 noon and 4 PM.

During each of these periods, the mean net load has been calculated and is used as the attribute set for clustering analysis. It is not obvious that three time periods is better than two or four, or that the time periods should be of this length and not longer or shorter. A number of experiments were made and it was found that these periods worked best. "Best" in this case is a somewhat subjective judgment based on observation of the net load curves assigned to each cluster and judging how well they seem to follow the shape of the prototype. In addition, an extra emphasis has been given to the net load values during off-peak periods by multiplying the load in this period by 4. Since the fuzzy c-means algorithm does not compensate for relative scaling between the attributes, this multiplication causes this attribute to take extra weight in the clustering.

Because the linear problem is not very taxing numerically, it is not essential that the number of prototypes be kept very small. Since the prototypes found through clustering analysis will be used to approximate the continuous distribution of real data, more prototypes should lead to a more accurate approximation.

The first step in applying fuzzy clustering to the data that is available for the test system is to import the data from the source Excel worksheets into MATLAB. The data from the real system is available on an hourly and semi-hourly basis for a series of five years. Since load and generation grow along the interval of time for which production data is available, it must be scaled to produce data points that are all comparable with one another and represent the load and generation levels chosen for the test system at the time that the pumped hydro project may be implemented.

Once the data is read in and appropriately scaled, the attributes for fuzzy clustering must be generated. That means calculating the net load obtained by the subtraction of wind and hydro production and finding averages for off-peak, peak, and intermediate periods. The net load time series is calculated in each hour by the following:

$$NetLoad = TotalLoad - HydroProduction - WindProduction$$

The data may then be passed to the appropriate fuzzy clustering function from the Fuzzy Clustering and Data Analysis Toolbox to produce fuzzy partitions of the data for a range of number of clusters. The function returns the fuzzy cluster membership values for each cluster and the prototype points. Since what is needed for the problem is a set of hourly series, the representative day for each cluster is produced by averagine the days with largest membership values. This reduces the chance that some atypical day ends up being used for a scenario while not doing large-scale averaging that ends up masking the variations that appear along the course of individual days.

After looking at the clusters and prototypes produced by a variety of number of clusters, a final decision may be made as to the number of scenarios to be used. It is generally accepted that "about seven" is a good number; however, if problem continues to be numerically tractable with more scenarios, a larger number may be chosen. Quality indices for the fuzzy clusters may not indicate their usefulness for the application in this problem because what is sought is a simplified approximation for the data set, while the validation indices are generally formulated to indicate the *simplest* partition that still is faithful to the data. Nonetheless, the indices should be calculated and examined in case something interesting might show up.

With the final decision about the number of clusters made and the clusters and prototypes found, the probabilities for each cluster may be found. Two methods were considered for this calculation. The first approach was to harden the clusters by assigning each data point to a cluster according to the largest membership value of the point, then counting the number of data points that are assigned to each cluster and dividing this counted number by the total number of data points to get the relative frequencies.

The second method was to sum the fuzzy membership values of the data points in each cluster and divide by the number of data points considered. The difference between the two methods is small and neither seems to have clear theoretical preference. The second approach has been adopted for simplicity and to avoid the information loss that occurs in when the fuzzy clusters are hardened.

Once the prototype series have been determined and the probabilities calculated, they may then be coded for the numeric resolution of the problem, as described in the next subsection.

4.4.3 Coding and Solving

The linear program described in Section 4.3 contains several variables and constraints that must be applied to every time period of every scenario. For 24 time periods and 20 scenarios, this leads to over nine thousand problem variables and nearly seventeen thousand constraints. Defining all of the problem variables and constraint equation coefficients individually is extremely time-consuming, subject to errors,

and difficult to change if some modification to the program is desired.

It is much more practical to use a modeling language to define the problem. A modeling language allows the objective function and constraints to be specified using a high-level language. In this way, the coding of the program is very similar to the mathematical formulation that has been developed. The modeling interpreter then expands subscripted variables and constraints and sets up the full problem vector and coefficient matrix automatically in a format appropriate for an linear program solver.

A number of modeling languages for linear programs are available in both commercial and free packages. One free package available is the GNU Linear Programming Kit (GLPK), which includes the MathProg modeling language [75]. Modeling languages available in commercial packages include LINGO (from LINDO Systems, Inc.) [76], GAMS [77], AMPL [78], and several others. Additionally, there are some programming libraries that provide API's to implement linear programming models using standard programming languages. Examples include FlopC++ for C++ [79] and PuLP for Python [80]. Additional examples are referred to in [81].

Coding the problem in a modeling language such as MathProg is not much different from specifying the original mathematical formulation. In the first part, all of the symbols of the model are defined: set names, variables, constraints, and the objective function. Linear operations such as multiplication by constants and summation may be done on the variables in the definition of the constraints.

Once defined completely, the `glpsol` program available in GLPK may be used to solve the linear program. It is not as fast as commercial solvers, however, it is freely available and proved to be sufficient for this problem. Although an interior point method is available in the solver, in this formulation it fails to converge, while the simplex method is able to solve the problem without difficulty.

The disadvantage to using `glpsol` is that the output is not easily parsed for transfer of the results to MATLAB or a similar program to visualize the solution. The FlopC++ libraries offer the possibility to create a C++ program that solves the problem while still taking advantage of modeling-language-type syntax. FlopC++ may link with several linear program solvers to solve the problem after expanding all the variables and constraints. The open-source CLP solver from the COIN package is easily integrated since FlopC++ is also part of COIN.

One difference in using FlopC++ instead of `glpsol` is that the C++ program has to be compiled and the resulting executable run in order to get results. However, being able to output results in a format suitable for importing the data into MATLAB for further treatment simplifies and speeds up the process considerably. After making a change in the model, all the figures of results can be generated in a few minutes.

It is worth noting that this problem presents a structure that lends to the application of Bender's decomposition [82]. Bender's decomposition takes advantage of the fact that the problem can be factored into a master problem and several sub-problems.

To apply Bender's decomposition, it is necessary to implement the solution using a programming API

so as to have the ability to add constraints to the master problem based on the dual variables resulting from the sub-problems or use a more advanced modeling language that allows some procedural commands, as has been done, for example, with GAMS in [83]. Since an adequate solution to the problem was available without the use of Bender's decomposition, some experimental efforts were made to implement a solution based on Bender's decomposition, however, the effort was abandoned for the sake of expediency. This possibility is mentioned here only to give direction for possible future work.

4.5 Summary of Methodology

The methodology to be followed to optimize the installed capacity of pumped storage is the following:

1. Create net load scenarios using fuzzy clustering techniques
2. Solve the linear program for capacity optimization and optimal operating strategies for scenarios
3. Compare costs and renewable integration with and without pumped storage

Results may be found in Chapter 7.

Chapter 5

Test System

A test system was created based upon a real island system. By using real-world data, the studies performed in this work provide insight into the challenges that are in fact encountered by system planners and operators. In this chapter, an overview of the system is provided. More complete technical details are provided in appendices.

The test system is an island system with peak system load of about 180 MW and off-peak load of about 80 MW. Energy is supplied by a combined wind-hydro-thermal system that includes several wind parks, significant hydropower generation, and two thermal generating stations. The mix of available generating capacity is shown in Table 5.1.

Table 5.1: Generating Capacity

Source	Capacity (MW)
Thermal	220
Hydro	50
Wind	60

The test system uses a transmission network comprised of 30 kV and 60 kV lines. A one-line diagram of the network is shown in Figures 5.4 and 5.5.

Figure 5.1 shows the annual evolution of load. There are clear dips in peak and average load on the weekend and holidays as well as seasonal variations. Peak and off-peak loads show seasonal variations different from one another. Figure 5.2 shows a typical weekday load diagrams while Figure 5.3 shows a typical weekend load diagram.

5.1 Diesel groups

The test system includes twenty-three diesel generating sets. These generators are an indispensable part of the energy supply of the test system, providing more than 80% of the energy required to supply load. They are dispatched as necessary to cover whatever load remains after wind and hydro power

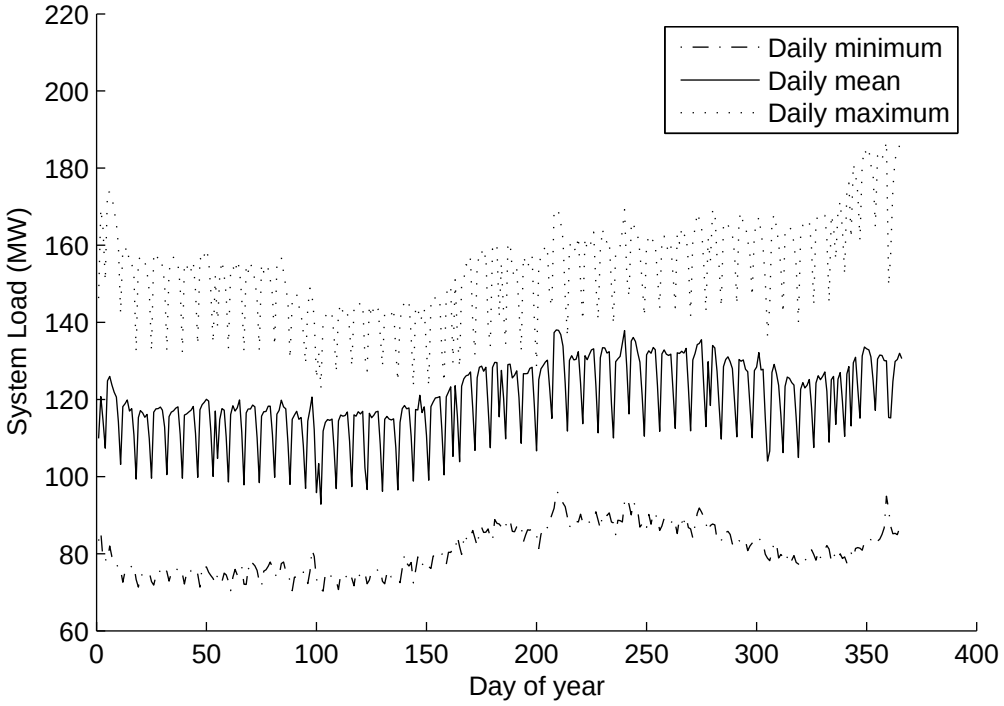

Figure 5.1: System Annual Load Evolution

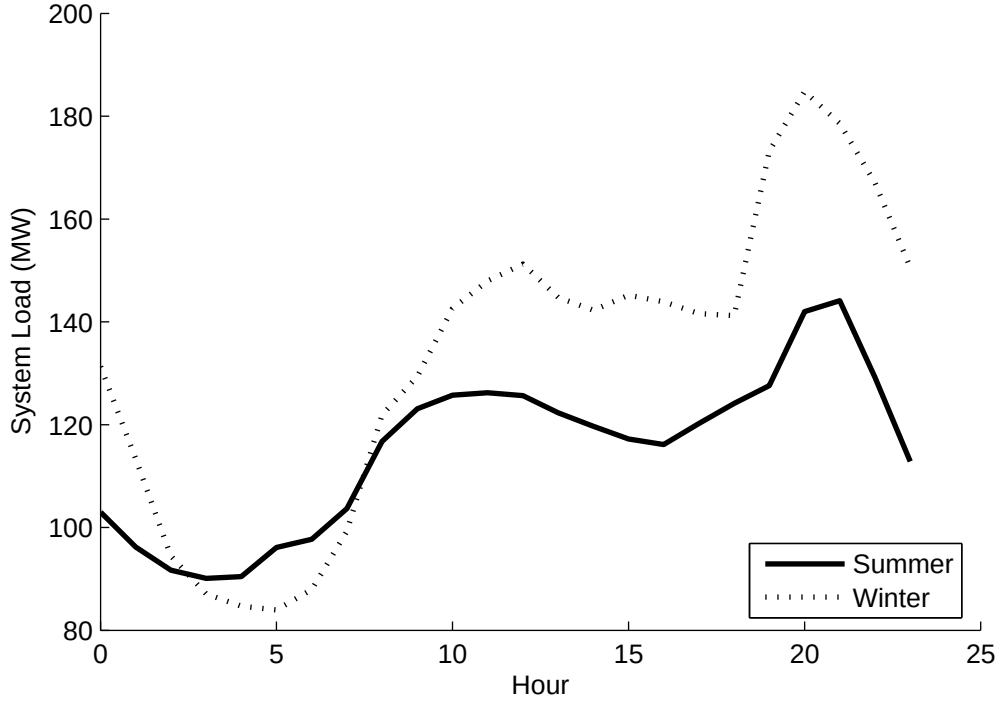

Figure 5.2: Typical Weekday Load Diagrams

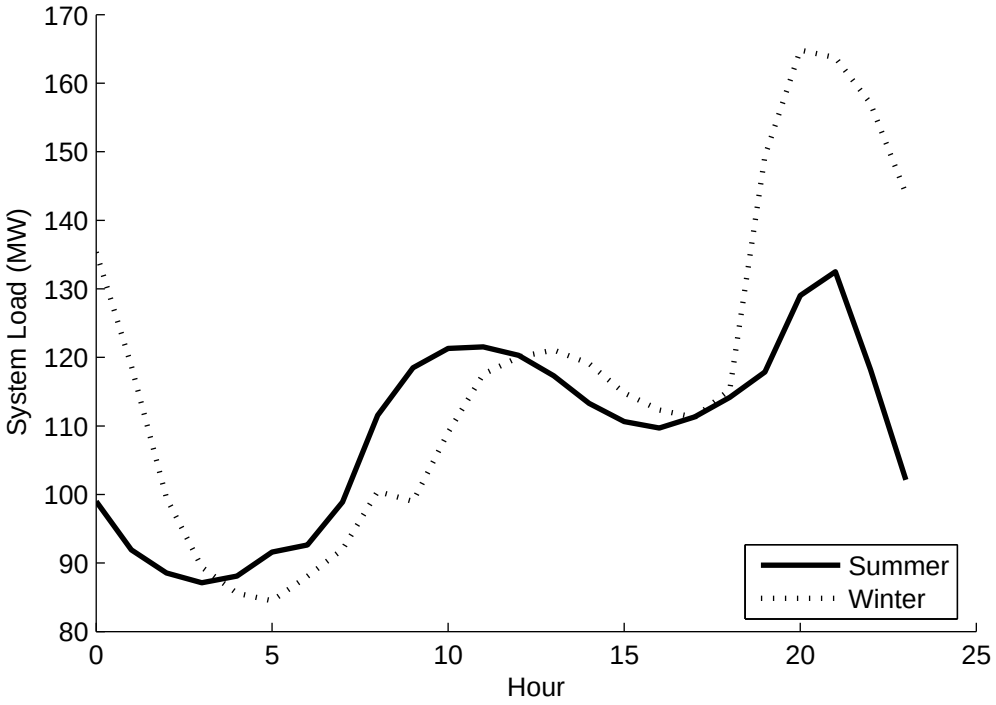

Figure 5.3: Typical Weekend Load Diagrams

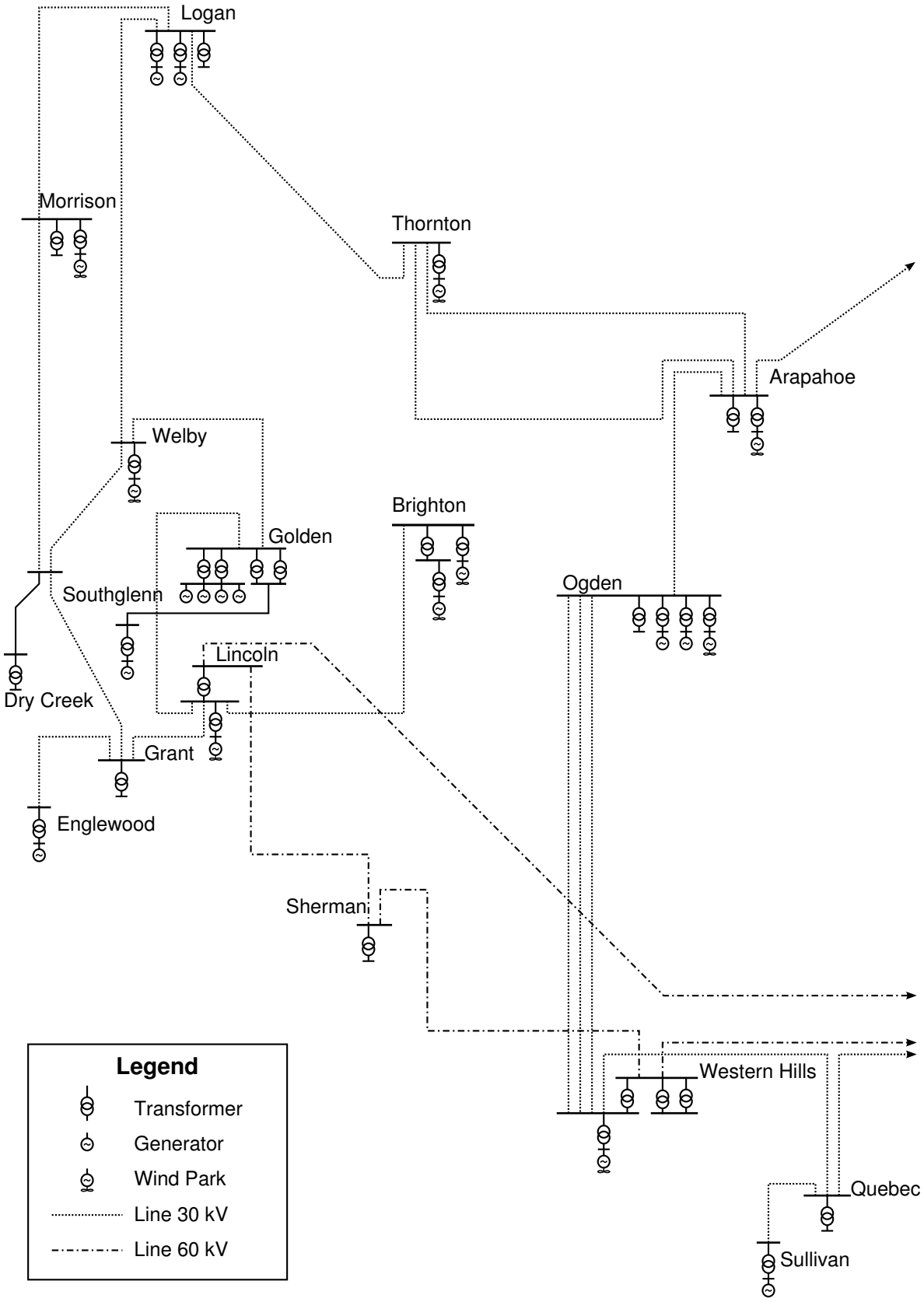

Figure 5.4: Test System Oneline Diagram (West)

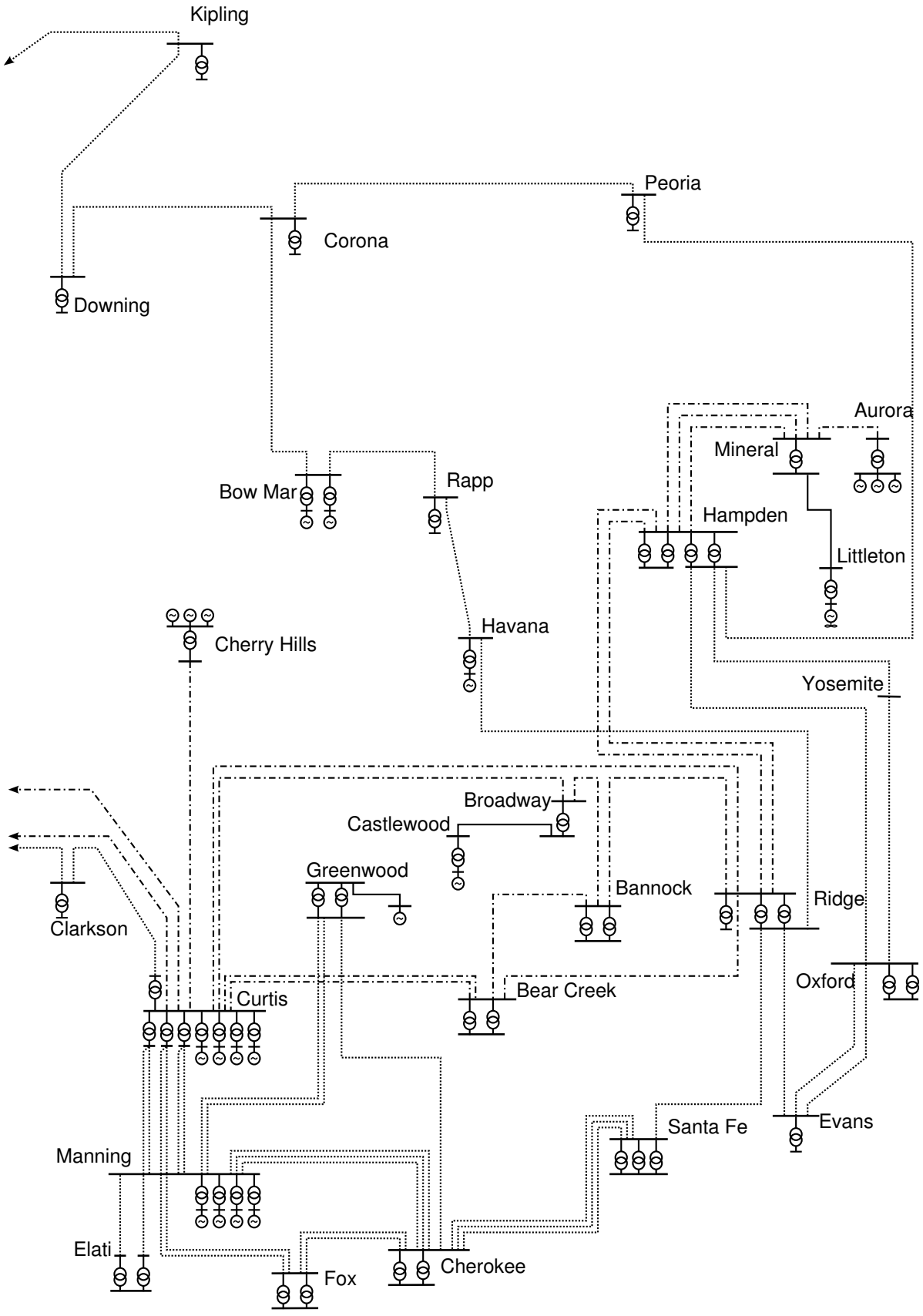

Figure 5.5: Test System Oneline Diagram (East)

contributions have been accounted for. They are also the primary element responsible for frequency regulation and load following.

The diesel groups are also primarily responsible for providing the spinning reserve requirements of the test system. That means that there must be sufficient unused capacity online to be able to cover the most extreme expected generation loss or load increase.

Diesel generating groups operate most efficiently when outputting their rated power and should not be operated below their minimum technical limit. Fuel consumption per unit of power output at minimum loading can be up to 50 % more than the fuel consumption when operating at rated power [84].

The diesel groups are located at two thermal stations. A large majority are located at the Manning Thermal Station and are interconnected at the Manning 30 kV bus or the Curtis 60 kV bus as shown in the one-line diagram in in Figure 5.5. Another three units are located on the eastern edge of the system at the Aurora Thermal Station as shown in the same figure. In order to maintain flow in the cooling systems at these stations, at least two units are always left online at the Manning station and at least one unit at the Aurora station.

The diesel generating sets are not equipped with under-frequency protection and in the case of system collapse rely on mechanical or thermal protection devices to operate or the station operator to perform manual disconnection.

5.2 Hydropower stations

The test system includes several run-of-the-river hydro and small hydro units ranging from 0.5 MW to 8 MW. The output of these units depends on rainfall and is highly seasonal. The annual cycle has a winter season of wet weather and a summer season of dry weather. Figure 5.6 shows daily peaks and averages for hydropower production over the course of a year. Very strong seasonal variations can be seen. Figure 5.7 shows the distribution of hourly hydro plant production over the period for which data is available.

The Cherry Hills Hydropower Station (see Figure 5.5 consists of three 8 MW units that have some limited storage capability and may be dispatched and participate in frequency regulation along with the diesel units. However, due to pressure effects, the hydraulic system at this station does not allow sudden changes in water flow and thus these units have been set with only loose regulation parameters.

All of the hydro units with the exception of Cherry Hills have under/over-frequency protection that disconnect them for frequency variations of greater than 0.5 Hz. They also have over/under-voltage protection set to trip for voltages above 1.2 p.u. or less than 0.8 p.u. With this kind of sensitivity, faults often lead to the tripping of hydro units in the area of the fault, or in the case of a major system event that leads to significant frequency variations, widespread tripping of the hydro units.

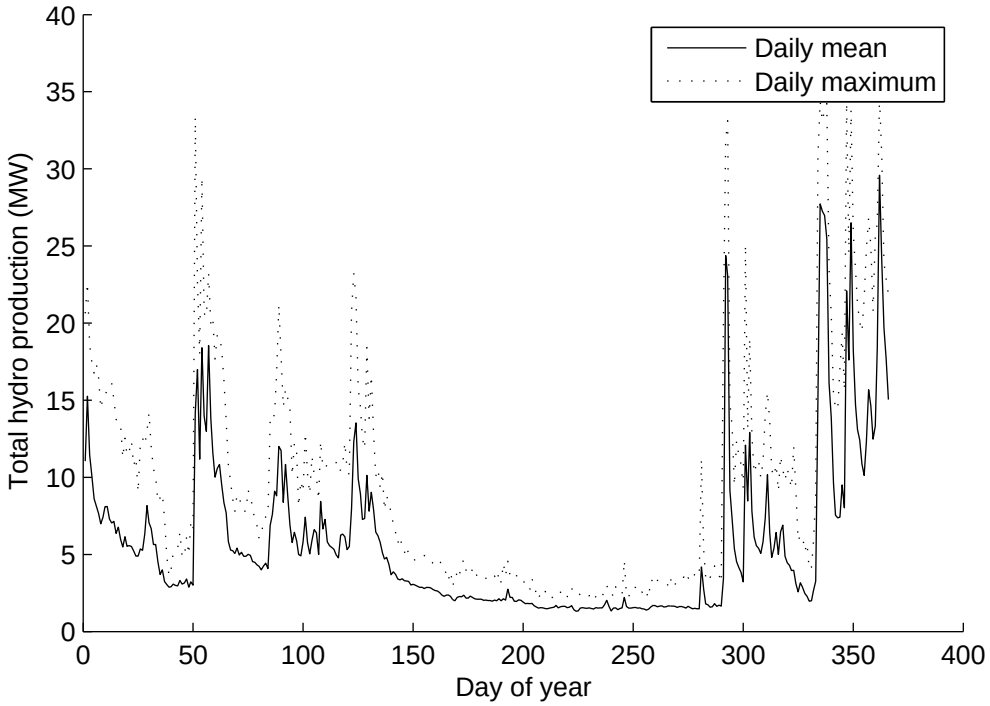

Figure 5.6: Annual Hydropower Evolution

5.3 Wind parks

The test system also includes several wind parks. Some are based on older technology and use standard asynchronous machines to inject power to the network. Most of the installed capacity, however, is based on newer double-fed induction machines. These machines have been required to include ride-through-the-fault capability as well as reactive power/voltage control. Table 5.2 lists the wind parks in the test system.

Table 5.2: Wind Parks

Interconnect Bus	Capacity (MW)	Technology
Arapahoe	6.6	DFIM
Brighton	1.8 + 2.6	Standard asynch.
Brighton	3.3 + 3.3	DFIM
Lincoln	10	DFIM
Littleton	0.9	Standard asynch.
Morrison	6	DFIM
Ogden	7.92	DFIM
Thornton	6.6	DFIM
Welby	3.3	DFIM
Western Hills	9	DFIM

One particular region of the test system island has favorable wind conditions and is far enough from the population center that extensive wind development is acceptable. Grid reinforcement has been done in this area to allow the integration of the wind parks. The interconnection points are shown in the one-line diagram of Figures 5.4 and 5.5. Nearly all the wind parks are connected in the western half of

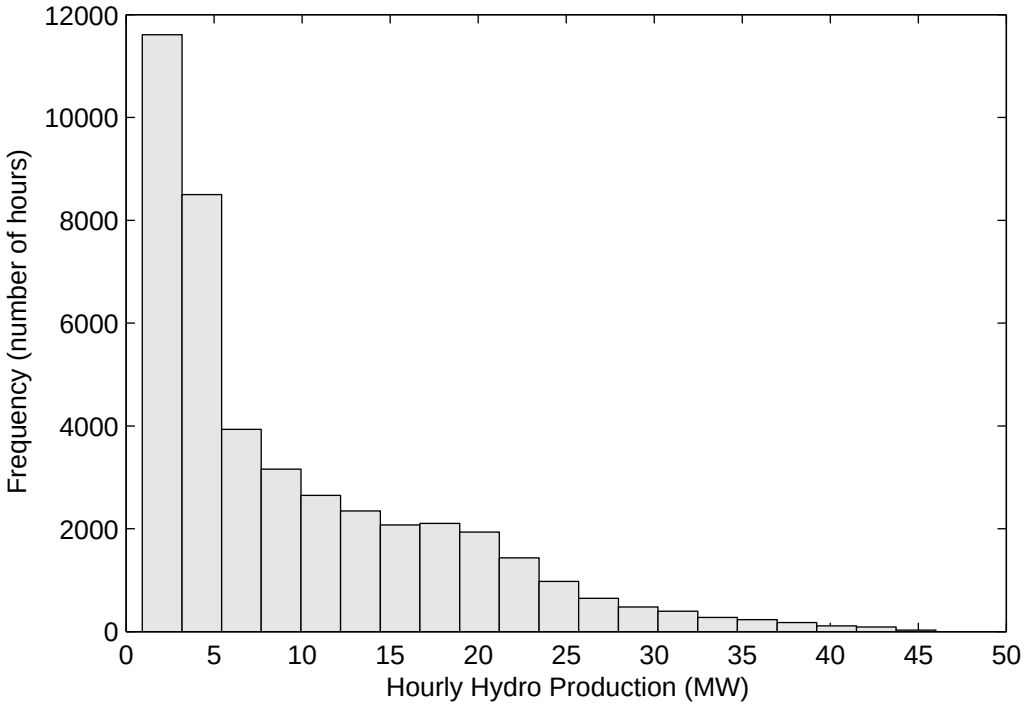

Figure 5.7: Distribution of Hourly Hydro Production

the system; only Littleton can be found in the eastern half.

Figure 5.8 shows daily peaks and averages for wind park production over the course of a year. There is some seasonality to wind park production, but it is much weaker than that of the hydro stations. Figure 5.9 shows the distribution of hourly wind park production over the years for which data is available.

5.4 Potential Pumped Storage Station

A promising location in the test system has already been identified for possible development of a pumped storage station. The area is near the hydro generation facilities at Golden and would be integrated at the same substation. There is a crater available to be used for the upper reservoir, allowing sufficient head and volume for the development of a reasonably sized storage station economically. The pumped storage station is projected to be based upon a reversible synchronous generator coupled to a reversible single-stage pump-turbine set.

5.5 Frequency Regulation Problems

Of the generators connected in the test system, only the diesel-fueled generating sets and the hydro units at Cherry Hills Station are capable of frequency regulation. Almost all of the hydropower stations are run-of-the-river and do not have the ability to adjust their output in response to system needs. A significant amount of wind power is also installed. This provides another potentially large block of power that does

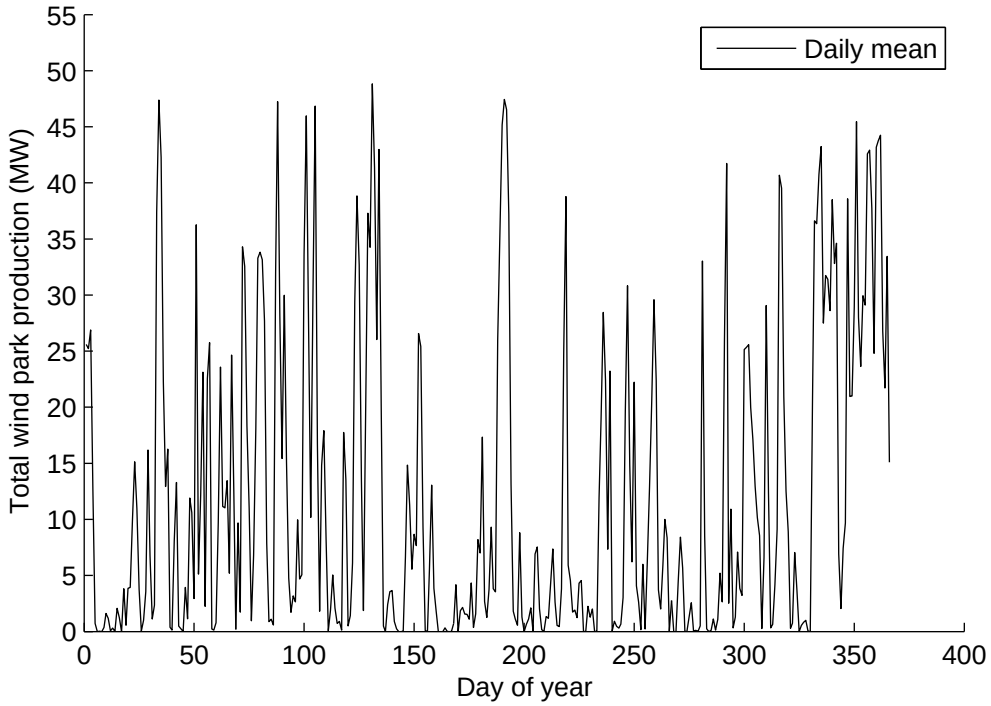

Figure 5.8: Annual Wind Park Evolution

not provide frequency regulation.

During off-peak hours the power provided by wind parks and hydro stations may at times be a large portion of the total power demand of the system. This leaves only a small amount to be carried by the diesel generating units. From an economic point of view this is good since it means that fuel is not being used to provide energy, but from the perspective of frequency regulation it is bad since it means that a relatively small number units are responsible for regulating frequency for the entire island. A small number of units means low rotating inertia, little spinning reserve, and weak response to frequency deviations.

Under these conditions, the system may exhibit frequency variations larger than desired and will be vulnerable to collapse if a major system event occurs. System collapse becomes an even more apparent threat when the voltage and frequency protection of wind and hydro generation is considered. When a major system disturbance occurs, it is likely that a large portion of the wind and hydro units will disconnect. Even when ride-through-the-fault capability is considered for the wind parks, sufficient frequency deviation will result in the disconnection of these units.

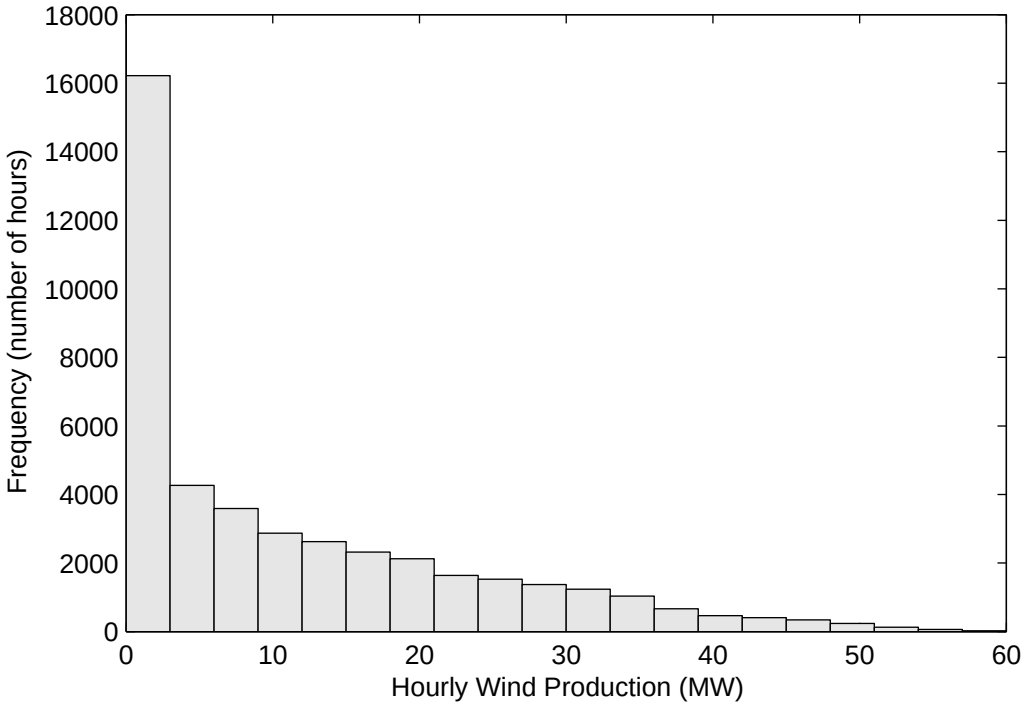

Figure 5.9: Distribution of Hourly Wind Production

Chapter 6

Dynamics Results

In this chapter, the results of the dynamic studies described in Chapter 3 are presented. First, the results of validation of the minimum frequency estimation expression is given. Following this, the results of simulations to compare the application of the new spinning reserve criteria and the inclusion of pumped storage are shown. Finally, the adequacy of the tools used will be evaluated.

6.1 Validation of Minimum Frequency Estimation

In Section 3.2 an expression for the frequency variation resulting from a load variation was developed, as expressed in (3.5). An adjustment factor a is included, the value of which must be determined by observing the behavior of the system after known disturbances.

A series of simulations were made in which all protection devices were disabled, load variations were applied, and the maximum frequency deviation recorded. The factor a was found to have typical value of 0.85. The predicted and observed minimum frequencies are shown in Table 6.1 for estimated a = 0.85 and droop r = 0.06.

In the test system used, all of the thermal generating units have similar droops (6% on active power base). The only unit that is different is the Cherry Hills generating station, which has a droop of 20%. The $r_{typical}$ is then chosen to be 0.06 and the capacity of Cherry Hills multiplied by a factor of 0.3 when included in calculations of minimum frequency regulation requirements.

With the model validated and a determined, the the criterion given in (3.6) can be evaluated for the test system using the values shown in Table 6.2. The evaluation of the criterion gives minimum frequency regulating generation online of 75.7 MW for no pumping load, 50.2 MW for 5 MW of pumped storage load, and 24.7 MW for 10 MW of pumped storage load.

Table 6.1: Simulation Results for Verification of Min. Freq Expression

P_{base}	47.9			
ΔP	4.1	8.2	12.3	16.4
Δf - observed	0.2	0.4	0.59	0.78
Δf - predicted	0.22	0.44	0.65	0.87
Δf - error	0.02	0.04	0.06	0.09
P_{base}	55.1			
ΔP	4.1	8.2	12.3	16.4
Δf - observed	0.19	0.37	0.54	0.73
Δf - predicted	0.19	0.38	0.57	0.76
Δf - error	0.00	0.01	0.03	0.03
P_{base}	60.1			
ΔP	4.1	8.2	12.3	16.4
Δf - observed	0.17	0.34	0.50	0.66
Δf - predicted	0.17	0.35	0.52	0.70
Δf - error	0.00	0.00	0.02	0.03
P_{base}	76.6			
ΔP	4.1	8.2	12.3	16.4
Δf - observed	0.14	0.27	0.41	0.54
Δf - predicted	0.14	0.27	0.41	0.55
Δf - error	0.00	0.00	0.00	0.01

Table 6.2: Parameters for Frequency Regulation Criterion

Parameter		Value
f_{base}	=	50 Hz
Δf_{max}	=	0.5 Hz
a	=	0.85
r	=	0.06
ΔP_{max}	=	11.6 MW (load carried by largest unit)
$P_{genlost}$	=	16.5 MW (capacity of largest unit)

6.2 Simulations Results

In Chapter 3, pumped storage was proposed as a means to help with the dynamic problems of the test system. An addition to the spinning reserve criteria was proposed, taking into account the need to recover system frequency without allowing it to fall to the point at which wind and hydro generation units begin to trip. Three scenarios and seven disturbances were selected to be simulated in order to compare the dynamic performance of the system with and without the suggested modifications.

The first set of simulations are made for faults in the area of the wind parks and several hydro plants. This is a concern because the application of the fault could lead to large-scale tripping of these renewable generation. If the amount of production from wind and hydro production is large, this could be a very significant loss of generation.

First, a fault on the 60 kV line from Curtis to Lincoln is considered. This is a strong fault that is felt throughout the network. The fault is applied at t=1000 s and cleared in 300 ms. Figures 6.1 and 6.2 show the fault current contribution and voltages at each end of the faulted line. Figure 6.3 shows the evolution of system frequency as a consequence of the fault.

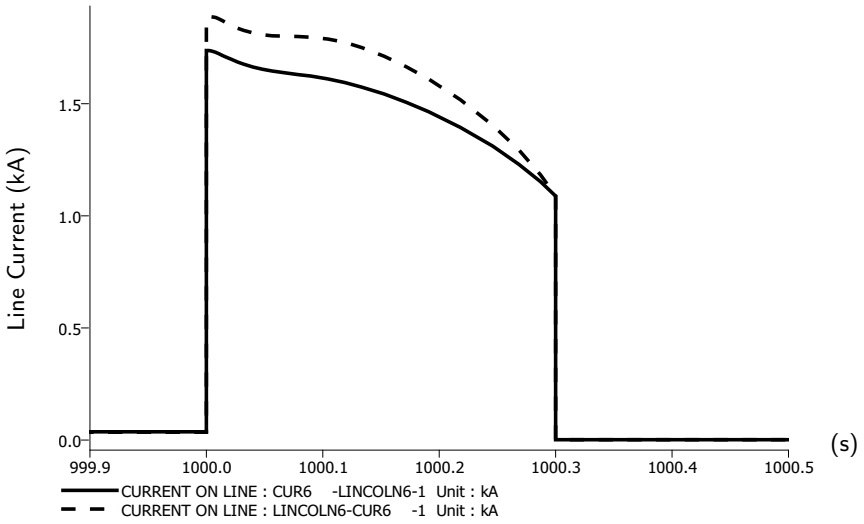

Figure 6.1: Fault on Line from Curtis to Lincoln: Current

During the fault on the Curtis-Lincoln line, system voltages are significantly depressed. This results in operation of the undervoltage protection of the run-of-river hydro plants. If these protection devices did not operate, these machines would accelerate and lose synchronism. In the scenario that includes the pumped storage unit, the pumping load is tripped shortly after the hydro plants go offline. Following the loss of the hydro plants, system frequency falls and the wind parks are lost as well. Frequency continues to fall and eventually stabilizes and recovers. In none of the scenarios does the frequency fall enough to initiate system underfrequency load shedding.

Next, a fault on the 30 kV line from Lincoln to Brighton is considered. This is not such a strong fault as the fault in the 60 kV network. Figures 6.4 and 6.5 show the fault current contribution and voltages

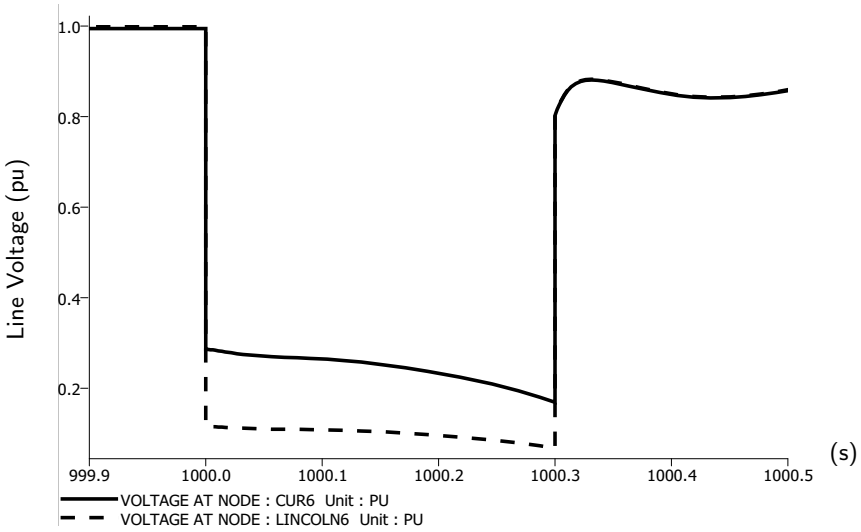

Figure 6.2: Fault on Line from Curtis to Lincoln: Voltage

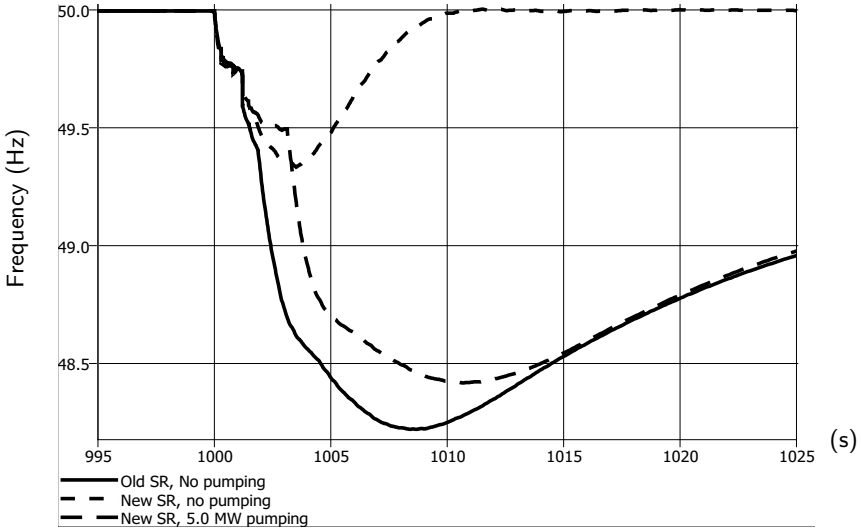

Figure 6.3: Curtis-Lincoln Fault: System Frequency Evolution

at each end of the faulted line. Figure 6.6 shows the evolution of system frequency following the fault.

The fault near Brighton results in depressed voltages in the area, leading to the tripping of the hydro units at Golden and Englewood. In the scenario in which the new spinning reserve criteria are used but there is no pumped storage load, the hydro unit Ogden trips on undervoltage as well. For this disturbance, neither the fault nor the generation loss that occurs because of it is sufficient to cause widespread tripping of renewable generation.

The next disturbance that was considered was the loss of a unit at Manning. This is the largest disturbance that is considered by the security criteria, so it is useful to see whether the system is in fact able to sustain this loss. Figure 6.7 shows system frequency following the unit trip.

In the scenario in which the old spinning reserve criteria was applied, the system frequency falls to 49.5 Hz, at which point the hydro and wind parks trip. The frequency decline continues to 48 Hz where the first stage of load shedding takes place. At 47.5 and 47 Hz the second and third system load shedding

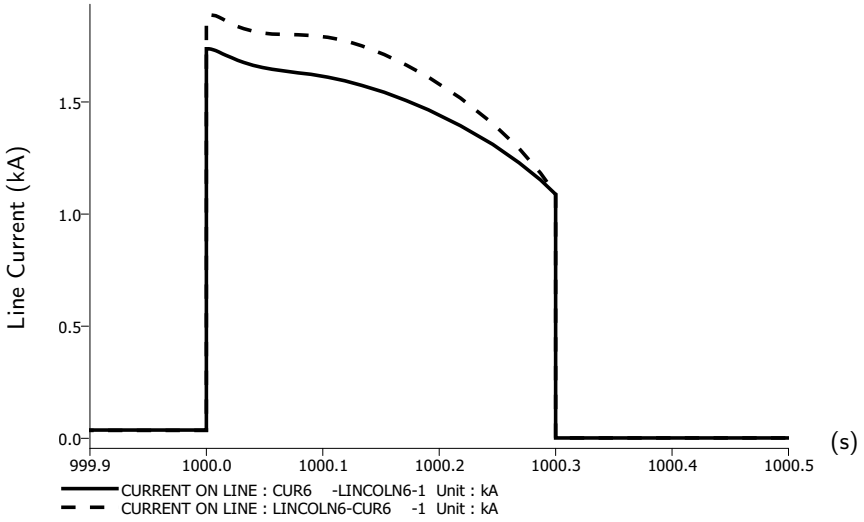

Figure 6.4: Fault on Line from Lincoln to Brighton: Current

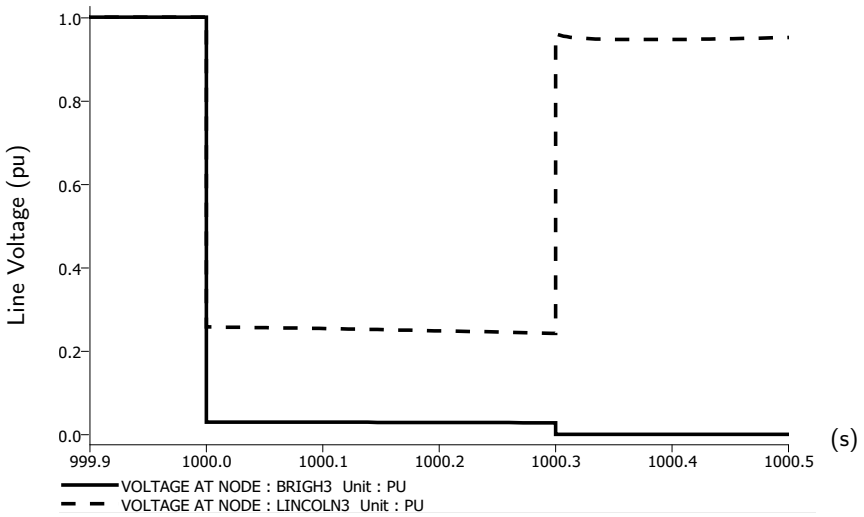

Figure 6.5: Fault on Line from Lincoln to Brighton: Voltage

steps are activated, but the system frequency continues to fall, leading eventually to complete collapse.

The last set of simulations that were performed were a set of nearly instantaneous load increases. Although these do not represent real load behavior, they are useful for showing the dynamic behavior of the system for disturbances of increasing magnitude. Figure 6.8 shows the system frequency following increasingly severe load steps for the scenario in which only the existing spinning reserve criteria is applied. Figure 6.9 shows the system frequency following the same load steps for the scenario in which the modification to the security criteria is adopted but no pumped storage is operating. Finally, Figure 6.10 shows the system frequency for the same step in load when the modification to security criteria is used and 5 MW of pumped storage is online.

The load step simulations for the scenario in which only the old spinning reserve criteria is used show clearly the divergence in system reponse when the frequency reaches the point at which hydro and wind generation trips. For the first three load steps, of 5%, 10%, and 15%, the minimum frequency is above

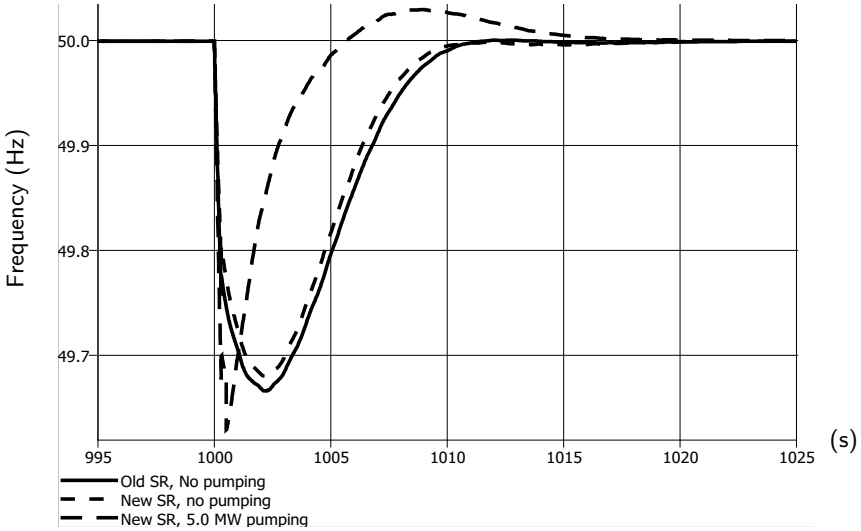

Figure 6.6: Lincoln-Brighton Fault: System Frequency Evolution

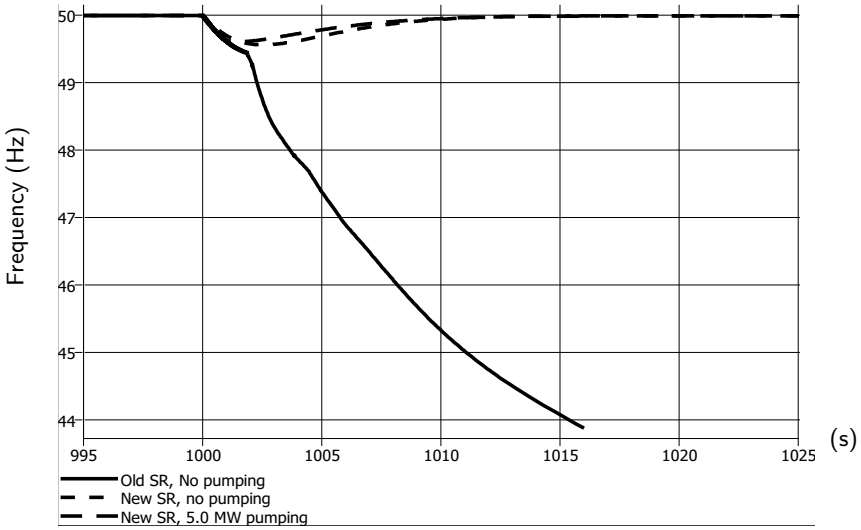

Figure 6.7: Manning Unit Trip: System Frequency Evolution

49.5 Hz and the system recovers without the operation of any protetive devices. In the fourth load step disturbance, of 20%, the frequency reaches 49.5 Hz and the hydro and wind generation trips, all three load shedding steps are activated, and the system collapses.

In the scenario in which the new spinning reserve criteria are applied but in which there is no pumped storage load, the system does not reach load shedding for any of the load step sizes. In the largest step, there is a visible downturn in the system frequency when it falls to 49.5 Hz and the wind and hydro plants trip, but since in this scenario the production of these units is limited, the impact of this loss is not very large.

When the new spinning reserve criteria is used and 5 MW of pumped storage load is considered, the system is again able to support all four load steps without the occurrence of system underfrequency load shedding. For the load increases of 10, 15, and 20 percent, shedding of the pumped storage load is activated. This slows or reverses the frequency decline and avoids any protection device actions.

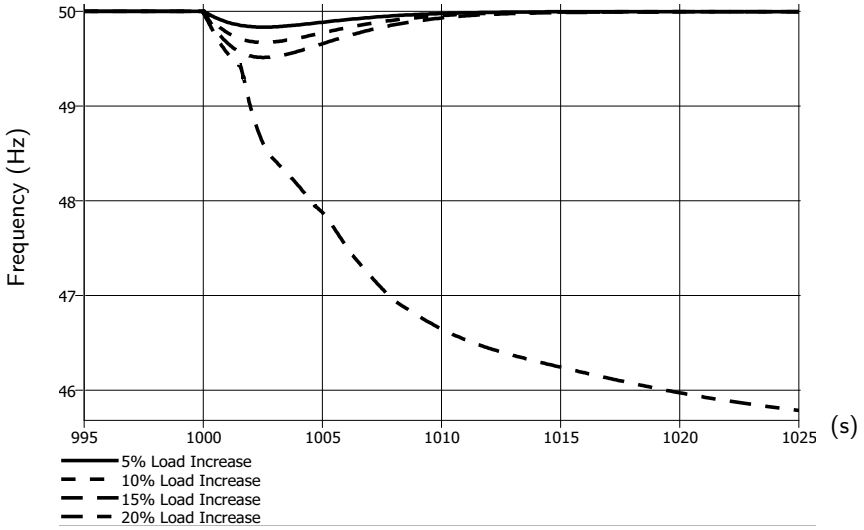

Figure 6.8: Load steps: Frequency Evolution (Old SR criteria only)

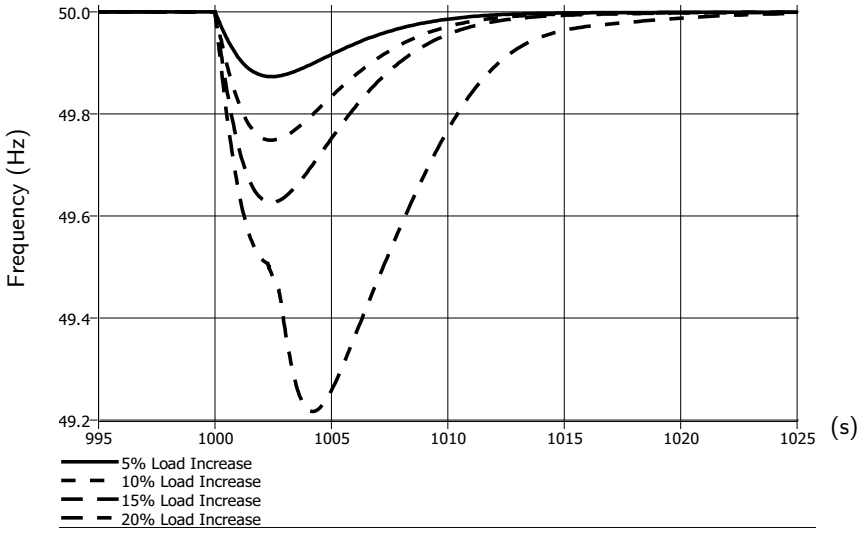

Figure 6.9: Load steps: Frequency Evolution (New SR, no pumping)

From these simulations, it is clear that the new spinning reserve criteria has a positive effect on the security of system operation. Of the disturbances that were simulated, system collapse occurred two of them when only the old spinning reserve criteria was used. The application of the new spinning reserve criteria requires the unit commitment to include adequate frequency-regulating capability, and in these most severe cases, system collapse is avoided.

Comparing the three scenarios, the scenario in which only the old spinning reserve criteria was applied and the scenario with the new spinning reserve criteria and 5 MW of pumped storage result in the same amount of renewable generation being admitted. However, when only the old spinning reserve criteria is applied, the system does not operate as securely as in the latter case.

Thus, the work done reveals two effects:

- Applying the new spinning reserve criteria improves the security of system operation but reduces the amount of renewable generation that may be integrated

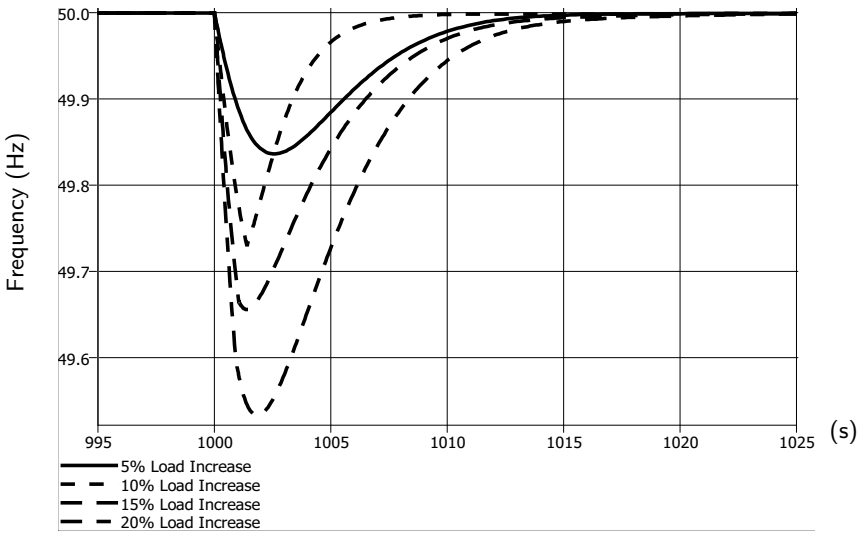

Figure 6.10: Load steps: Frequency Evolution (New SR, 5 MW pumping)

- Adding pumped storage in conjunction with the new spinning reserve criteria maintains system security while allowing more renewable generation to be integrated

6.3 Adequacy of Tools

Based on the work done, the EuroSTAG platform was well suited for the simulations performed. Standard models were available for the electrical machines and macroblock modeling enabled the development of the additional controllers and simplified wind park model. The EuroSTAG post-processing module allows macros for the figures, so after making a new simulation run it is simple to generate new figures. Since all the input files are in plain text format, it is possible to take advantage of the copy/paste and comparison features of a text editor to develop the scenarios and verify that everything is consistent within all the necessary files, while for more complex elements a graphical interface is still available for setting parameters. A Windows batch script was used to automate the simulation process, a measure that reduced the time and effort of making minor changes and re-running all the scenarios.

Chapter 7

Optimization Results

7.1 Scenario Selection

Section 4.4.2 describes how fuzzy clustering was to be applied to produce scenarios for the storage capacity optimization problem. The results of applying these steps is described in this section.

First was to be chosen the number of clusters. FCM clustering was applied partition the data into two to twenty clusters. Table 7.1 shows the validation indices calculated for these cluster sets.

Table 7.1: Validation Indices for Various Numbers of Clusters

c	PC min	PE max	S*1000 min	XB min
2	0.8031	0.3252	0.0035	10.4974
3	0.7055	0.5285	0.0045	6.6886
4	0.6234	0.7077	0.0035	5.7243
5	0.5571	0.8632	0.0036	4.1908
6	0.5060	0.9960	0.0033	5.1192
7	0.4618	1.1166	0.0033	3.2631
8	0.4331	1.2131	0.0031	3.0341
9	0.4138	1.2904	0.0031	3.8863
10	0.3985	1.3615	0.0032	2.8366
11	0.3908	1.4123	0.0031	2.7643
12	0.3744	1.4812	0.0031	2.4630
13	**0.3658**	**1.5229**	**0.0030**	**2.3342**
14	0.3540	1.5763	0.0030	3.0536
15	0.3404	1.6303	0.0029	2.2534
16	0.3293	1.6824	0.0030	3.1128
17	0.3203	1.7293	0.0029	2.5349
18	**0.3089**	**1.7797**	**0.0030**	**1.7215**
19	0.3043	1.8095	0.0028	1.8010
20	0.2996	1.8433	0.0028	2.0597

Note that of the four indices calculated, PC and PE monotonically increase or decrease in the direction of improving index values and S is nearly so. If the data exhibited clear clusters, it would be expected that the value would get worse when too many clusters are used.

Only the XB index shows significant variation, and it indicates that good cluster numbers in this range are 13 or 18. Thirteen clusters is chosen. The thirteen resulting scenarios for net load diagrams ($Load - Hydro - Wind$) are shown in Figure 7.1 with their probabilities listed in Table 7.2. As described in Section 4.4.2 the probabilities of the scenarios have been calculated by summing the membership values of all data points to each cluster and dividing by the number of datapoints. The net load diagrams assigned to each cluster are shown in Figures 7.2 to 7.14 with diagrams with strong membership values in darker gray and the scenario prototype shown in solid black. The clustering seems to have produced quite good results as the net load diagrams assigned to each cluster generally follow the shape of the prototype diagram quite well. The squeezing effect of scaling the off-peak net load values is visible in the clusters as the variation among the net load diagrams assigned to each cluster is smaller during off-peak hours than it is in intermediate and peak periods.

Once the scenario prototypes have been determined, the data is formatted for inclusion in the data section of the LP model. Each net load cluster defines an operational scenario for which the optimal pumping/generating schedule is determined.

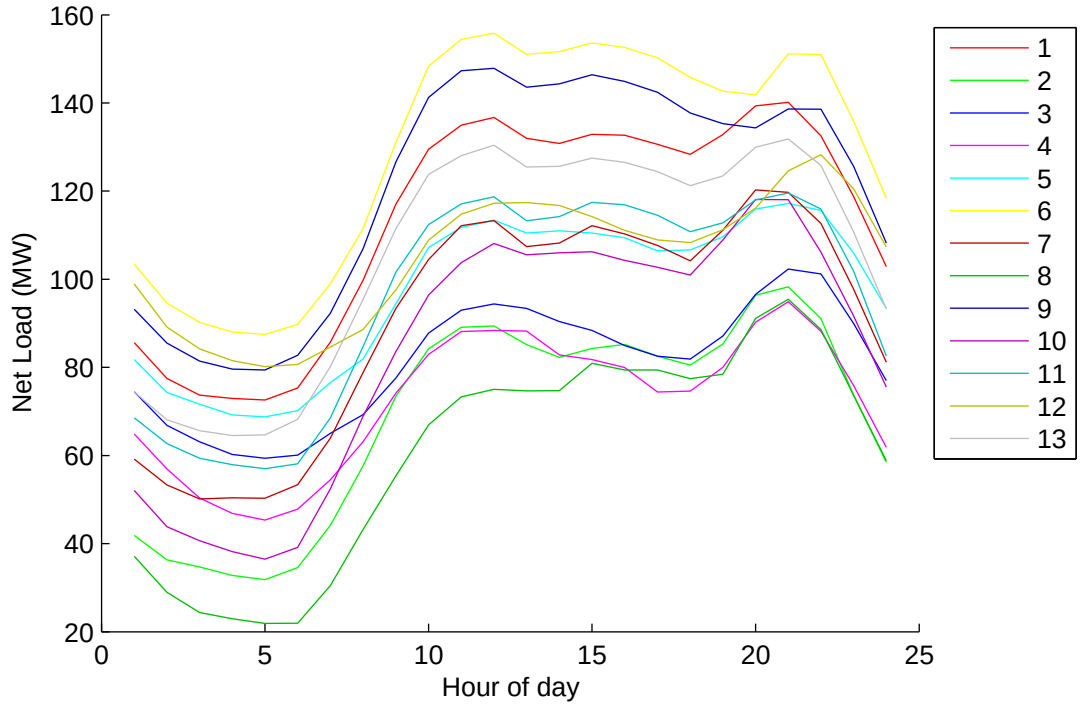

Figure 7.1: Clustering Results: Net Load Scenarios

Table 7.2: Scenario Probabilities

n	Probability
1	0.107
2	0.049
3	0.070
4	0.060
5	0.083
6	0.083
7	0.080
8	0.031
9	0.110
10	0.058
11	0.092
12	0.076
13	0.102

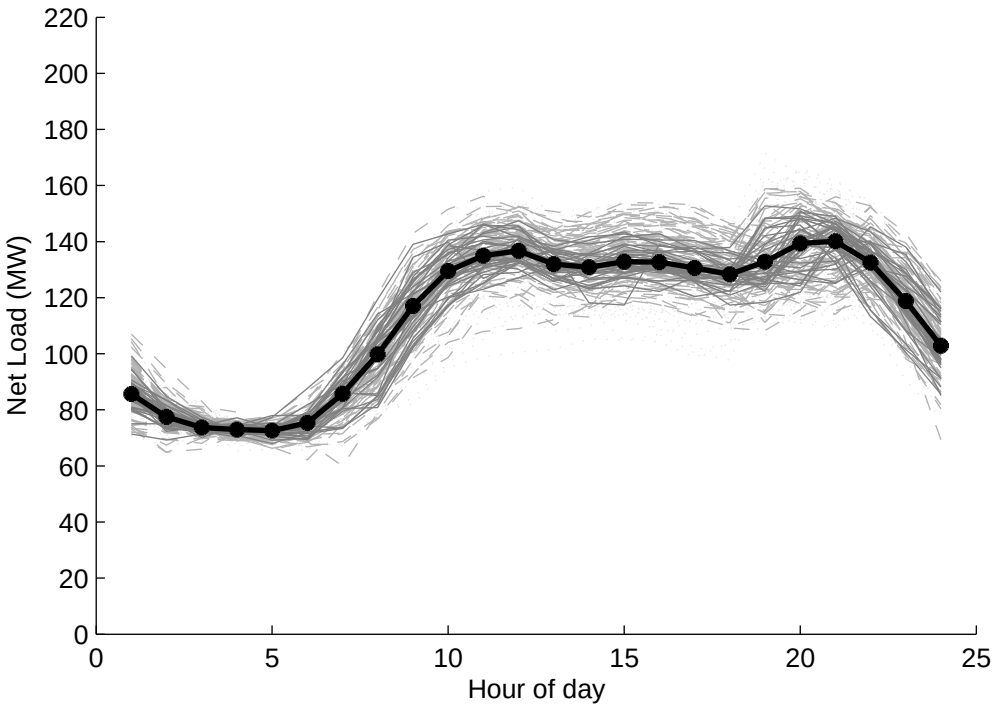

Figure 7.2: Clustering Results: Cluster 1

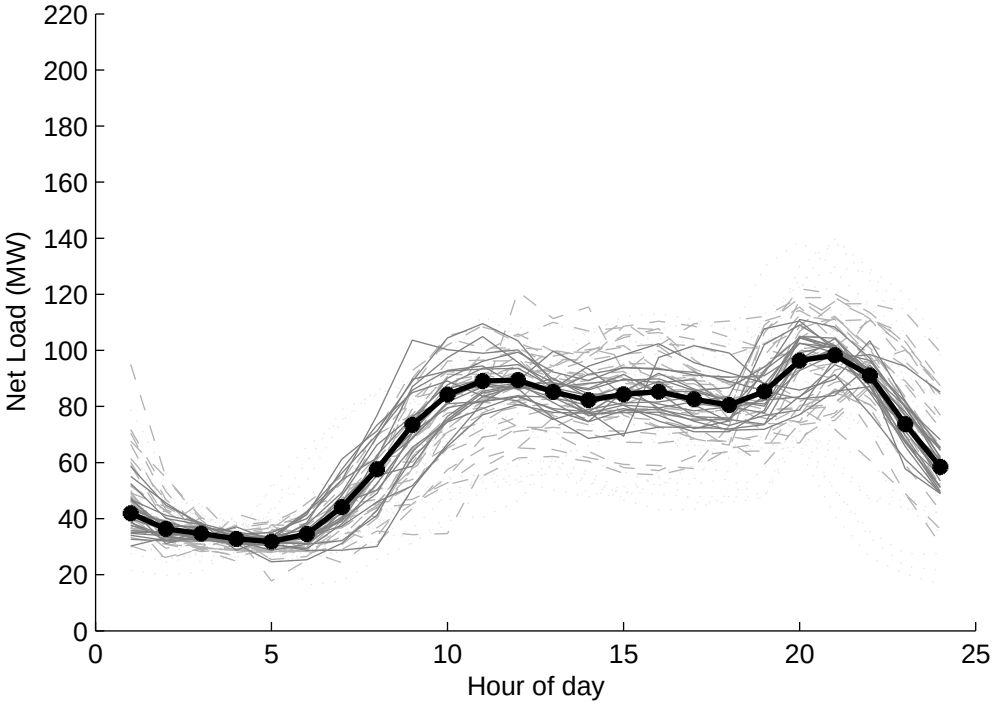

Figure 7.3: Clustering Results: Cluster 2

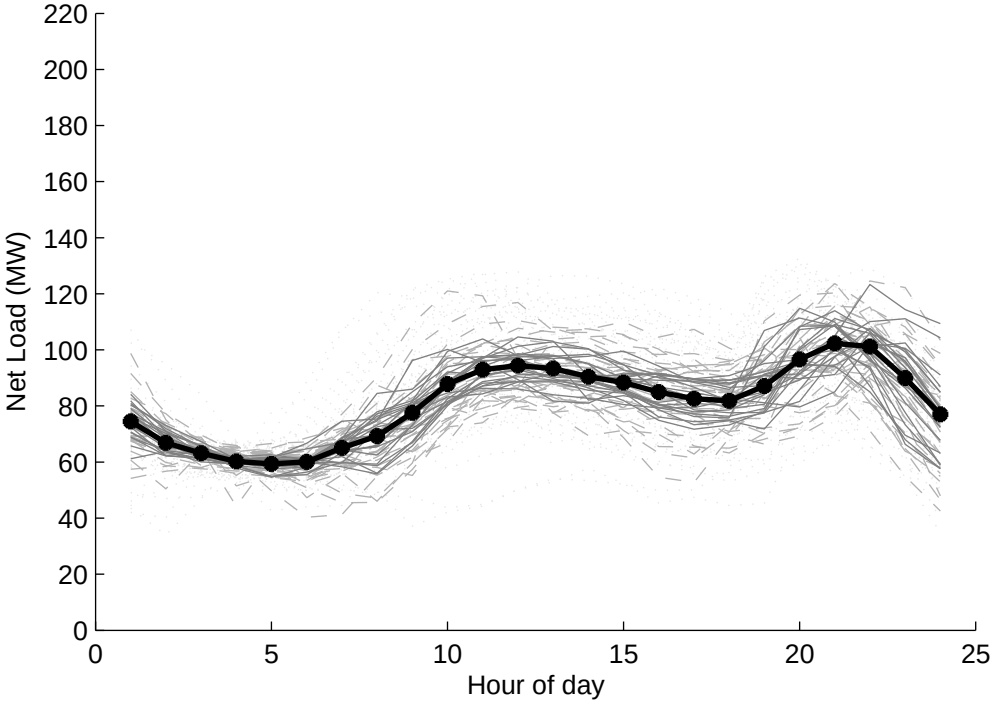

Figure 7.4: Clustering Results: Cluster 3

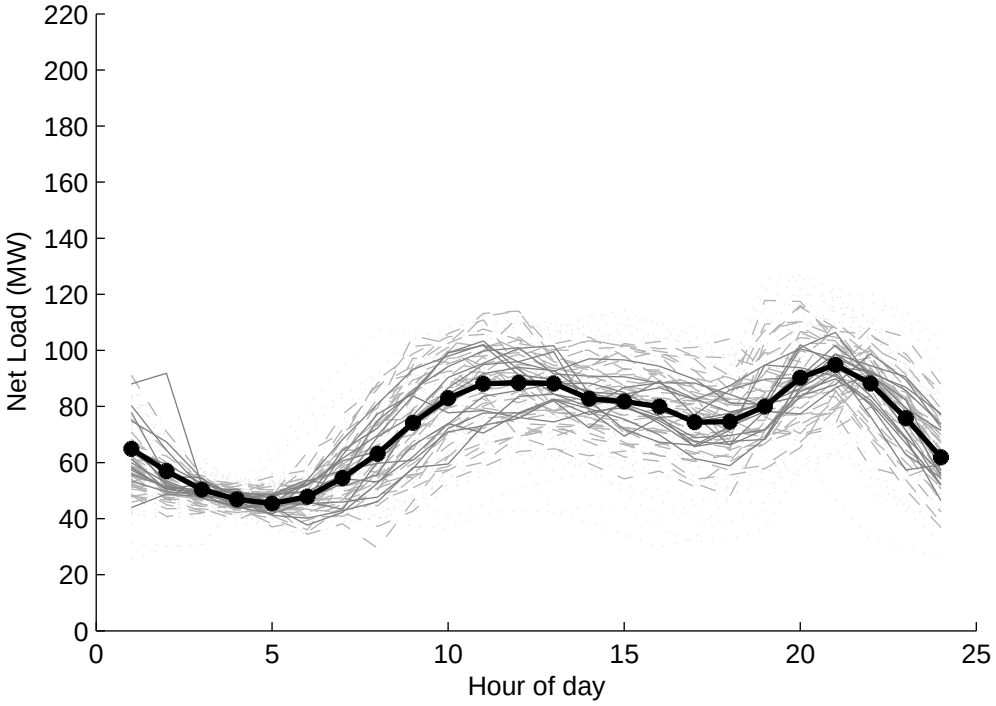

Figure 7.5: Clustering Results: Cluster 4

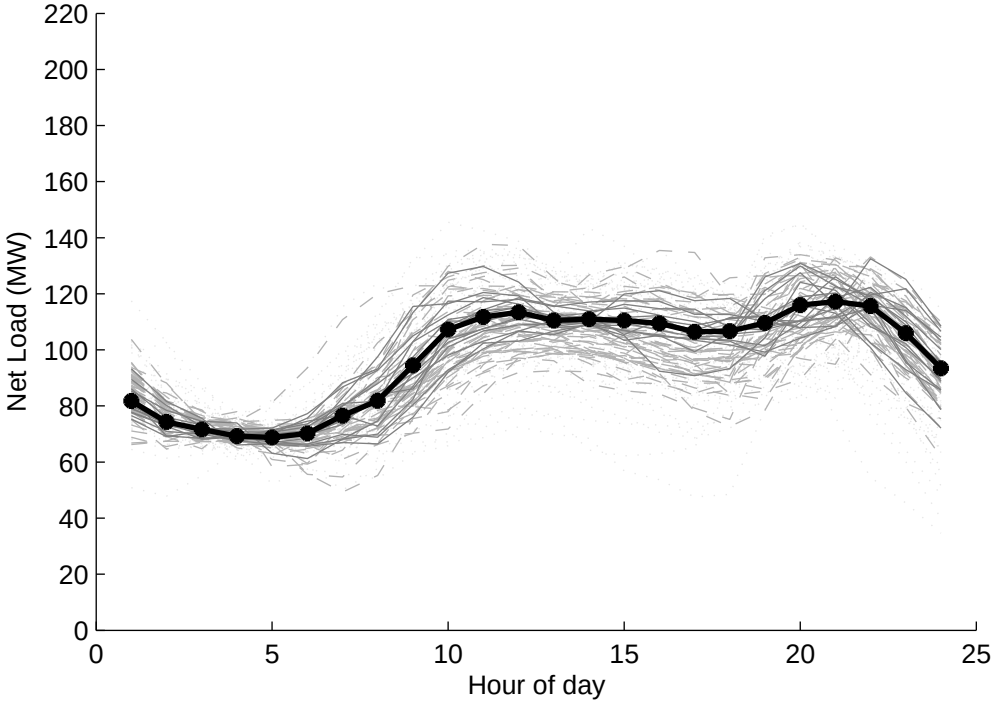

Figure 7.6: Clustering Results: Cluster 5

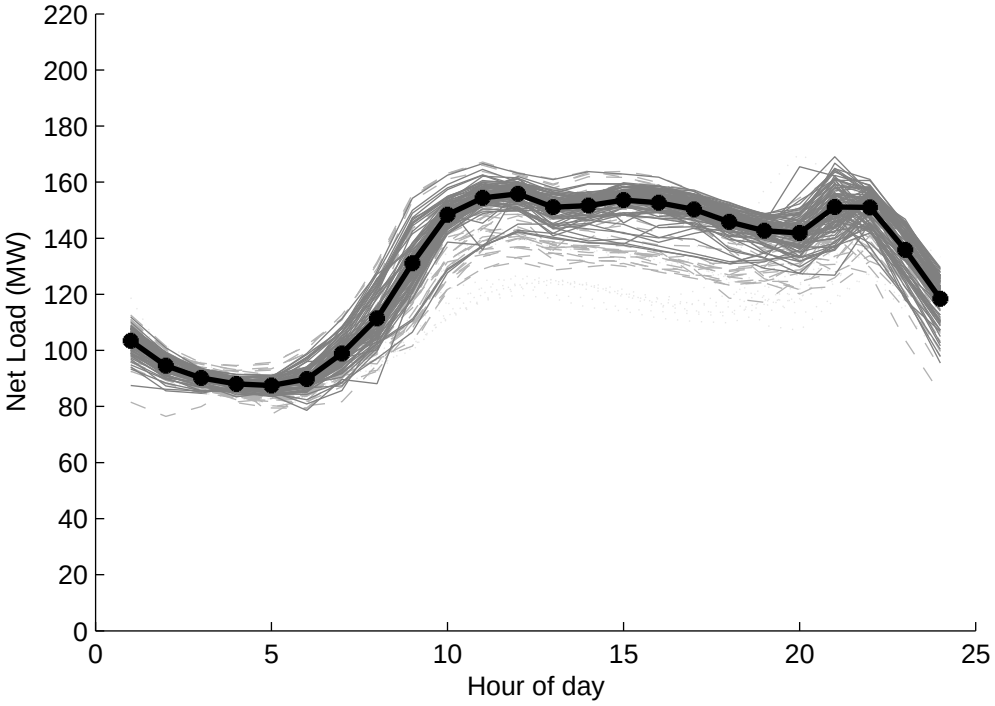

Figure 7.7: Clustering Results: Cluster 6

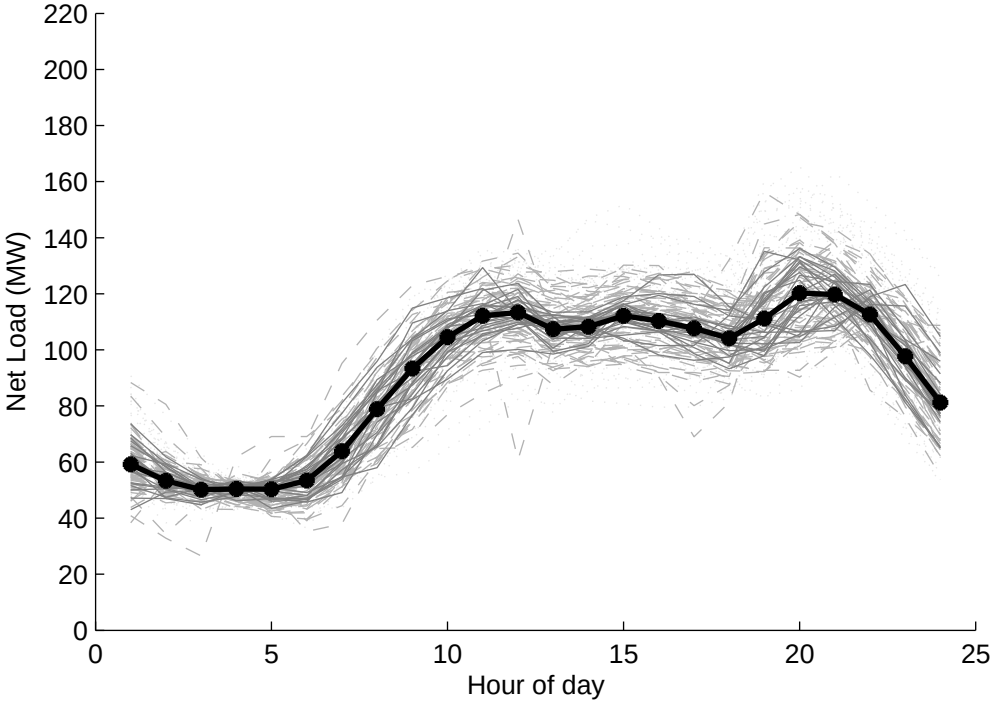

Figure 7.8: Clustering Results: Cluster 7

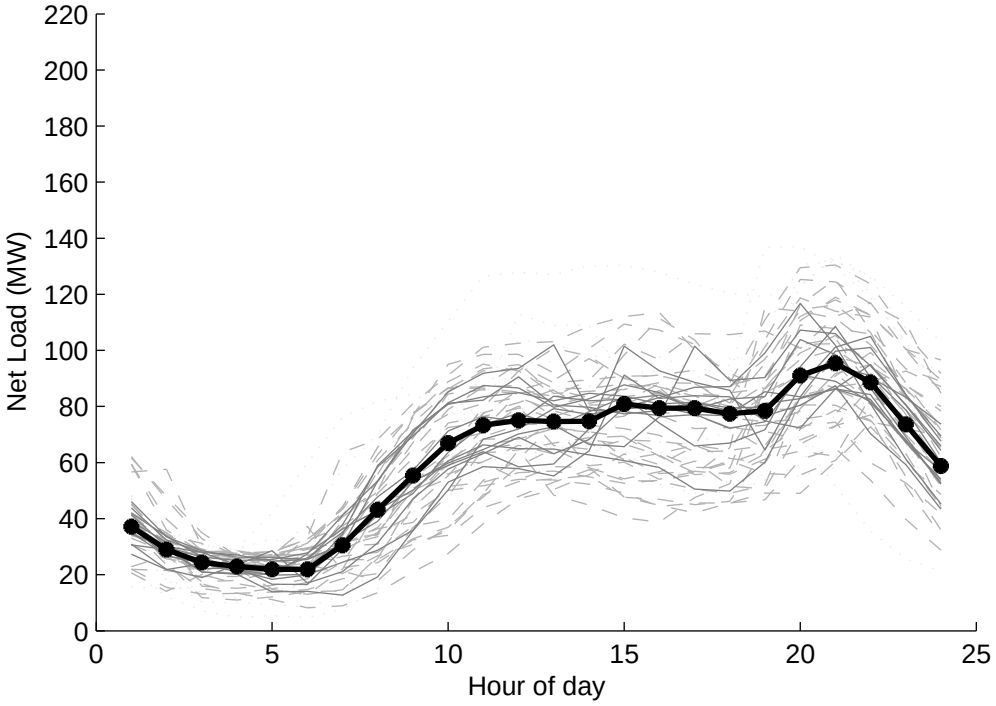

Figure 7.9: Clustering Results: Cluster 8

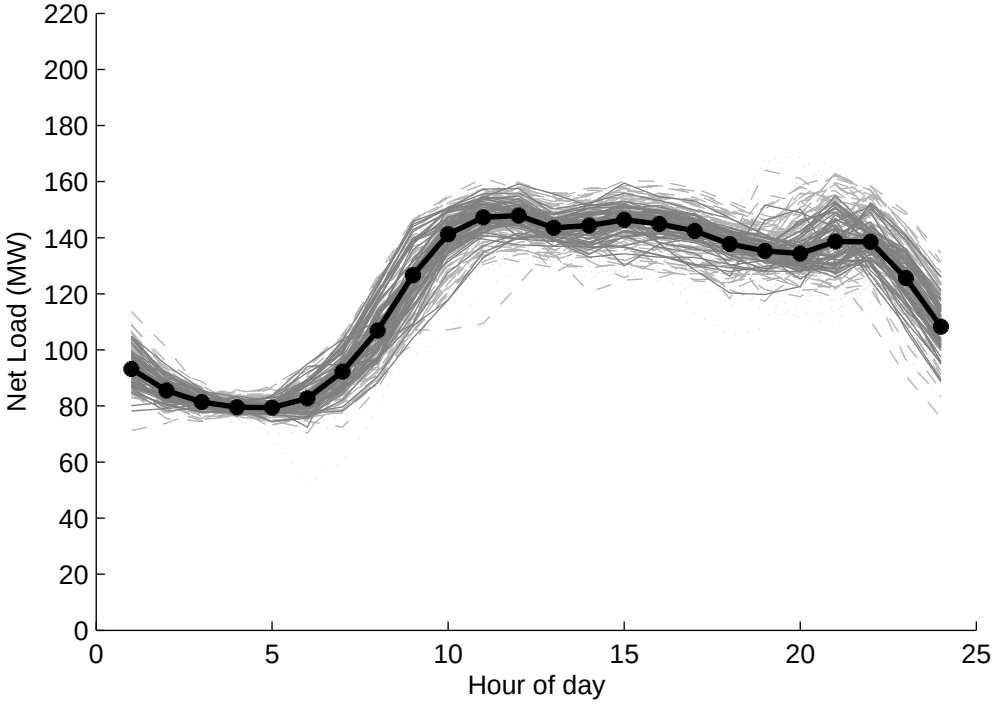

Figure 7.10: Clustering Results: Cluster 9

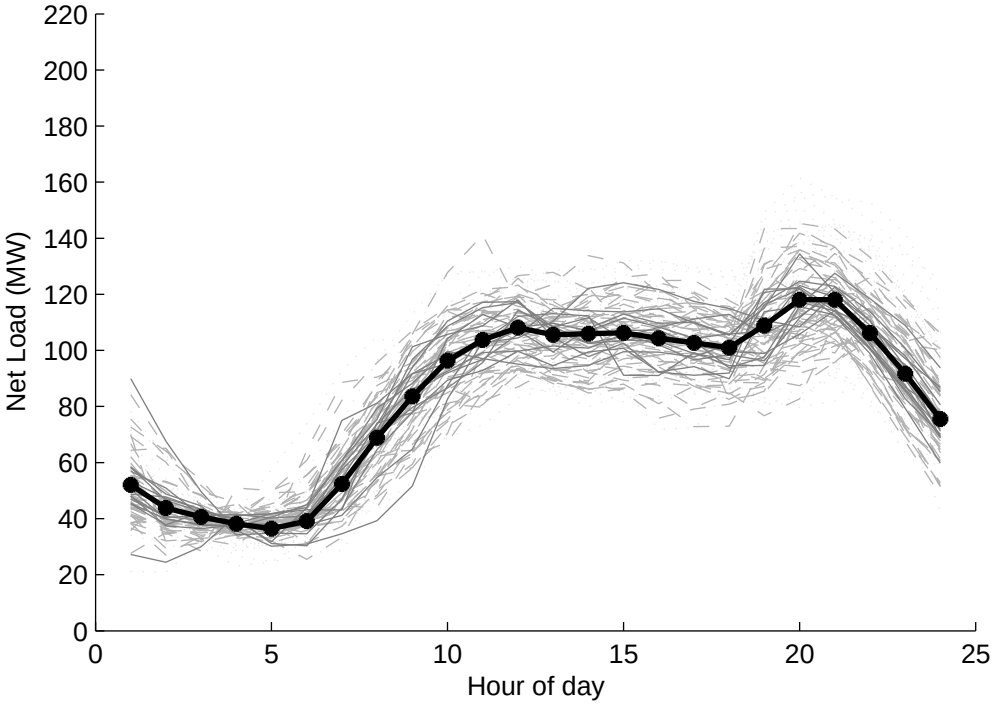

Figure 7.11: Clustering Results: Cluster 10

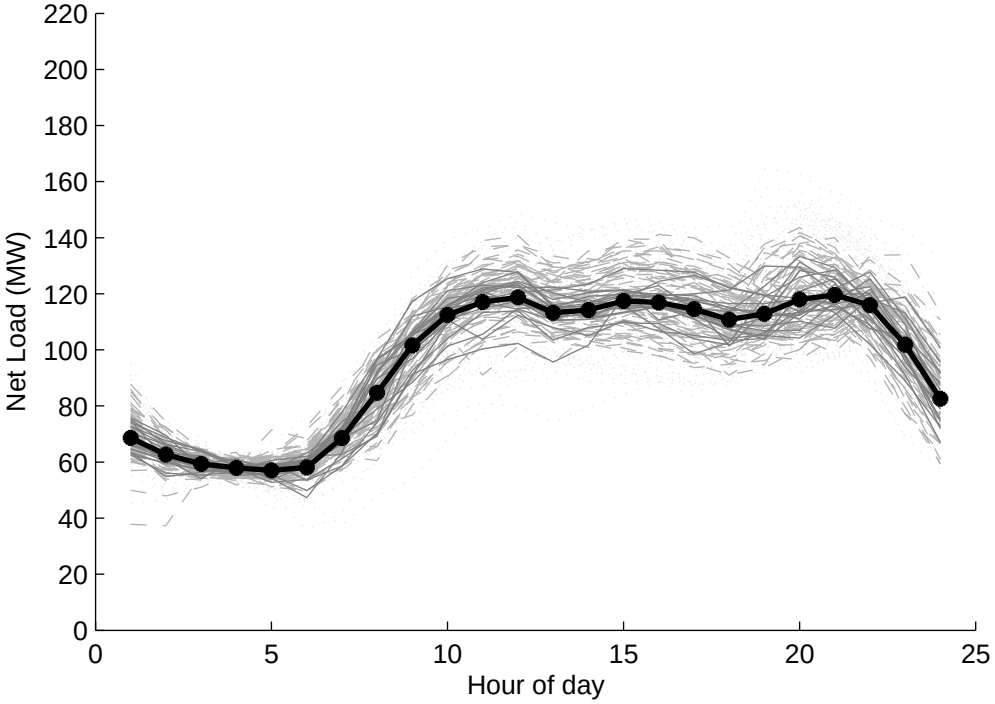

Figure 7.12: Clustering Results: Cluster 11

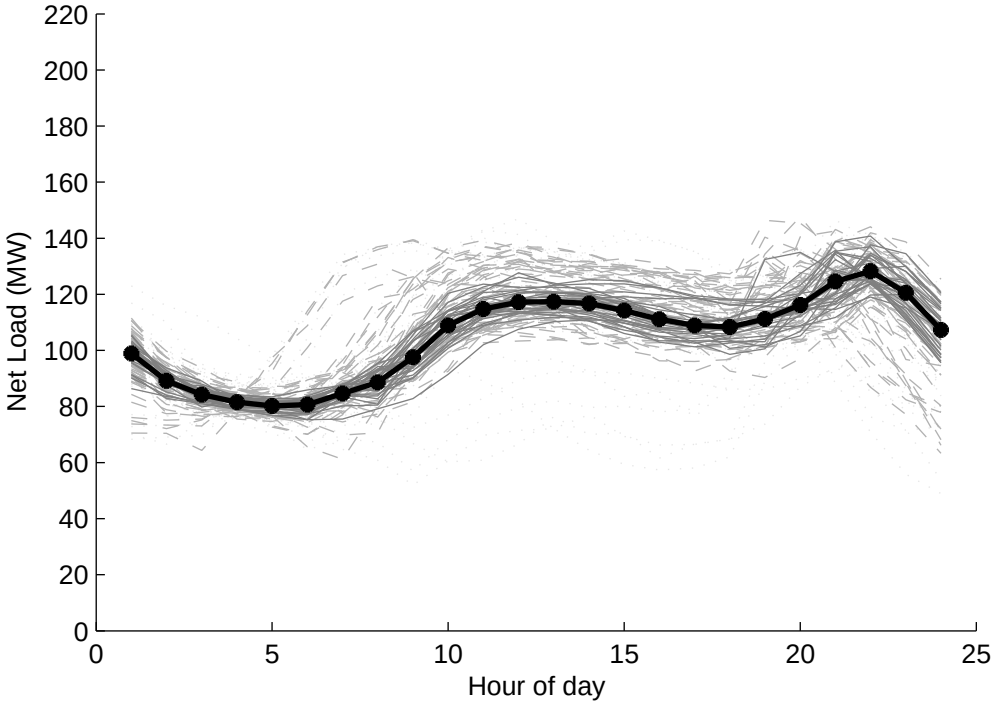

Figure 7.13: Clustering Results: Cluster 12

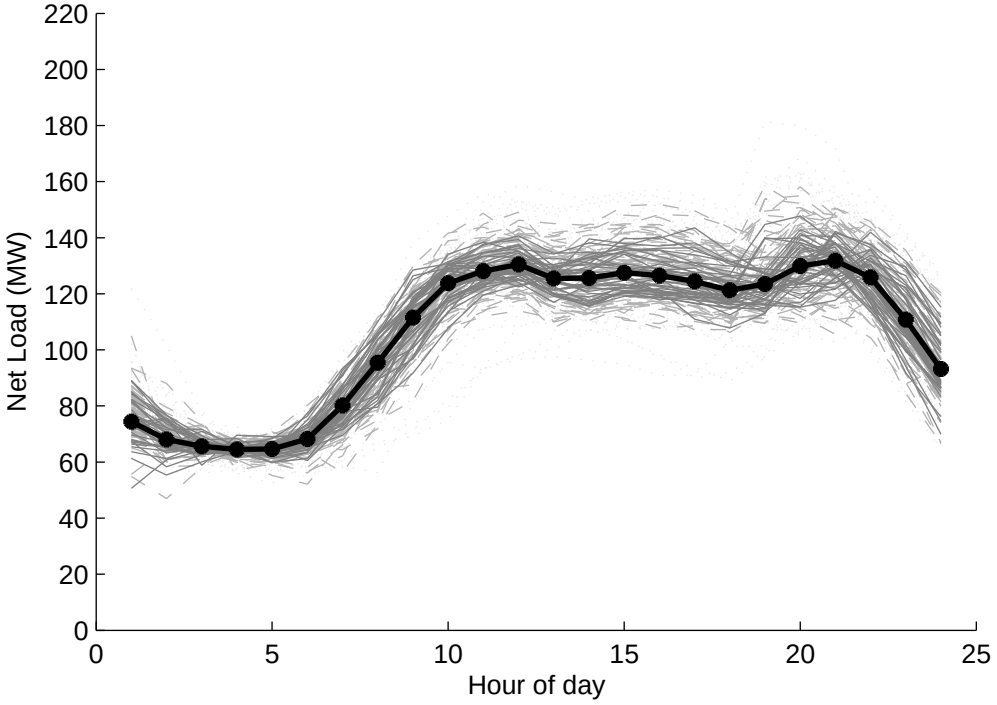

Figure 7.14: Clustering Results: Cluster 13

7.2 Results

The primary solution results obtained from the solution of the optimization problem defined by (4.1) are the values for the capacity of the pumped storage station and the amount of energy that can be stored. These results are shown in Table 7.3.

Table 7.3: Optimal Storage Capacity

Limit	Value
P_{max}	10.9 MW
E_{max}	80.2 MWh

This gives a total project cost of 5.07 million EUR, which is divided as 3.96 million for the power capacity and 1.11 million for the reservoir storage capacity. Amortized over a 30-year equipment lifespan, this gives 881 EUR per day. The expected fuel cost savings from using the pumped storage plant is 1363 EUR per day, or 0.6% of the total fuel cost. The expected average daily curtailment of renewable generation is reduced from 25.8 MWh to 10.2 MWh.

The optimal operation strategy for each scenario is shown in Figures 7.15 to 7.27. The results are generally intuitive: the large increase in the marginal cost of thermal generation occurs at 90 MW. The results show the pumped storage station in pumping mode for net load less than 90 MW and in generating mode for net load greater than 90 MW.

As an illustrative example, consider Scenario 1, results shown in Figure 7.15. During off-peak hours, the net load is below the cost breakpoint at 90 MW and the storage station operates at full pumping power. As the net load rises through the morning, the pumped storage station is switched off. When the load reaches the peak that is sustained throughout the day, the storage station enters into service in generating mode and shaves the peaks off of the net load giving thermal generation production that is nearly constant for a period of twelve hours. The daily peak is reduced by about 10 MW, the generating capacity of the pumped storage station.

It should be noted that the solution shown in the figures is not necessarily unique. Since the cost of thermal generation is represented by a piecewise linear function, there may be (and often are) several time periods that all have the same marginal cost and there is no economic preference to use pumped storage in one period rather than another. Several small breakpoints in the cost function (see Table 4.1) reduce this effect. The use of the simplex algorithm to solve the problem results in solutions that tend to lie on extreme points of either not generating or pumping at all during a period or generating or pumping at the upper limit. An interior-point algorithm would not necessarily show this same behavior.

Scenarios 2, 4, 8, and 10 show some interesting behavior. These are four scenarios in which there is a large amount of wind and hydro power available during off-peak hours. For reasons of dynamic security, the system is not able to accept all of this generation. With the pumped storage unit pumping and available to be tripped early in the case of an underfrequency event, more of the wind and hydro

power is able to be accepted than would be the case without it.

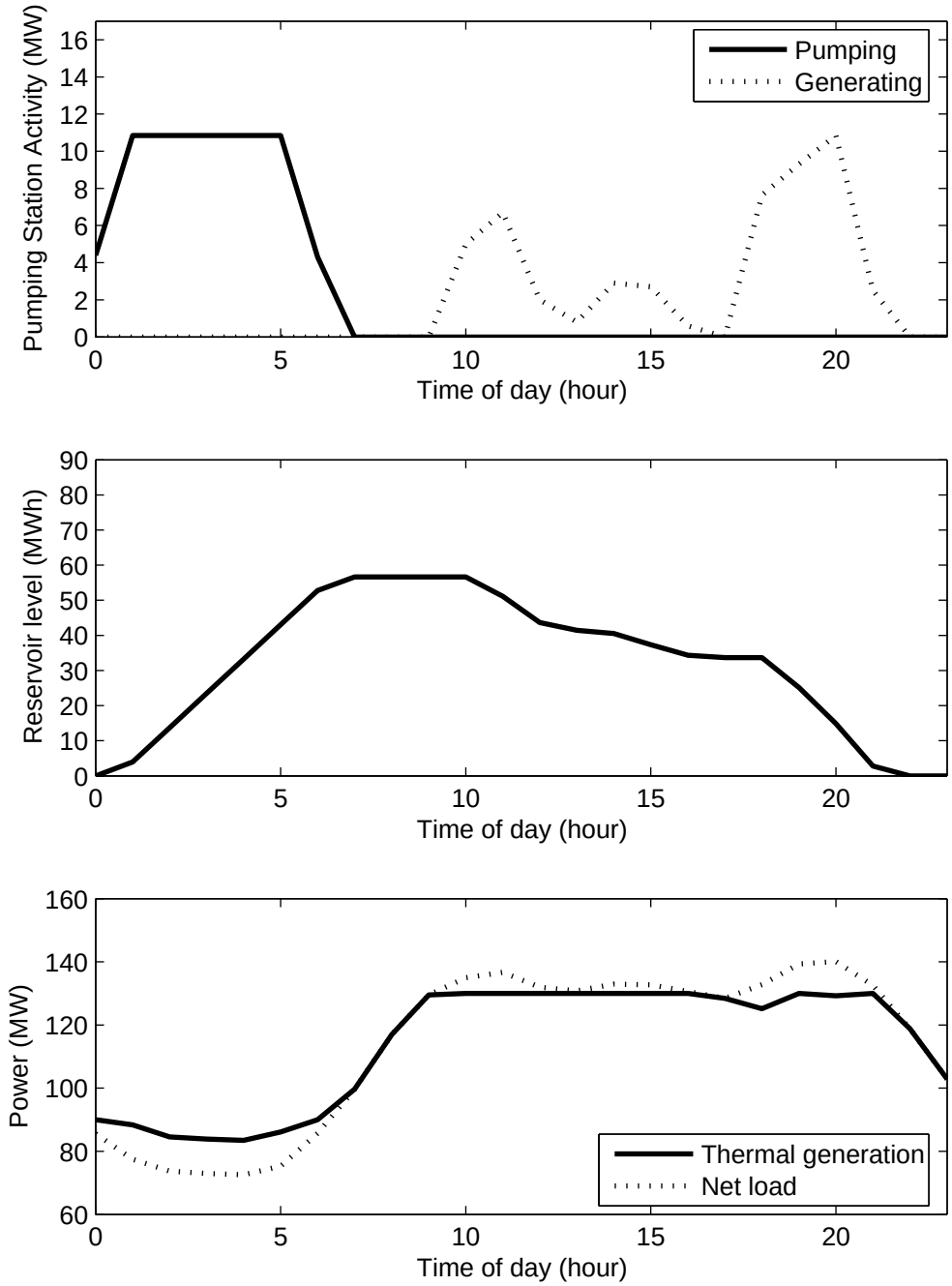

Figure 7.15: Optimization Results: Scenario 1

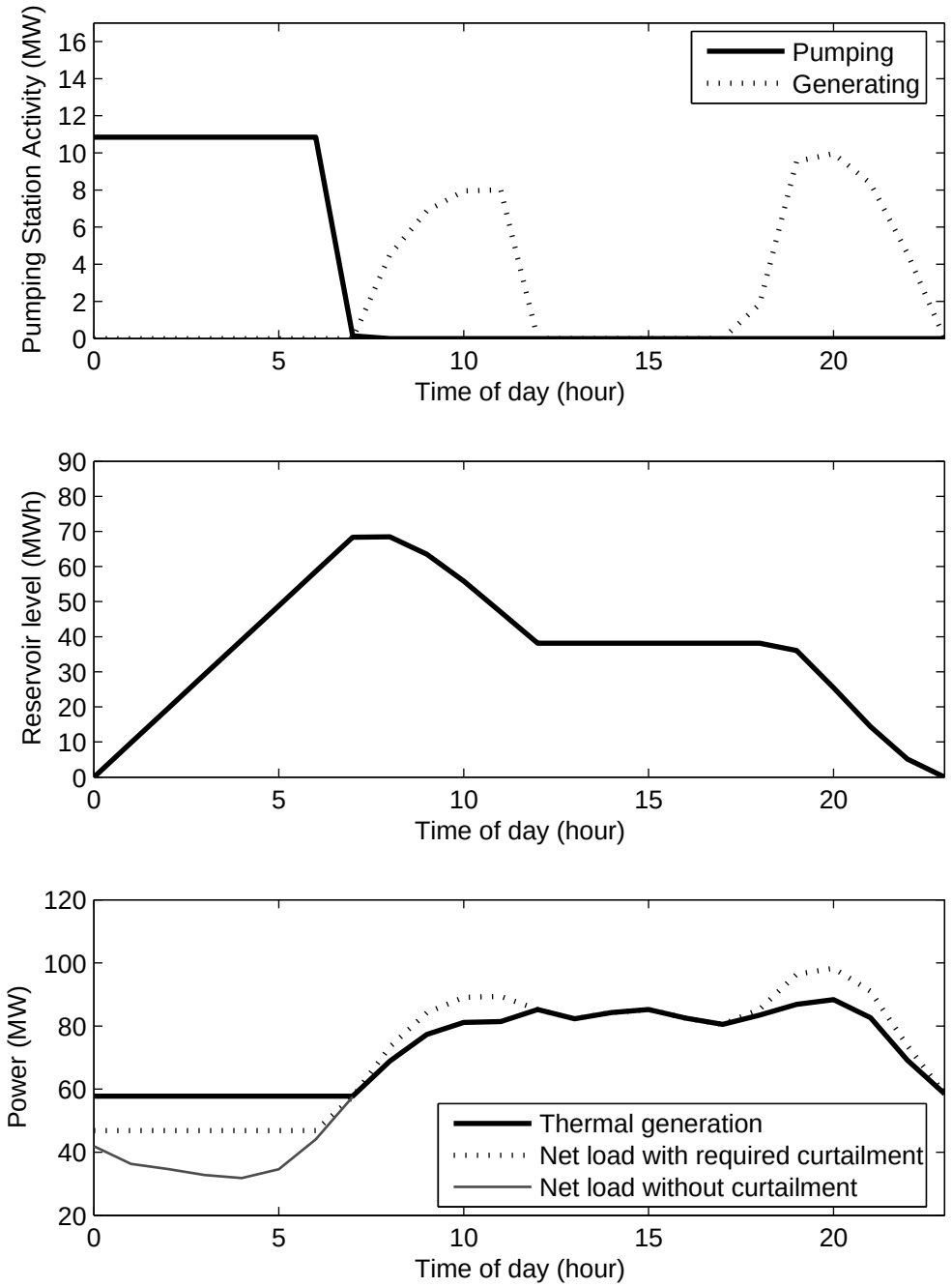

Figure 7.16: Optimization Results: Scenario 2

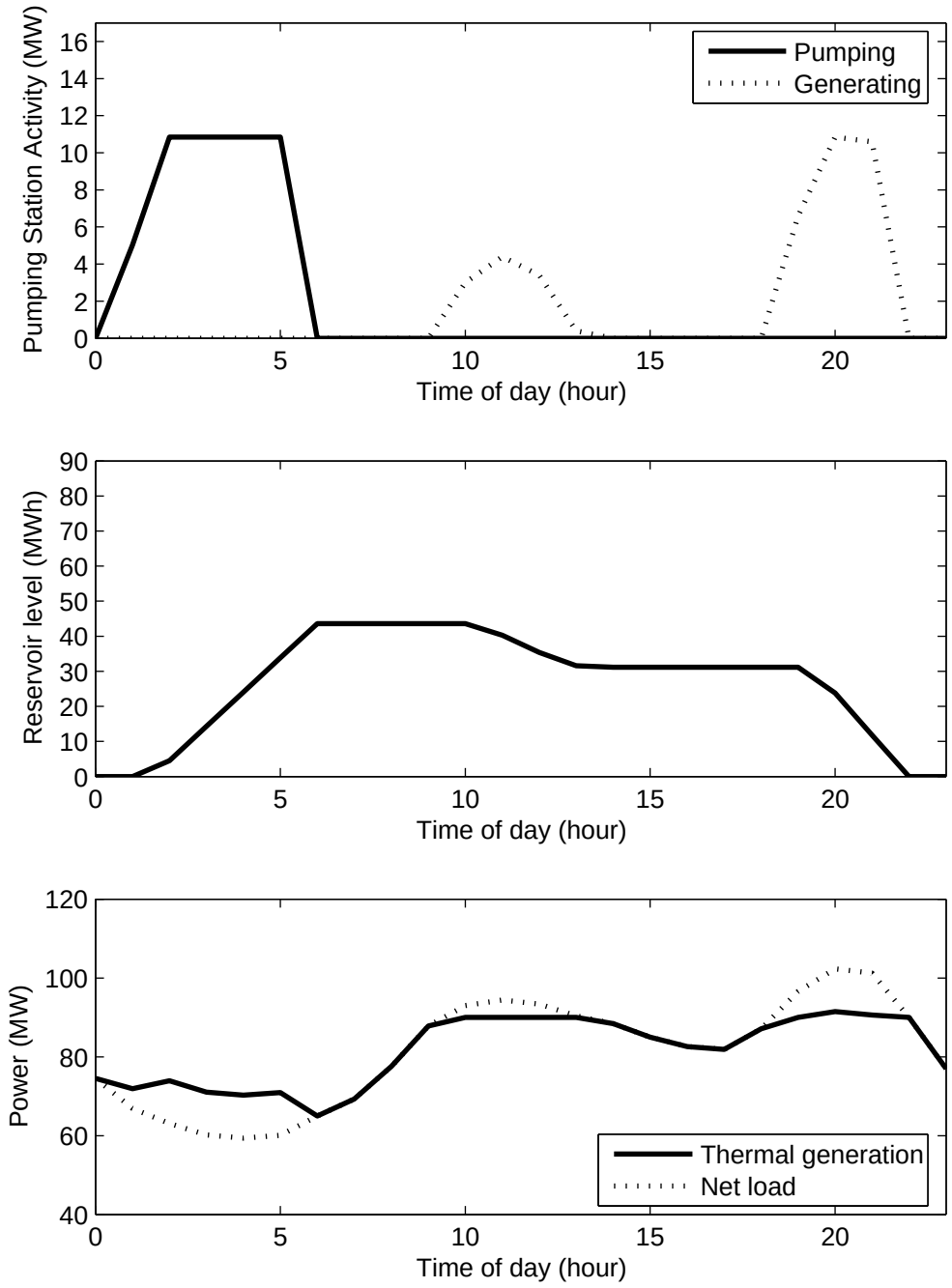

Figure 7.17: Optimization Results: Scenario 3

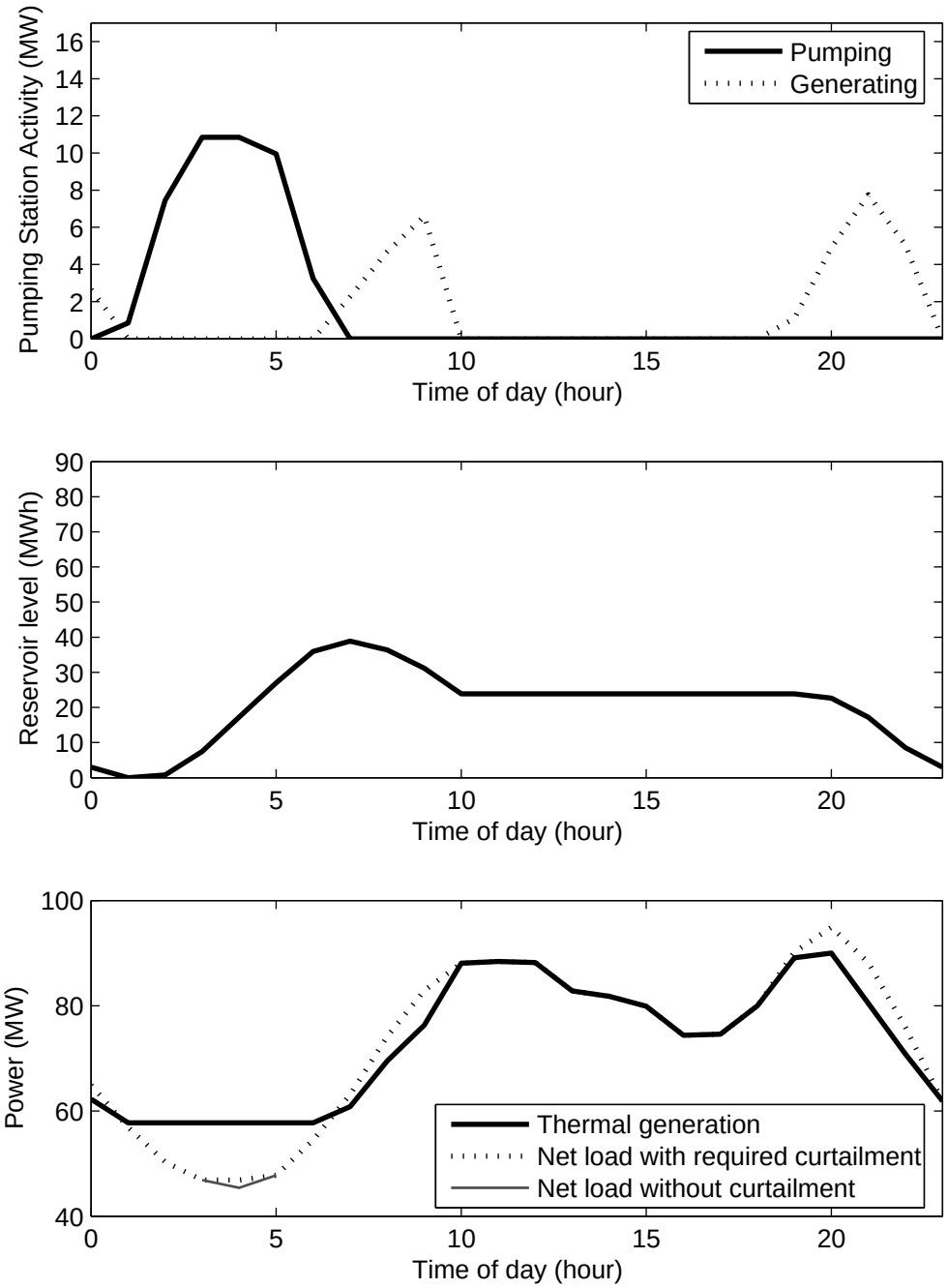

Figure 7.18: Optimization Results: Scenario 4

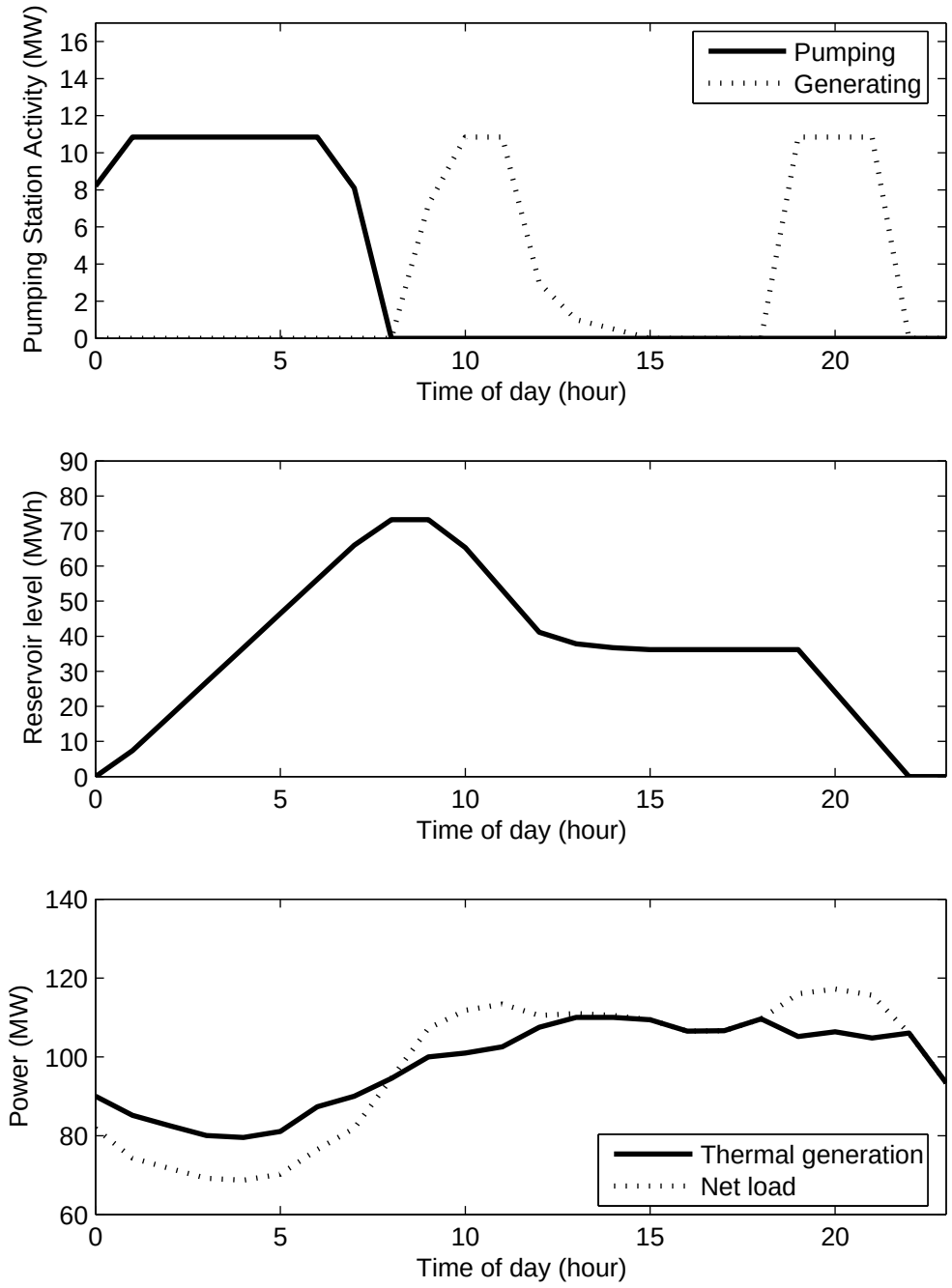

Figure 7.19: Optimization Results: Scenario 5

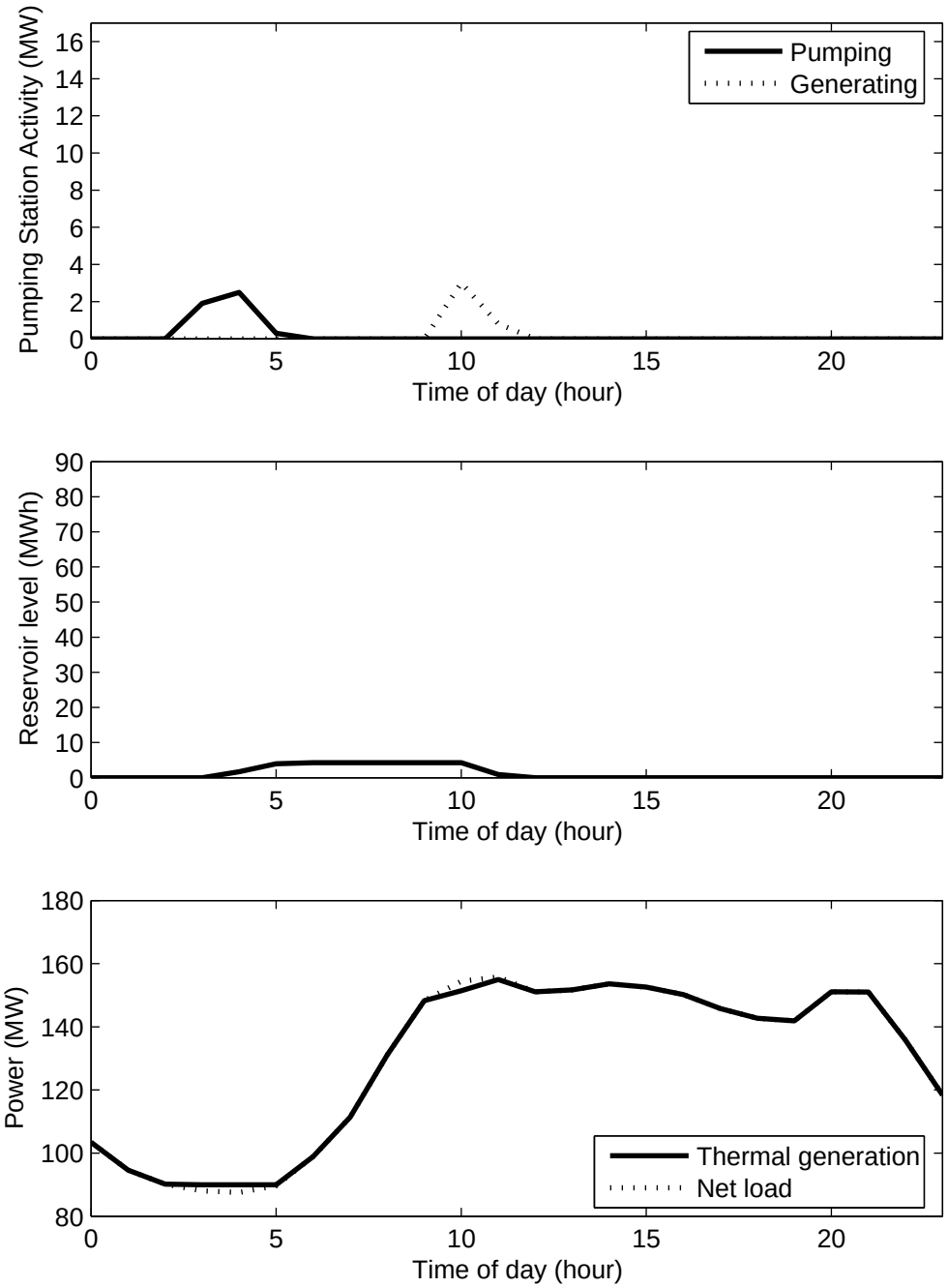

Figure 7.20: Optimization Results: Scenario 6

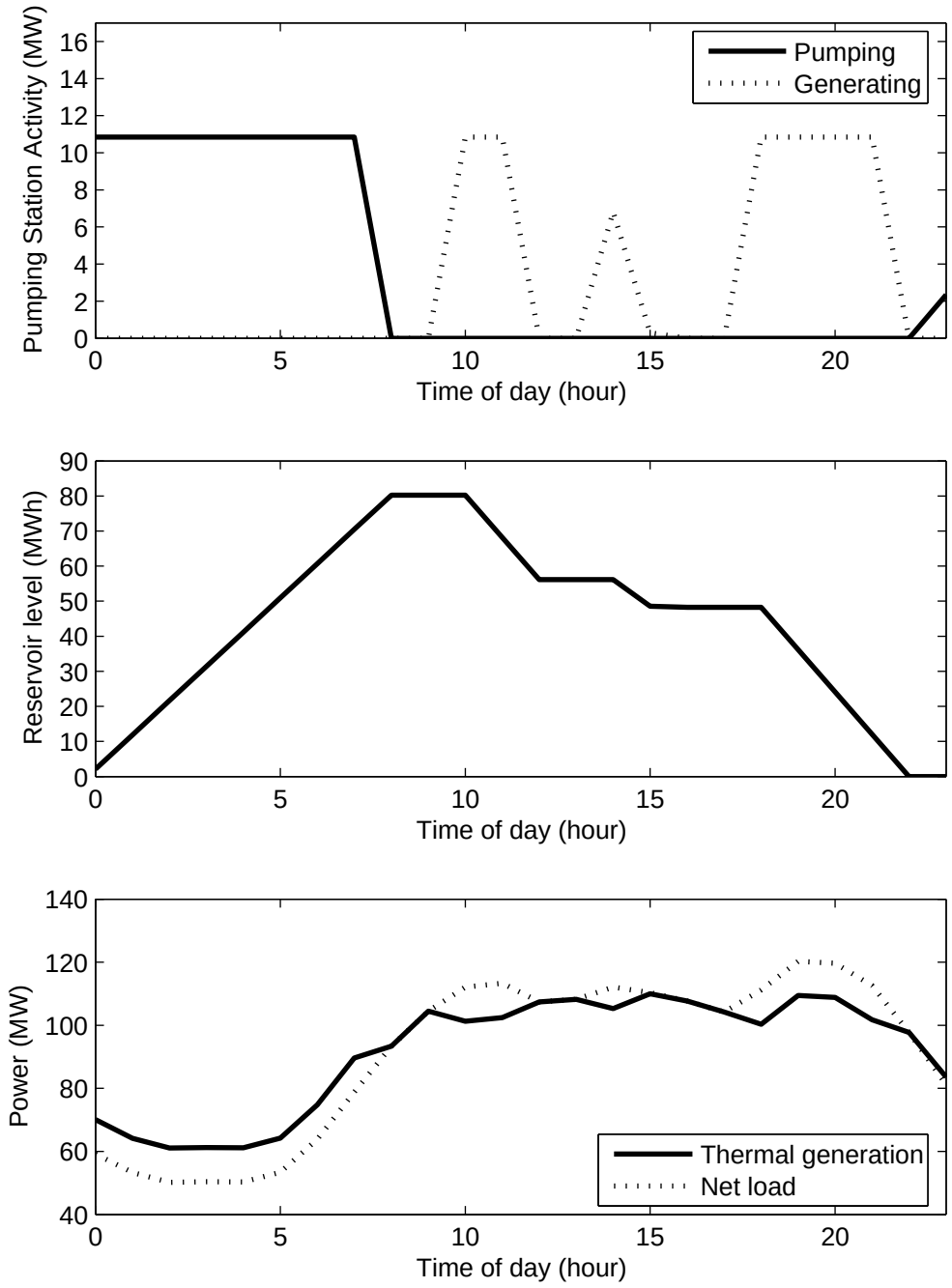

Figure 7.21: Optimization Results: Scenario 7

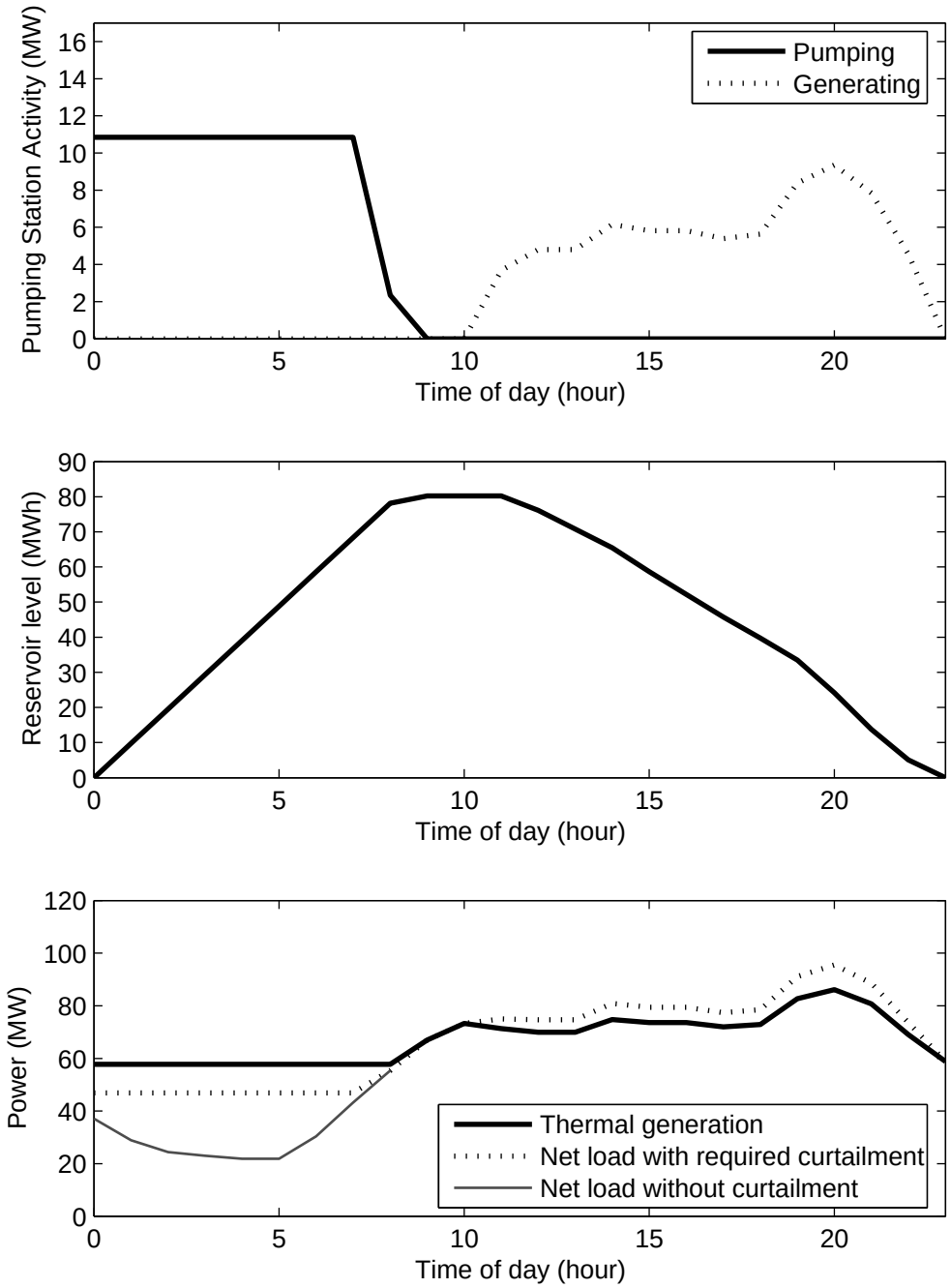

Figure 7.22: Optimization Results: Scenario 8

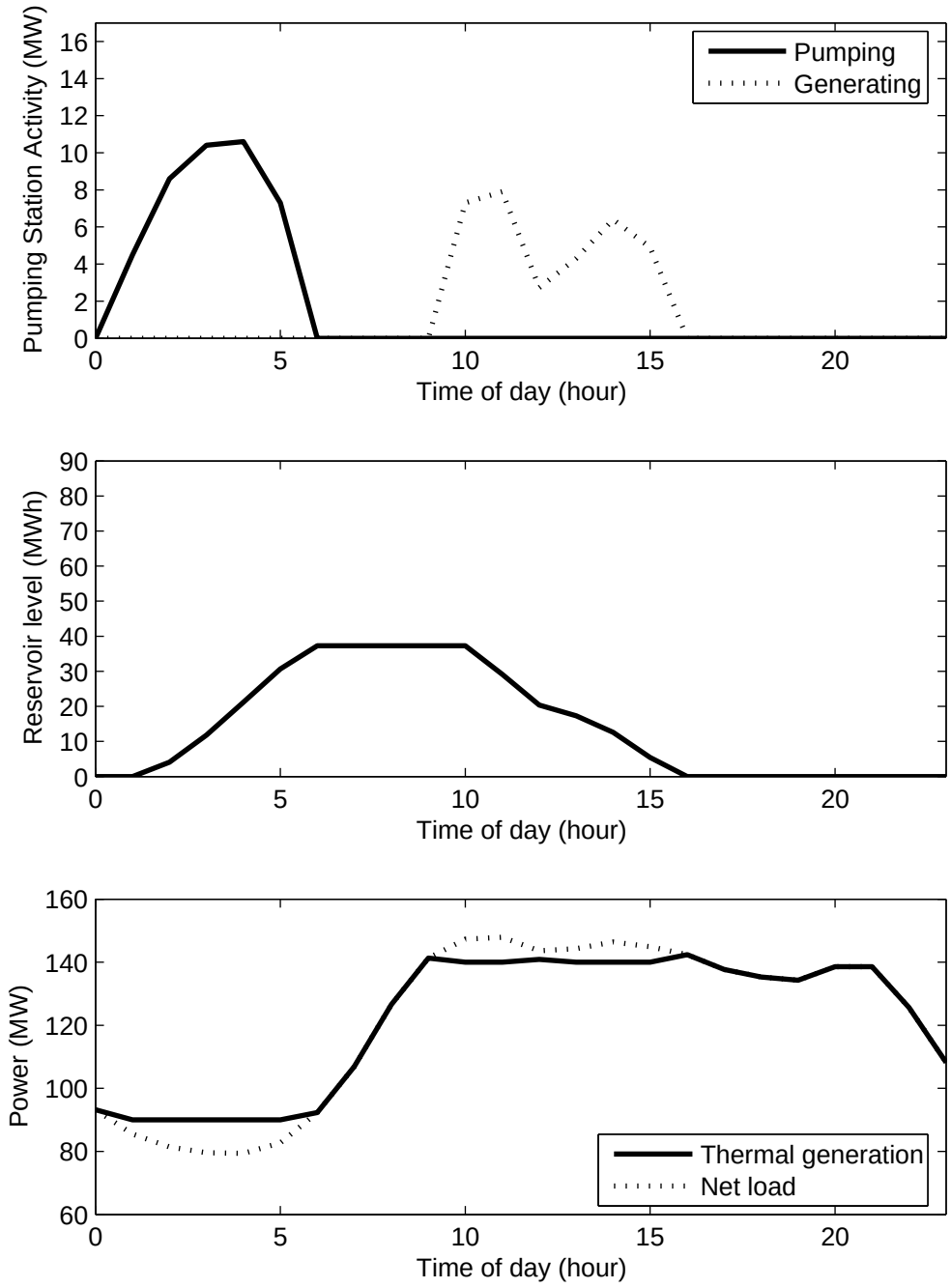

Figure 7.23: Optimization Results: Scenario 9

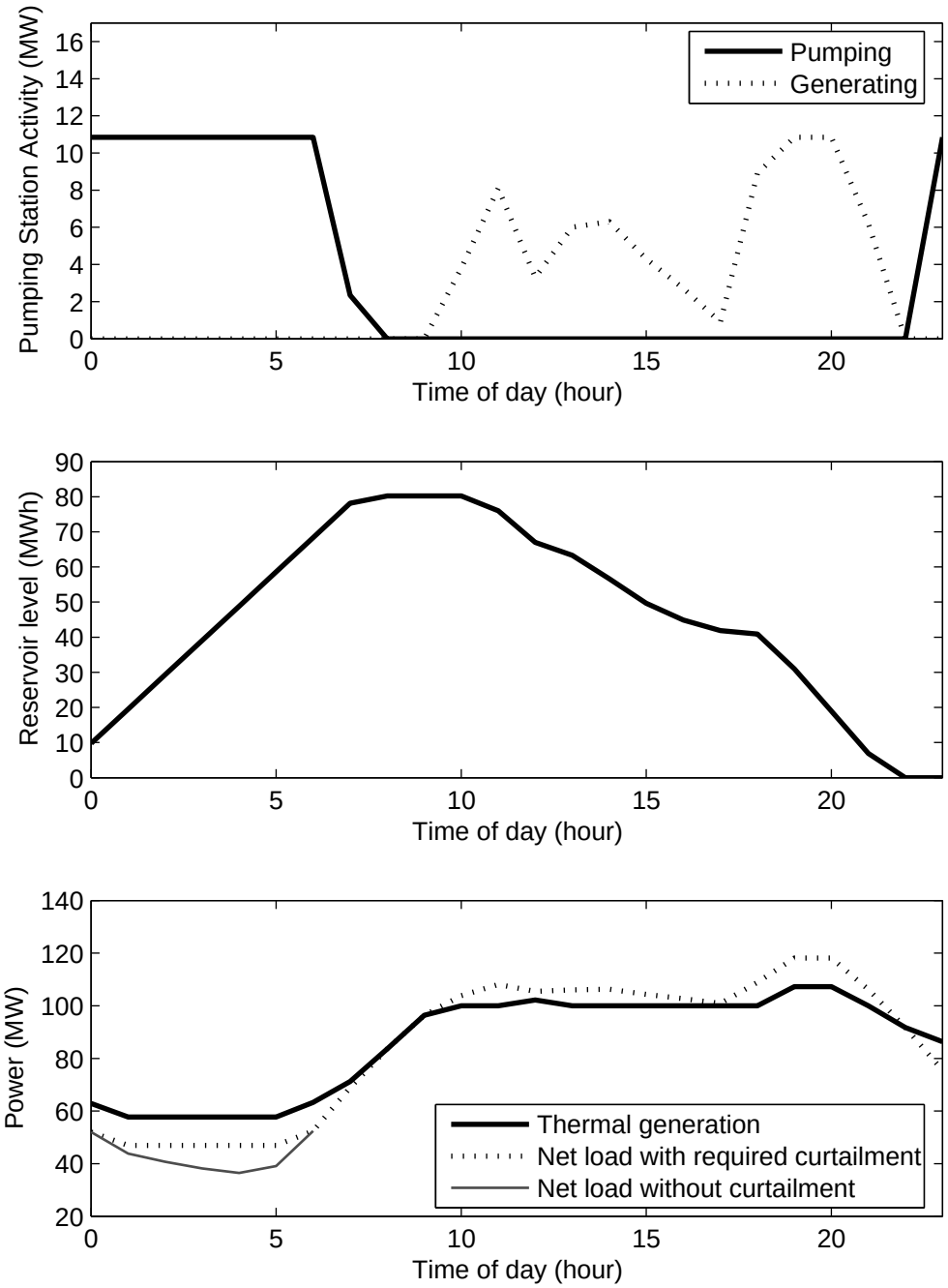

Figure 7.24: Optimization Results: Scenario 10

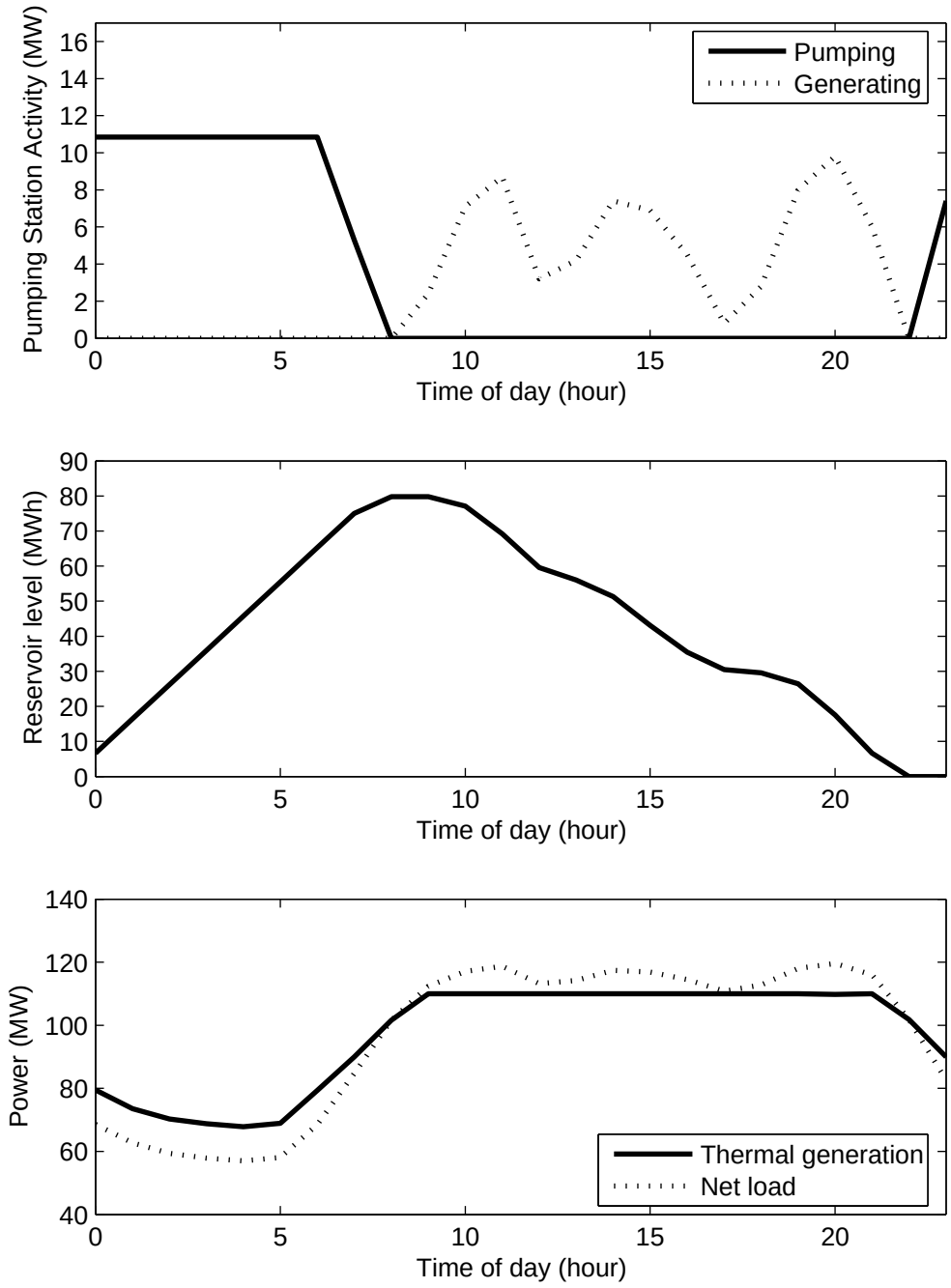

Figure 7.25: Optimization Results: Scenario 11

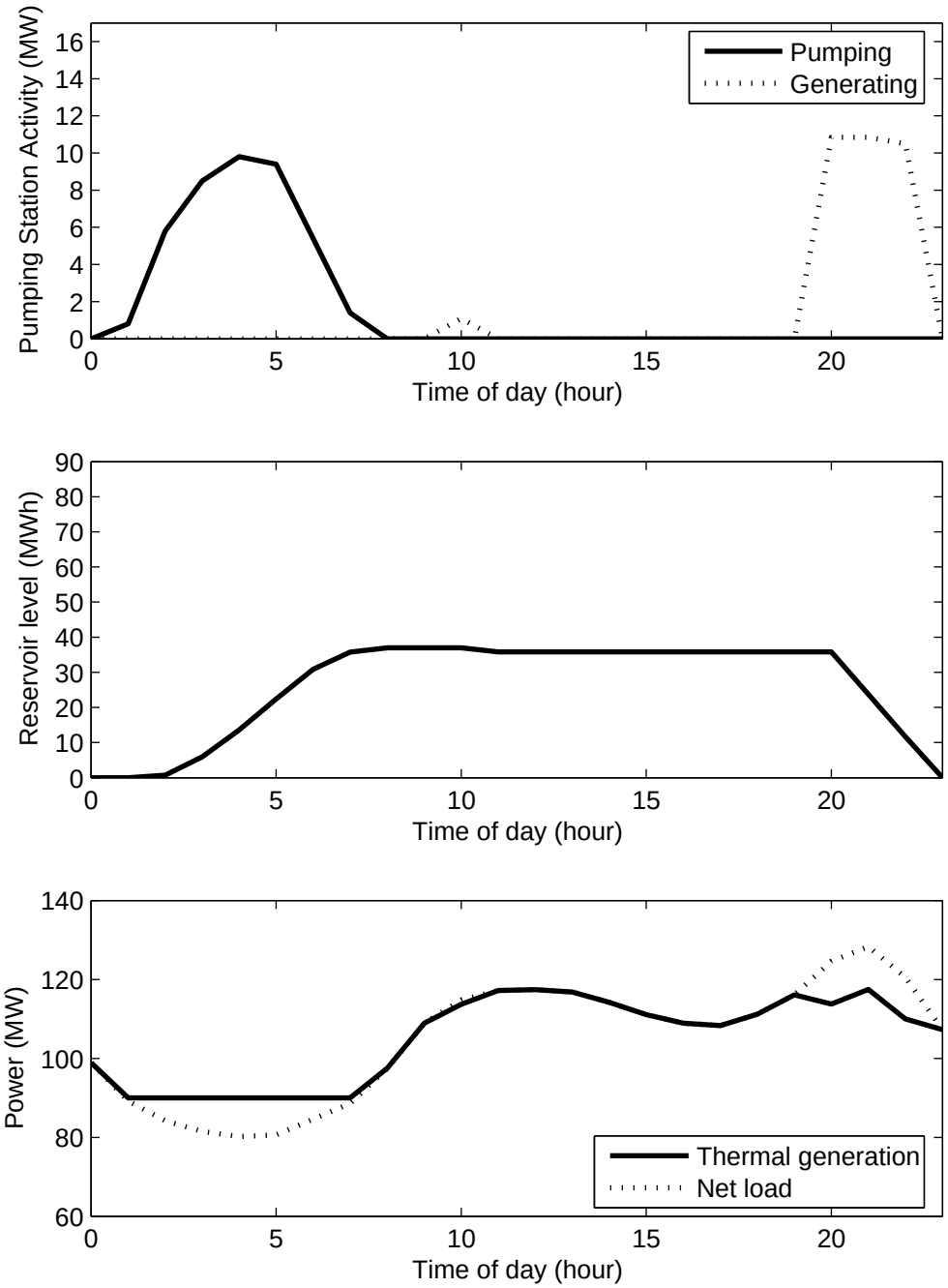

Figure 7.26: Optimization Results: Scenario 12

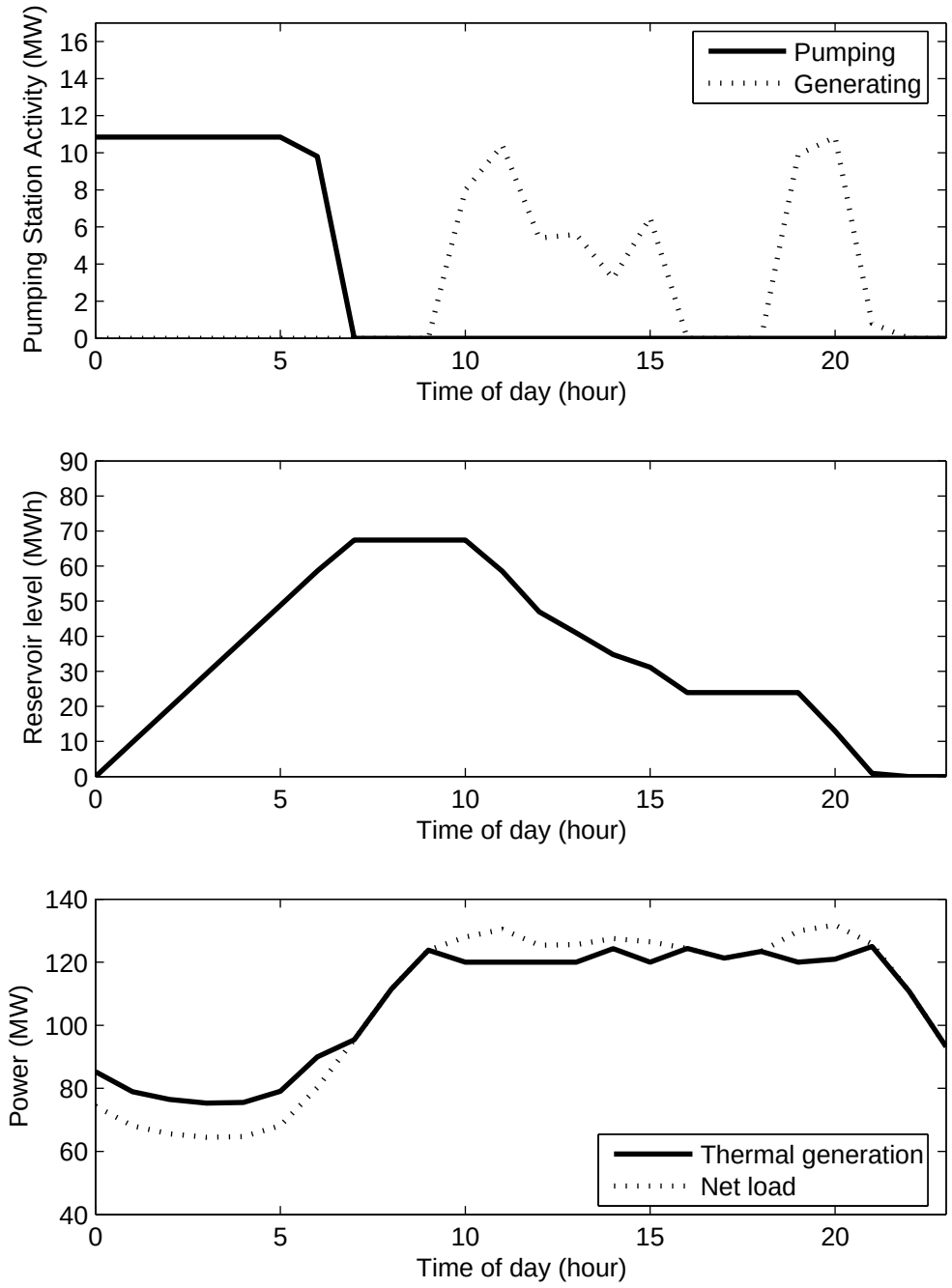

Figure 7.27: Optimization Results: Scenario 13

7.3 Sensitivity Analysis

In order to see the effect that each problem parameter has on the results, a sensitivity analysis was performed. In this analysis, each parameter is changed by a small amount and the new optimum solution is compared to the original solution. The results of this analysis are shown in Table 7.4.

Table 7.4: Sensitivity Analysis Results

Parameter	Value	Value Change (%)	P'_{max} (MW)	E'_{max} (MWh)	P_{max} Change (%)	E_{max} Change (%)
Reference	–	–	**10.9**	**80.2**	–	–
$C_{E_{max}}$ (EUR/MWh)	12398	−10.	10.9	80.2	0.0	0.0
$C_{E_{max}}$ (EUR/MWh)	15154	+10.	10.4	77.0	−4.6	−4.0
$C_{P_{max}}$ (EUR/MW)	339480	−10.	12.4	91.0	+13.8	+13.5
$C_{P_{max}}$ (EUR/MW)	414920	+10.	9.8	72.7	−10.1	−9.4
$\eta_p \cdot \eta_g$	0.72	−10.	7.5	44.5	−35.2	−45.5
$\eta_p \cdot \eta_g$	0.88	+10.	12.4	88.2	+13.8	+10.0
$UnitSize$ (MW)	14.9	−10.	6.8	48.6	−37.6	−39.4
$UnitSize$ (MW)	18.1	+10.	13.1	91.8	+20.2	+14.5
$TechMin$ (pu)	0.63	−10.	0.5	3.4	−95.4	−95.7
$TechMin$ (pu)	0.77	+10.	21.1	136.3	+93.6	+70.0
$RegFactor$	4.6	−10.	10.9	80.2	0.0	0.0
$RegFactor$	5.6	+10.	10.0	71.3	−8.3	−11.1
Fuel Price (USD/barrel)	63	−10.	8.1	60.4	−25.6	−24.7
Fuel Price (USD/barrel)	77	+10.	12.4	91.0	+13.8	+13.5

The optimization problem as also been solved with the spinning reserve security constraints removed, allowing all renewable generation available to be used. In this case, no pumped storage is indicated to be installed at all. It is clear that it is the security constraints that make the installation of the pumped storage unit economically viable. The strong dependence of the security constraints on the size of the largest thermal unit and the technical minimums of the diesel generators is reflected in the large changes that occur in the optimal sizing of the pumped storage when changes are made to these parameters.

It is also worth noting that in the case that the efficiency difference between old and new machines is reduced, the pumped storage that is installed is only placed in operation when it is allows additional renewable energy to be used; it is not used for normal load transfer from peak to off-peak hours. This occurs when the cost difference between the older and newer generators does not compensate for the energy lost in the pumping/generating process.

7.4 Adequacy of Tools

From the experiments performed, it is possible to conclude that the overall toolchain worked quite well. Each part could be scripted to give output in the format needed for the next step. Once everything was scripted, the entire process, starting from choosing the number of clusters to finally looking at figures of results, took only a few minutes, and changes at any point could be made readily.

For clustering the `FCMclust` function of the Fuzzy Clustering and Data Analysis Toolbox for MATLAB worked very well. The functions from this toolbox for calculating the validation indices for the clusters worked correctly, but the indices were not extremely helpful in identifying good sets of clusters. This can be attributed to the use of clustering methods on data that is only weakly clustered. Nonetheless, the scenarios produced seem to do a good job of grouping the net load curves according to similar shapes and providing the approximation to their probability distribution that was needed for the problem as it was formulated. Because the clustering was done in MATLAB scripts, the output could be formatted exactly as was necessary to include in the FlopC++ or MathProg programs.

The GLPK `glpsol` was adequate to solve the linear programming problem with ease, but it did not give results in a form that could be used for visualization and further treatment. The FlopC++ program was not difficult to write and gave results that could easily be pasted into MATLAB. The time to expand the variables and constraints and solve the linear program was quite good in both systems, taking only a few seconds to execute. The solution for E_{max} and P_{max} between the two solvers was equal as was the minimizing value of the objective function. This increases the confidence that there has been no numerical error in the solver to arrive at an incorrect solution.

Chapter 8

Conclusions

8.1 Achievements/Contributions

In this thesis, a number of contributions have been made. Pumped storage was proposed as a measure to allow the increase of renewable intermittent generation into the system and to improve the dynamic performance and security of an isolated island system. A method of including the pumped storage load in the security criteria was proposed and tested by dynamic simulation. The effectiveness of shedding pumped storage to assist in restoring system frequency after major system events is confirmed.

In the second part, these dynamic security criteria have been included in an optimization problem that is able to determine both the power capacity and the best reservoir capacity for a potential pumped storage station in an island system. Fuzzy clustering techniques have been used to deal with the stochastic nature of load and renewable production and produce scenarios for the optimization problem.

Results showed that including pumped storage can be an effective means of allowing larger penetration of intermittent renewable energy sources, improving both the dynamic security and the economic operation of a test system. Including the dynamic security criteria in the economic question of dimensioning the pumped storage unit proved to make a significant difference in the optimal pumped storage capacity.

8.2 Future Developments

The pumped storage station has been considered in this work as a source of emergency or secondary reserve. In an island system, these reserves are likely to be arranged by the system operator itself or by contracts made by the operator. However, in power systems of larger size, market structures are responsible for providing reserves. In this situation, the operator of a storage station would have the possibility of entering both into the energy market as well as the reserve markets. Further work could be done to investigate the rules and limitations of such participation. The optimization of the capacity of

the storage station under market rules could also be considered.

The sensitivity analysis of the results of the optimization showed that the security criteria are what primarily provide the economic incentive for the installation of pumped storage in the test system. Since the dynamic security issues are of primary importance, it may be worthwhile to consider the use of another storage technology to better meet the reserve needs. The shedding of pumped storage load is able to limit large frequency excursions, however, it is not a substitute for spinning reserve, and the use of renewable generation continues to be limited by the dynamic security constraints. A technology that is able to provide full spinning reserve and frequency regulation services could be a very good option. Several of the technologies described in Chapter 2 have already been used in this type of application, among them lead-acid or nickel-cadmium batteries [26, 7] and flow batteries [85].

The approach to the optimization problem could also be adapted for application to optimizing the operation of a pumped storage station. While this problem in simpler in that the capacity of pumped storage is known rather than a problem variable, and there is no need for various scenarios, it is more complex because the result must be physically possible. A mixed-integer formulation may be needed in order to account for the fact that a fixed-speed pump operates either full-on or off, not in intermediate power levels. This would also be required in order to determine which specific thermal units should be committed at any given time. Some cost could be given to start-up and shut-down of all units so as to limit the switching actions necessary during operation.

Bibliography

[1] T. Malyshev, D. Justus, L. P. Alisse, and T. Gül, *Renewable Energy: Market & Policy Trends in IEA Countries*. Paris: International Energy Agency, 2004. [Online]. Available: http://www.iea.org/textbase/nppdf/free/2004/renewable1.pdf

[2] J. Barton and D. Infield, "Energy storage and its use with intermittent renewable energy," *IEEE Trans. Energy Conversion*, vol. 19, no. 2, pp. 441–448, 2004.

[3] R. Schainker, "Executive overview: energy storage options for a sustainable energy future," in *Power Engineering Society General Meeting, 2004. IEEE*, 2004, pp. 2309–2314.

[4] W. Leonhard and E. Grobe, "Sustainable electrical energy supply with wind and pumped storage - a realistic long-term strategy or utopia?" in *Power Engineering Society General Meeting, 2004. IEEE*, 2004, pp. 1221–1225.

[5] P. Symons, "Opportunities for energy storage in stressed electricity supply systems," in *Power Engineering Society Summer Meeting, 2001. IEEE*, vol. 1, Vancouver, BC, 2001, pp. 448–449.

[6] *Power Engineering Journal*, vol. 13, no. 3, June 1999.

[7] B. Roberts and J. McDowall, "Commercial successes in power storage," *IEEE Power Energy Mag.*, vol. 3, no. 2, pp. 24–30, 2005.

[8] I. Gyuk, P. Kulkarni, J. Sayer, J. Boyes, G. Corey, and G. Peek, "The United States of Storage," *IEEE Power Energy Mag.*, vol. 3, no. 2, pp. 31–39, 2005.

[9] A. Nourai, B. Martin, and D. Fitchett, "Testing the limits," *IEEE Power Energy Mag.*, vol. 3, no. 2, pp. 40–46, 2005.

[10] Energy Storage Program. U.S. Department of Energy. [Online]. Available: http://www.electricity.doe.gov/program/electric_rd_estorage.cfm?section=divisions&level2=estorage

[11] "European Technology Platform: SmartGrids," Dec. 2005, Draft Version 2.0.

[12] J. Lopes, C. Moreira, and A. Madureira, "Defining Control Strategies for Microgrids Islanded Operation," *IEEE Trans. Power Syst.*, vol. 21, no. 2, pp. 916–924, May 2006.

[13] G. Hunt, "Valve regulated lead/acid battery systems," *Power Engineering Journal*, vol. 13, no. 3, pp. 113–116, 1999.

[14] A. Malik and B. Cory, "An application of frequency and duration approach in generation planning," *IEEE Trans. Power Syst.*, vol. 12, no. 3, pp. 1076–1084, 1997.

[15] A. J. Wood and B. F. Wollenberg, *Power Generation, Operation, and Control*, 2nd ed. New York: John Willey & Sons, 1996, ch. Pumped-Storage Hydroplants, pp. 230 – 263.

[16] A. Price and B. Davidson, "Recent developments in the design and applications of utility-scale energy storage plant," in *Electricity Distribution, 2001. Part 1: Contributions. CIRED. 16th International Conference and Exhibition on (IEE Conf. Publ No. 482)*, vol. 4, Amsterdam, 2001.

[17] Storage Technology. [Online]. Available: http://www.electricitystorage.org/tech/technologies_technologies.htm

[18] J. Baker and A. Collinson, "Electrical energy storage at the turn of the Millennium," *Power Engineering Journal*, vol. 13, no. 3, pp. 107–112, 1999.

[19] K. Mandle, "Dinorwig pumped-storage scheme," *Power Engineering Journal*, vol. 2, no. 5, pp. 259–262, 1988.

[20] T. Kuwabara, A. Shibuya, H. Furuta, E. Kita, and K. Mitsuhashi, "Design and dynamic response characteristics of 400 MW adjustable speed pumped storage unit for Ohkawachi Power Station," *IEEE Trans. Energy Conversion*, vol. 11, no. 2, pp. 376–384, 1996.

[21] B. Lam, F. Prabhakara, D. Mincheng, and G. Jiatian, "Transmission contingency, voltage collapse and transfer limits evaluation for the THP pumped storage hydro project," in *Power System Technology, 1998. Proceedings. POWERCON '98. 1998 International Conference on*, vol. 2, Beijing, 1998, pp. 1459–1463.

[22] L. Hannett, B. Lam, F. Prabhakara, Q. Guofu, D. Mincheng, and B. Beilei, "Modeling of a pumped storage hydro plant for power system stability studies," in *Power System Technology, 1998. Proceedings. POWERCON '98. 1998 International Conference on*, vol. 2, Beijing, 1998, pp. 1300–1304.

[23] S. Schoenung and C. Burns, "Utility energy storage applications studies," *IEEE Trans. Energy Conversion*, vol. 11, no. 3, pp. 658–665, 1996.

[24] C. A. Vincent and B. Scrosati, *Modern Batteries*, 2nd ed. London: Arnold, 1997, pp. 14 – 16.

[25] ——, *Modern Batteries*, 2nd ed. London: Arnold, 1997, ch. 5, Secondary Lead-Acid Cells, pp. 142 – 161.

[26] G. Rodriguez, "Operating experience with the Chino 10 MW/40 MWh battery energy storage facility," in *Energy Conversion Engineering Conference, 1989. IECEC-89. Proceedings of the 24th Intersociety*, Washington, DC, 1989, pp. 1641–1645.

[27] D. Daly, "20 MW battery power conditioning system for Puerto Rico Electric Power Authority," in *Battery Conference on Applications and Advances, 1995., Proceedings of the Tenth Annual*, Long Beach, CA, 1995, pp. 233–237.

[28] A. Green, "The characteristics of the nickel-cadmium battery for energy storage," *Power Engineering Journal*, vol. 13, no. 3, pp. 117–121, 1999.

[29] C. A. Vincent and B. Scrosati, *Modern Batteries*, 2nd ed. London: Arnold, 1997, ch. 8, High Temperature Cells, pp. 243 – 274.

[30] E. Kodama and Y. Kurashima, "Development of a compact sodium sulphur battery," *Power Engineering Journal*, vol. 13, no. 3, pp. 136–141, 1999.

[31] P. Lex and B. Jonshagen, "The zinc/bromine battery system for utility and remote area applications," *Power Engineering Journal*, vol. 13, no. 3, pp. 142–148, 1999.

[32] C. A. Vincent and B. Scrosati, *Modern Batteries*, 2nd ed. London: Arnold, 1997, ch. 9.3, Redox cells, pp. 300 – 302.

[33] A. Price, S. Bartley, S. Male, and G. Cooley, "A novel approach to utility scale energy storage [regenerative fuel cells]," *Power Engineering Journal*, vol. 13, no. 3, pp. 122–129, 1999.

[34] TVA - Regenesys. [Online]. Available: http://www.tva.gov/environment/reports/envreport01/regenesys.htm

[35] "Company pulls plug on power storage plant in Lowndes County," *Sun-Herald*, Dec. 2003, archived by archive.org. [Online]. Available: http://web.archive.org/web/20040326194736/http://www.sunherald.com/mld/sunherald/7451410.htm

[36] "Innogy pulls plug on Regenesys," *The Guardian*, Dec. 2003. [Online]. Available: http://business.guardian.co.uk/story/0,3604,1107840,00.html

[37] The Vanadium Redox Battery. [Online]. Available: http://www.vrb.unsw.edu.au/

[38] VRB Power Systems Inc. [Online]. Available: http://www.vrbpower.com/

[39] "The VRB Energy Storage System: The Multiple Benefits of Integrating the VRB-ESS with Wind Energy Producers – a Case Study in MWH Applications," VRB Power Systems Inc. [Online]. Available: http://www.vrbpower.com/docs/casestudies/VRB-ESS%20-%20Case%20Study%20Wind.pdf

[40] R. Hebner, J. Beno, and A. Walls, "Flywheel batteries come around again," *IEEE Spectr.*, vol. 39, no. 4, pp. 46–51, 2002.

[41] C. Tarrant, "Revolutionary flywheel energy storage system for quality power," *Power Engineering Journal*, vol. 13, no. 3, pp. 159–163, 1999.

[42] C. A. Vincent and B. Scrosati, *Modern Batteries*, 2nd ed. London: Arnold, 1997, ch. 9.5 Supercapacitors, pp. 305 – 310.

[43] R. Schottler and R. Coney, "Commercial application experiences with SMES," *Power Engineering Journal*, vol. 13, no. 3, pp. 149–152, 1999.

[44] X. Huang, S. Kral, G. Lehmann, Y. Lvovsky, and M. Xu, "30 MW Babcock and Wilcox SMES program for utility applications," *IEEE Trans. Appl. Superconduct.*, vol. 5, pp. 428–432, 1995.

[45] International Partnership for the Hydrogen Economy. [Online]. Available: http://www.iphe.net

[46] B. Roberts, Ed., *IEEE Power Energy Mag.*, vol. 2, no. 2, Mar./Apr. 2004.

[47] R. Bleischwitz and K. Fuhrmann, Eds., *Energy Policy*, vol. 34, no. 11, July 2006.

[48] J. Gurney, "Building a case for the hydrogen economy," *IEEE Power Energy Mag.*, vol. 2, no. 2, pp. 35–39, 2004.

[49] O. Weinmann, "Hydrogen-the flexible storage for electrical energy," *Power Engineering Journal*, vol. 13, no. 3, pp. 164–170, 1999.

[50] M. Korpaas, R. Hildrum, and A. Holen, "Optimal operation of hydrogen storage for energy sources with stochastic input," in *Power Tech Conference Proceedings, 2003 IEEE Bologna*, vol. 4, 2003.

[51] R. Gazey, S. Salman, and D. Aklil-D'Halluin, "A field application experience of integrating hydrogen technology with wind power in a remote island location," *Journal of Power Sources*, vol. In Press, Corrected Proof. [Online]. Available: http://www.sciencedirect.com/science/article/B6TH1-4J2M4FG-2/2/6afc74ceb30e3cf8752088ebdde28b03

[52] M. Jog, *Hydroelectric and pumped storage plants*. New York: Wiley, 1989.

[53] Planning and development of hydropower. Asian Institute of Technology School of Civil Engineering. Lecture Material for Course CE74.81 "Planning and Development of Hydropower". [Online]. Available: http://www.sce.ait.ac.th/people/faculty/z_ahmad/

[54] T.-H. Kuan, "Basic planning analysis of pumped-storage," Ph.D. dissertation, Colorado State University, 1989.

[55] G. Contaxis and A. Vlachos, "Optimal power flow considering operation of wind parks and pump storage hydro units under large scale integration of renewable energy sources," in *Power Engineering Society Winter Meeting, 2000. IEEE*, vol. 3, 2000, pp. 1745–1750.

[56] E. Castronuovo and J. Lopes, "On the optimization of the daily operation of a wind-hydro power plant," *IEEE Trans. Power Syst.*, vol. 19, no. 3, pp. 1599–1606, 2004.

[57] C. Bueno and J. Carta, "Wind powered pumped hydro storage systems, a means of increasing the penetration of renewable energy in the canary islands," *Renewable and Sustainable Energy Reviews*, vol. 10, pp. 312–340, 2006.

[58] C. Madureira and V. Baptista, *Hidroelectricidade em Portugal: Memória e Desafio*. Lisbon: REN-Rede Eléctrica Nacional, S.A., 2002.

[59] A. J. Wood and B. F. Wollenberg, *Power Generation, Operation, and Control*, 2nd ed. New York: John Willey & Sons, 1996, ch. Control of Generation, pp. 328 – 362.

[60] J. Horne, D. Flynn, and T. Littler, "Frequency stability issues for islanded power systems," in *Power Systems Conference and Exposition, 2004. IEEE PES*, 2004, pp. 299–306.

[61] S.-J. Huang and C.-C. Huang, "An automatic load shedding scheme including pumped-storage units," *IEEE Trans. Energy Conversion*, vol. 15, no. 4, pp. 427–432, 2000.

[62] *Transfer function block diagram for 14K60MC-S with Woodward DEC723 and EGB actuator*, ver. 1.2, Mann B&W Diesel, 2005, document reference 2440/ER/LLL/3090407-3.

[63] P. Kundur, *Power System Stability and Control*. New York: McGraw-Hill, 1994.

[64] *EUROSTAG Theory Manual*, 4th ed., Tractabel – EDF, Oct. 2002.

[65] J. Slootweg, S. de Haan, H. Polinder, and W. Kling, "General model for representing variable speed wind turbines in power system dynamics simulations," *IEEE Trans. Power Syst.*, vol. 18, no. 1, pp. 144–151, 2003.

[66] J. G. Slootweg, "Wind power: Modelling and impact on power system dynamics," Ph.D. dissertation, Delft University of Technology, 2003.

[67] *Grid Code: High and extra high voltage*, E.ON Netz GmbH, Aug. 2003. [Online]. Available: http://www.eon-netz.com/Ressources/downloads/enenarhseng1.pdf

[68] U. I. T. F. on Load Representation for Dynamic Performance, "Load representation for dynamic performance analysis [of power systems]," *IEEE Trans. Power Syst.*, vol. 8, no. 2, pp. 472–482, 1993.

[69] E. D. Castronuovo and J. A. P. Lopes, "Optimal operation and hydro storage sizing of a wind-hydro power plant," *International Journal of Electrical Power and Energy Systems*, vol. 26, no. 10, pp. 771 – 778, Dec. 2004.

[70] M. Kandil, S. Farghal, and N. Hasanin, "Economic assessment of energy storage options in generation expansion planning," *Generation, Transmission and Distribution [see also IEE Proceedings-Generation, Transmission and Distribution], IEE Proceedings C*, vol. 137, no. 4, pp. 298–306, 1990.

[71] J. C. Bezdek, *Handbook of Fuzzy Computation*. IOP Publishing Ltd, 1998, ch. F6.2 Fuzzy Clustering.

[72] B. Balasko, J. Abonyi, and B. Feil, *Fuzzy Clustering and Data Analysis Toolbox (for use with Matlab)*. [Online]. Available: http://www.fmt.vein.hu/softcomp/fclusttoolbox/

[73] X. Xie and G. Beni, "A validity measure for fuzzy clustering," *IEEE Trans. Pattern Anal. Machine Intell.*, vol. 13, no. 8, pp. 841–847, 1991.

[74] J. C. Bezdek, *Handbook of Fuzzy Computation*. IOP Publishing Ltd, 1998, ch. F6.3 Cluster validity for volumetric clusters.

[75] A. Makhorin. Gnu linear programming kit. Free Software Foundation, Inc. [Online]. Available: http://www.gnu.org/software/glpk/glpk.html

[76] Lindo Systems, Inc. [Online]. Available: http://www.lindo.com/

[77] GAMS Development Corporation. [Online]. Available: http://www.gams.com/

[78] AMPL Optimization LLC. [Online]. Available: http://www.ampl.com/

[79] COIN-OR (COmputational INfrastructure for Operations Research). [Online]. Available: http://projects.coin-or.org/FlopC++

[80] J.-S. Roy. Pulp : A linear programming modeler in python. [Online]. Available: http://www.jeannot.org/~js/code/index.en.html#PuLP

[81] T. H. Hultberg, "Topics in computational linear optimization," Ph.D. dissertation, Informatics and Mathematical Modelling, Technical University of Denmark, DTU, Richard Petersens Plads, Building 321, DK-2800 Kgs. Lyngby, 2000. [Online]. Available: http://www2.imm.dtu.dk/pubdb/p.php?2370

[82] J. R. Birge, "Decomposition and partitioning methods for multistage stochastic linear programs," *Operations Research*, vol. 33, no. 5, pp. 989 – 1007, 1985.

[83] S. S. Nielsen and S. A. Zenios, "Scalable parallel benders decomposition for stochastic linear programming," *Parallel Computing*, vol. 23, no. 8, pp. 1069 – 1088, 1997.

[84] "The VRB Energy Storage System: Remote Area Power Supplies (RAPS)," VRB Power Systems Inc. [Online]. Available: http://www.vrbpower.com/docs/whitepapers/VRB-ESS%20RAPS-Diesel%20Application.pdf

[85] "Remote Area Power Systems: King Island," VRB Power Systems Inc. [Online]. Available: http://www.vrbpower.com/docs/casestudies/RAPS%20Case%20Study%20(King%20Isl)%20March%202006%20(HR).pdf

Appendix A

Network Data

This appendix presents the network data used in the test system. This includes the lines, transformers, and generation units. Details of the dynamic parameters of the machines are included in Appendix B.

A.1 Lines

Table A.1 shows the transmission lines in the test system. Values are presented on a 100 MVA per-unit basis. The shunt admittance values are the semi-shunt values as appear at each end of the line in a pi transmission line model [64]. Lines that are not in service in the normal switching configuration that has been used are typeset in italics.

Table A.1: Transmission Lines

SEND	RECV	R	X	GS	BS	MVA
CUR6	LINCOLN6	0.07586	0.08171	0.	0.00056	59.23614
CUR6	BROAD6	0.02043	0.02201	0.	0.00015	59.23614
BROAD6	BANNO6	0.00742	0.00799	0.	0.00005	59.23614
CUR6	BANNO6	0.02827	0.03045	0.	0.00021	59.23614
BANNO6	RIDGE6	0.02478	0.02669	0.	0.00018	59.23614
CUR6	RIDGE6	0.03776	0.04068	0.	0.00028	59.23614
CUR6	CHERR6	0.00792	0.00853	0.	0.00006	59.23614
RIDGE6	HAMPD6	0.04002	0.04311	0.	0.0003	59.23614
HAMPD6	MINER6	0.03793	0.01928	0.	0.00023	31.59261
MINER6	AURORA6	0.00226	0.00243	0.	0.00002	59.23614
DRYCR3	PRZE3	0.10279	0.02075	0.	0.00001	5.19615
PRZE3	GRANT3	0.06069	0.03086	0.	0.00001	15.7963
PRZE3	MLWELBY3	0.09423	0.01902	0.	0.00001	5.19615
MLWELBY3	*WELBY3*	0.15603	0.04315	0.	0.00001	6.49519
WELBY3	LOGAN3	0.63328	0.17512	0.	0.00006	6.49519
WELBY3	*GOLDE3*	0.36467	0.10084	0.	0.00003	6.49519
LINCOLN3	GOLDE3	0.03642	0.01851	0.	0.00001	15.7963
LINCOLN3	BRIGH3	0.26401	0.13422	0.	0.00005	15.7963
LINCOLN3	GRANT3	0.03642	0.01851	0.	0.00001	15.7963

Continued on next page

Table A.1: – continued from previous page

SEND	RECV	R	X	GS	BS	MVA
ENGLE3	GRANT3	0.10044	0.05107	0.	0.00002	15.7963
MANNING3	CUR3TR1	0.00705	0.00921	0.	0.00007	19.53753
MANNING3	CUR3TR1	0.00705	0.00921	0.	0.00007	19.53753
MANNING3	CUR3TR2	0.00705	0.00921	0.	0.00007	19.53753
MANNING3	CUR3TR2	0.00705	0.00921	0.	0.00007	19.53753
MANNING3	CUR3TR3	0.00705	0.00921	0.	0.00007	19.53753
MANNING3	CUR3TR3	0.00705	0.00921	0.	0.00007	19.53753
MANNING3	ELATITR1	0.00034	0.00044	0.	0.0	19.53753
MANNING3	ELATITR2	0.00034	0.00044	0.	0.0	19.53753
MANNING3	SAMAN3S1	0.00688	0.00899	0.	0.00007	19.53753
MANNING3	SAMAN3S2	0.00688	0.00899	0.	0.00007	19.53753
SAMAN3S1	ASMAN3S1	0.01686	0.01626	0.	0.00001	29.61807
SAMAN3S2	ASMAN3S2	0.01686	0.01626	0.	0.00001	29.61807
ASMAN3S1	GREENW	0.01678	0.02193	0.	0.00018	19.53753
ASMAN3S2	GREENW	0.01678	0.02193	0.	0.00018	19.53753
MANNING3	CHERO3	0.10752	0.07086	0.	0.00115	11.22369
MANNING3	CHERO3	0.10752	0.07086	0.	0.00115	11.22369
MANNING3	CHERO3	0.10752	0.07086	0.	0.00067	11.22369
CHERO3	SANTA3	0.06303	0.04154	0.	0.00067	11.22369
CHERO3	SANTA3	0.06303	0.04154	0.	0.00135	11.22369
CHERO3	SANTA3	0.06303	0.04154	0.	0.00135	11.22369
CHERO3	FOX3	0.03337	0.02199	0.	0.00036	11.22369
CHERO3	FOX3	0.03337	0.02199	0.	0.00036	11.22369
CHERO3	GREENW	0.05033	0.06579	0.	0.00053	19.53753
SANTA3	*SASAN3P1*	0.04026	0.05263	0.	0.00042	19.53753
SASAN3P1	*RIDGE3*	0.0348	0.03356	0.	0.00002	29.61807
SANTA3	*SASAN3P2*	0.03355	0.04386	0.	0.00035	19.53753
SASAN3P2	*RIDGE3*	0.0348	0.03356	0.	0.00002	29.61807
RIDGE3	HAVAN3	0.08092	0.07805	0.	0.00004	29.61807
HAVAN3	MLHAVAN3	0.06342	0.03224	0.	0.00001	15.7963
BOWMAR3	CORON3	0.3763	0.1041	0.	0.00003	6.495
RIDGE3	EVANS3	0.07633	0.09979	0.	0.0008	19.53753
OXFOR3	*ASOXF3L3*	0.01636	0.01578	0.	0.00001	29.618
ASOXF3L3	*EVANS3*	0.04194	0.05483	0.	0.00044	19.53753
HAMPD3	YOSEM3	0.05033	0.06579	0.	0.00053	19.53753
SULLI3	QUEBE3	0.10708	0.04131	0.	0.00001	8.31384
ARAPA3	OGDEN3	0.10569	0.13817	0.	0.00111	19.53753
CUR3	SACUR3F3	0.00168	0.00219	0.	0.00002	19.53753
SACUR3F3	CLARK3	0.0472	0.05084	0.	0.00002	29.61807
CLARK3	ASCLA3C3	0.03979	0.04285	0.	0.00002	29.61807
ASCLA3C3	QUEBE3	0.00956	0.0125	0.	0.0001	19.53753
HAMPD3	PEORI3	0.08268	0.07974	0.	0.00004	29.61807
PEORI3	CORON3	0.10115	0.09756	0.	0.00003	29.61807
CORON3	DOWNI3	0.06744	0.06504	0.	0.00003	29.61807
CASTL6.6	BROAD6.6	0.65006	0.21023	0.	0.00005	2.33203
SOUTH6.6	GOLDE6.6	0.75851	0.20975	0.	0.0	1.42894
WESTH3	OGDEN3	0.14596	0.1908	0.	0.00153	19.53753
HAMPD6	MINER6	0.01182	0.03434	0.	0.00534	62.35383
HAMPD6	MINER6	0.01182	0.03434	0.	0.00534	62.35383
CUR6	SACUR6A6	0.00066	0.0019	0.	0.0003	62.35383

Continued on next page

Table A.1: – continued from previous page

SEND	RECV	R	X	GS	BS	MVA
SACUR6A6	ASVT6MP6	0.00624	0.00672	0.	0.00005	59.23614
ASVT6MP6	BEARC6	0.00639	0.01856	0.	0.00289	59.35383
CUR6	SACUR6A2	0.00066	0.0019	0.	0.0003	62.35383
SACUR6A2	ASVT6MP2	0.00624	0.00672	0.	0.00005	59.23614
ASVT6MP2	BEARC6	0.00639	0.01856	0.	0.00289	59.35383
QUEBE3	SAQUE3P3	0.00956	0.0125	0.	0.0001	19.53753
SAQUE3P3	WESTH3	0.07216	0.07772	0.	0.00003	29.61807
MANNING3	SAMAN3A1	0.00688	0.00899	0.	0.00007	19.53753
SAMAN3A1	ASMAN3A1	0.02495	0.02687	0.	0.00001	29.61807
ASMAN3A1	FOX3	0.00755	0.00987	0.	0.00008	19.53753
MANNING3	SAMAN3A2	0.00688	0.00899	0.	0.00007	19.53753
SAMAN3A2	ASMAN3A2	0.02495	0.02687	0.	0.00001	29.61807
ASMAN3A2	FOX3	0.00755	0.00987	0.	0.00008	19.53753
BSS6	RIDGE6	0.0091	0.00981	0.	0.00007	59.2334
BEARC6	BSS6	0.00591	0.01717	0.	0.00267	62.352
ARAPA3	THORN3	0.19461	0.2544	0.	0.00204	19.53753
THORN3	LOGAN3	0.10569	0.13817	0.	0.00111	19.53753
ARAPA3	KIPLI3	0.1426	0.18641	0.	0.0015	19.53753
MLHAVAN3	RAPP3	0.01888	0.01821	0.	0.00001	29.61807
RAPP3	BOWMAR3	0.23251	0.0643	0.	0.00002	6.495
BANNO6	BEARC6	0.00447	0.01299	0.	0.00202	62.35383
MORRI3	PRZE3	0.08092	0.07805	0.	0.00004	29.61807
HAMPD6	OXFOR6	0.02866	0.03087	0.	0.00021	59.23614
HAMPD3	OXFOR3	0.11464	0.11057	0.	0.00006	29.61807
RIDGE6	OXFOR6	0.01433	0.01543	0.	0.00011	59.23614
KIPLI3	*DOWNI3*	0.13487	0.13008	0.	0.00007	29.61807
MORRI3	*LOGAN3*	0.13487	0.13008	0.	0.00007	29.61807
SHERM6	LINCOLN6	0.02057	0.02215	0.	0.00015	59.2344
WESTH6	SHERM6	0.01854	0.01997	0.	0.00014	59.2344
CUR6	SACUR3PV	0.00016	0.00046	0.	0.00007	62.352
SACUR3PV	WESTH6	0.04383	0.04721	0.	0.00032	59.2344
WESTH3	OGDEN3	0.11194	0.12057	0.	0.00005	29.6172
WESTH3	OGDEN3	0.11194	0.12057	0.	0.00005	29.6172

A.2 Transformers

Table A.2 lists the transformers in the test system that have a fixed tap ratio. Table A.3 lists transformers with variable tap ratios. Reactances are given on a 100 MVA per-unit base. In Table A.3, CONTR is the bus whose voltage is to be controlled, VCON is the target voltage, RATIO is the nominal per-unit transformer ratio, and TLOR and TUPR are the lower and upper limits of the tap ratio, in per-unit.

Table A.2: Fixed Ratio Transformers

SEND	RECV	X	MVA
LOGAN	LOGAN3	1.45	4
OGDEN	OGDEN3	1.583	3.6
OGDEN	OGDEN3	1.58	3.6
GOLDEN	GOLDE3	1.9666	3
GOLDEN	GOLDE3	1.9666	3
BOWMAR	BOWMAR3	3.86666	1.5
BOWMAR	BOWMAR3	3.86666	1.5
ENGLE	ENGLE3	0.802083	9.6
CASTLEW	TER6.6	7.5	0.8
SULLIV	SULLI3	1.45	2
CHERRYH	CHERR6	0.33333	30
SOUTHGL	LBR6.6	8	0.5
AURORA	AURORA6	0.27	48
VITGR1&2	MANNING3	0.385	20
MANGR3	MANNING3	0.77	10
MANGR4T6	MANNING3	0.23	30
MANGR710	MANNING3	0.23	30
MANG1115	MANNING3	0.11	65
MANGR16	MANNING3	0.333	30
MANGR17	CUR6	0.625	25
MANGR18	CUR6	0.625	25
MANGR16A	CUR6	0.625	25
MANGR19	CUR6	0.625	25
BRIGHT3	BDC6.6	1.583	3.6
DRYCR3	DRYCR6.6	2.7	2
OGDEN3	OGDEN6.6	1.4375	4
GOLDE3	GOLDE6.6	8	0.5
GOLDE3	GOLDE6.6	8	0.5
BRIGHTA1	BDC6.6	7.5	0.8
BRIGHTA2	BDC6.6	7.5	0.8
BRIGHTA3	BDC6.6	7.5	0.8
BRIGHTA4	BDC6.6	7.5	0.8
BRIGHTA5	BDC6.6	7.5	0.8
BRIGHTB1	BRIGHT3	2.3809	0.63
BRIGHTB2	BRIGHT3	2.3809	0.63
BRIGHTB3	BRIGHT3	2.3809	0.63
BRIGHTB4	BRIGHT3	2.3809	0.63
BRIGHTB5	BRIGHT3	2.3809	0.63
BRIGHTB6	BRIGHT3	2.3809	0.63
BRIGHTC1	BRIGHT3	2.3809	0.63
BRIGHTC2	BRIGHT3	2.3809	0.63
BRIGHTC3	BRIGHT3	2.3809	0.63
BRIGHTC4	BRIGHT3	2.3809	0.63
LITTLET1	MINER6.6	9.2	0.5
LITTLET2	MINER6.6	9.2	0.5
BRIGHTD	BRIGHT3	1.9666	3
OGDENA	OGDEN3	0.802083	9.6
ARAPA	ARAPA3	0.802083	9.6
THORNT	THORN3	0.802083	9.6
WELBY	WELBY3	1.9666	3

Continued on next page

Table A.2: – continued from previous page

SEND	RECV	X	MVA
RAPP3	RAPP6.6	2.7	2
MORRI3	MORRI6.6	2.7	2
KIPLI3	KIPLI6.6	1.425	4
MORRISA	MORRI3	0.802083	9.6
WESTERNA	WESTH3	0.802083	9.6
GOLDENN	GOLDE3	1.9666	3
GOLDENB	GOLDE3	1.9666	3

Table A.3: Tap-changing Transformers

SEND	RECV	X	CONTR	VCON	MVA	RATIO	TLOR	TUPR
HAVANA	HAVAN3	0.8	HAVAN3	30	10	1	0.9	1.1
CUR6	CUR3TR1	0.4	CUR3TR1	30	25	1	0.85	1.15
CUR6	CUR3TR2	0.4	CUR3TR2	30	25	1	0.85	1.15
CUR6	CUR3TR3	0.4	CUR3TR3	30	25	1	0.85	1.15
RIDGE6	RIDGE3	0.66667	RIDGE3	30	15	1	0.85	1.15
RIDGE6	RIDGE3	0.66667	RIDGE3	30	15	1	0.85	1.15
HAMPD6	HAMPD3	0.4	HAMPD3	30	15	1	0.85	1.15
LINCOLN6	LINCOLN3	0.4	LINCOLN3	30	25	1	0.85	1.15
CUR6	CUR3	0.4	CUR3	30	25	1	0.85	1.15
WESTH6	WESTH3	0.4	WESTH3	30	25	1	0.85	1.15
CORON3	CORON6.6	0.1	CORON6.6	6.6	6	1	0.9	1.1
LOGAN3	LOGAN6.6	0.1	LOGAN6.6	6.6	6	1	0.9	1.1
SHERM6	SHERM6.6	1	SHERM6.6	6.6	10	1	0.85	1.15
DRYCR3	DRYCR6.6	0.1	DRYCR6.6	6.6	6	1	0.9	1.1
FOX3	FOX6.6	0.8	FOX6.6	6.6	10	1	0.9	1.1
FOX3	FOX6.6	0.8	FOX6.6	6.6	10	1	0.9	1.1
OXFOR3	OXFOR6.6	0.8	OXFOR6.6	6.6	10	1	0.9	1.1
OXFOR3	OXFOR6.6	0.8	OXFOR6.6	6.6	10	1	0.9	1.1
RIDGE6	RIDGE6.6	1	RIDGE6.6	6.6	10	1	0.85	1.15
RIDGE6	RIDGE6.6	1	RIDGE6.6	6.6	10	1	0.85	1.15
BROAD6	BROAD6.6	1	BROAD6.6	6.6	10	1	0.85	1.15
GRANT3	GRANT6.6	0.66	GRANT6.6	6.6	10	1	0.9	1.1
QUEBE3	QUEBE6.6	0.66	QUEBE6.6	6.6	10	1	0.9	1.1
WESTH6	WESTH6.6	1	WESTH6.6	6.6	10	1	0.85	1.15
WESTH6	WESTH6.6	1	WESTH6.6	6.6	10	1	0.85	1.15
ELATITR 1	ELATI6.6	0.66	ELATI6.6	6.6	10	1	0.9	1.1
ELATITR 2	ELATI6.6	0.66	ELATI6.6	6.6	10	1	0.9	1.1
BANNO6	BANNO6.6	1	BANNO6.6	6.6	10	1	0.85	1.15
BANNO6	BANNO6.6	1	BANNO6.6	6.6	10	1	0.85	1.15
ARAPA3	ARAPA6.6	1	ARAPA6.6	6.6	6	1	0.9	1.1
DOWNI3	DOWNI6.6	0.8	DOWNI6.6	6.6	10	1	0.9	1.1
EVANS3	EVANS6.6	0.8	EVANS6.6	6.6	10	1	0.9	1.1
EVANS3	EVANS6.6	0.8	EVANS6.6	6.6	10	1	0.9	1.1
HAMPD6	HAMPD6.6	0.6666	HAMPD6.6	6.6	15	1	0.85	1.15
HAMPD6	HAMPD6.6	1	HAMPD6.6	6.6	10	1	0.85	1.15
MINER6	MINER6.6	1	MINER6.6	6.6	10	1	0.85	1.15
GREENW	GREEN6.6	0.8	GREEN6.6	6.6	10	1	0.9	1.1
SANTA3	SANTA6.6	0.8	SANTA6.6	6.6	10	1	0.9	1.1
SANTA3	SANTA6.6	0.8	SANTA6.6	6.6	10	1	0.9	1.1

Continued on next page

Table A.3: – continued from previous page

SEND	RECV	X	CONTR	VCON	MVA	RATIO	TLOR	TUPR
SANTA3	SANTA6.6	0.8	SANTA6.6	6.6	10	1	0.9	1.1
CHERO3	CHERO6.6	0.5333	CHERO6.6	6.6	15	1	0.88	1.12
CHERO3	CHERO6.6	0.5333	CHERO6.6	6.6	15	1	0.88	1.12
PEORI3	PEORI6.6	1	PEORI6.6	6.6	6	1	0.9	1.1
BEARC6	BEARC6.6	0.6666	BEARC6.6	6.6	15	1	0.85	1.15
BEARC6	BEARC6.6	0.6666	BEARC6.6	6.6	15	1	0.85	1.15
CLARK3	CLARK6.6	1	CLARK6.6	6.6	15	1	0.9	1.1

A.3 Loads

The loads for the test system are described in Table A.4. This represents an estimate of the off-peak load during winter (wet season).

Table A.4: Loads

NAME	MW	MVAR	MVA	cos(phi)
SANTA6.6	7.120	3.033	7.739	0.920
FOX6.6	5.779	1.701	6.024	0.959
ELATI6.6	4.550	2.343	5.118	0.889
GREEN6.6	1.291	0.272	1.320	0.979
CHERO6.6	8.447	2.548	8.823	0.957
BROAD6.6	2.976	1.811	3.484	0.854
BANNO6.6	6.182	2.297	6.595	0.937
WESTH6.6	3.274	1.496	3.599	0.910
SHERM6.6	1.740	1.063	2.038	0.853
GOLDE6.6	0.196	0.125	0.233	0.842
GRANT6.6	2.348	0.594	2.422	0.969
LOGAN6.6	1.083	0.230	1.107	0.978
OGDEN6.6	0.495	0.307	0.582	0.850
CORON6.6	0.886	0.849	1.227	0.722
DOWNI6.6	1.946	1.384	2.388	0.815
HAMPD6.6	5.505	2.779	6.167	0.893
OXFOR6.6	4.790	2.913	5.606	0.854
EVANS6.6	3.529	1.744	3.937	0.896
RIDGE6.6	3.076	1.247	3.319	0.927
ARAPA6.6	1.305	0.734	1.497	0.872
DRYCR6.6	1.039	0.633	1.217	0.854
MINER6.6	3.110	2.027	3.712	0.838
QUEBE6.6	1.711	1.036	2.000	0.856
YOSEM3	0.513	0.149	0.534	0.960
HAVAN3	1.056	0.587	1.208	0.874
PEORI6.6	1.263	0.767	1.477	0.855
BEARC6.6	4.504	1.648	4.796	0.939
CLARK6.6	0.965	1.233	1.566	0.617
RAPP6.6	0.343	0.213	0.404	0.850
KIPLI6.6	0.486	0.301	0.572	0.850
MORRI6.6	0.325	0.202	0.383	0.850
Total	81.833	38.265	90.337	0.906

A.4 Thermal Generation

Table A.5 lists the thermal generation units in the test system. They are all diesel generating sets with the exception of Havana, which is a generates from biomass. Units with similar characteristics have been grouped together in the table and are represented by a single equivalent unit in dynamic simulations.

Table A.5: Thermal Units

Gen. Station	Node	Group	Capacity (MW)
Aurora Thermal Station	AURORA	G1	10.1
		G2	10.1
		G3	10.1
Manning Thermal Station	MANGR1&2	G1	6.0
		G2	6.0
	MANGR3	G3	5.0
	MANGR4T6	G4	6.9
		G5	6.9
		G6	6.9
	MANGR710	G7	9.4
		G8	9.4
		G9	9.4
		G10	9.4
	MANG1115	G11	10.1
		G12	10.1
		G13	10.1
		G14	10.1
		G15	10.1
	MANGR16	G16	13.0
	MANGR16A	G16a	4.0
	MANGR17	G17	16.5
	MANGR18	G18	16.5
	MANGR19	G19	16.5
Havana	HAVANA	G1	6.5

A.5 Hydro Generation

Table A.6 lists the hydro generation available in the test system. This includes the 5.0 MW pumping station that has been considered in the dynamic studies.

Table A.6: Hydro Stations

Gen. Station	Node	Group	Capacity (MW)
Logan	LOGAN	G1	1.5
		G2	1.5
Ogden	OGDEN	G1	2.4
		G2	2.4
Golden	GOLDEN	G4	2.4
		G1	1.2
		G2	0.5
		G3	0.5
	GOLDENB	P1	5.0
Bow Mar	BOWMAR	G1	1.2
		G2	1.2
Englewood	ENGLE	G1	7.3
Cherry Hills	CHERRYH	G1	8.0
		G2	8.0
		G3	8.0
Castlewood	CASTLEW	G1	0.72
Sullivan	SULLIV	G1	1.7
Southglen	SOUTHGL	G1	0.15
Greenwood	GREENW	G1	1.7

Appendix B

Dynamic Model Parameters

This appendix presents the parameters used in the machine models for dynamic simulation. Table B.1 shows the parameters of the synchronous machines. The model description can be found in Appendix C. Table B.2 lists the parameters used in the voltage regulation controls of the synchronous generators. An IEEE Type 1 Exciter model has been used as described in Section 3.5.1. Table B.3 shows the parameters of the diesel speed governors. Table B.4 shows the parameters of the hydro speed regulation parameters as described in Section 3.5.2.

Table B.1: Synchronous Machine Model Parameters

Name	S_n	P_n	U_n	H	R_a	X_d	X'_d	T'_{do}	X_q
Logan	2.	1.5	6.6	4.	0.01	0.8	0.12	3.5	0.479
Ogden	3.6	2.4	6.6	3.056	0.01	1.44	0.217	4.5	0.863
Golden	4.5	3.6	6.6	4.263	0.01	1.14	0.1714	3.5	0.683
Golden (PS Stat.)	6.5	5.	6.6	4.236	0.01	1.13973	0.1714	3.5	0.683
Bow Mar	1.5	1.2	6.6	4.	0.01	0.6	0.09	3.5	0.360
Engle	8.75	7.3	6.6	2.057	0.01	1.54	0.2551	3.5	0.986
Castlewood	0.9	0.72	0.4	4.	0.01	1.5	0.25	3.5	0.9
Sullivan	2.13	1.7	0.4	4.	0.01	0.5	0.25	3.5	0.9
Southglen	0.19	0.15	0.4	4.	0.01	1.5	0.25	3.5	0.9
Greenwood	2.13	1.7	30.	4.	0.01	1.5	0.25	3.5	0.9
Cherry Hills (x3)	10.	8.	6.6	8.497	0.01	0.278	0.056	5.66	0.167
Aurora	12.5	10.1	11	7.457	0.0302	1.87	0.324	5.3	0.86
Manning 1 & 2	10.	8.	6.6	2.098	0.0323	1.74	0.411	4.4	0.741
Manning 3	9.8	5.	6.6	2.098	0.0323	1.74	0.411	4.4	0.741
Manning 4-6	10	7.	6.6	2.056	0.0218	2.	0.301	3.531	1.241
Manning 7-10	12.5	8.36	6.6	3.838	0.0091	1.183	0.278	4.471	0.752
Manning 11-15	12.5	8.9	6.6	6.251	0.0106	1.431	0.288	2.981	0.941
Manning 16	15	13	6.6	6.251	0.0106	1.431	0.288	2.981	0.941
Manning 16A	5.25	4.	6.6	6.251	0.0106	1.431	0.288	2.981	0.941
Manning 17-19	20.6	16.5	6.6	6.251	0.0106	1.431	0.288	2.981	0.941
For all units: X_l= 0.1 and D = 0.05									

Table B.2: Voltage Regulator Parameters

Name	K_a	K_e	K_s	T_a	T_e	T_r	T_s	V_{max}	V_{min}
Logan	200	1	0.44	0.84	0.3	0.023	1	5	-2.5
Ogden	200	1	0.44	0.84	0.3	0.023	1	5	-2.5
Golden	400	1	0.04	0.05	0.8	0.02	0.1	7.3	-7.3
Bow Mar	200	1	0.44	0.84	0.3	0.023	1	5	-2.5
Englewood	187	1	0.058	0.98	1	0.02	0.62	5	-3.5
Castlewood	200	1	0.44	0.84	0.3	0.023	1	5	-2.5
Sullivan	200	1	0.44	0.84	0.3	0.023	1	5	-2.5
Southglen	200	1	0.44	0.84	0.3	0.023	1	5	-2.5
Greenwood	200	1	0.44	0.84	0.3	0.023	1	5	-2.5
Cherry Hills	200	1	0.44	0.84	0.3	0.023	1	5	-2.5
Aurora	200	1	0.44	0.84	0.3	0.023	1	5	-2.5
Manning (all)	200	1	0.44	0.84	0.3	0.023	1	5	-2.5

Table B.3: Diesel Speed Governor Parameters

Name	r	K_I	T_g	T_h	P_{max}	P_{min}
Aurora	0.07	3	0.1	0.4	1.15	0
Manning 1 & 2	0.075	3	0.1	0.4	1.15	0
Manning 3	0.075	3	0.1	0.4	1.15	0
Manning 4-6	0.075	3	0.1	0.4	1.15	0
Manning 7-10	0.07	3	0.1	0.4	1.15	0
Manning 11-15	0.07	3	0.1	0.4	1.15	0
Manning 16	0.07	3.5	0.1	0.4	1.15	0
Manning 16A	0.07	3.5	0.1	0.4	1.15	0
Manning 17-19	0.07	3.5	0.1	0.4	1.15	0

Table B.4: Hydro Speed Governor Parameters

Name	r	K_I	T_g	T_w	P_{max}	P_{min}
Cherry Hills	0.25	0.5	0.1	0.575	1.0	0

Appendix C

Synchronous Machine Model

This appendix describes EuroSTAG's simplified model for synchronous machines as described in the manual [64]. The entire derivation is not included here but may be found in [64].

The simplified model is a third-order model that represents the rotor with a single winding in the direct axis. The schematic diagram of the circuit equivalent is shown in Figure C.1.

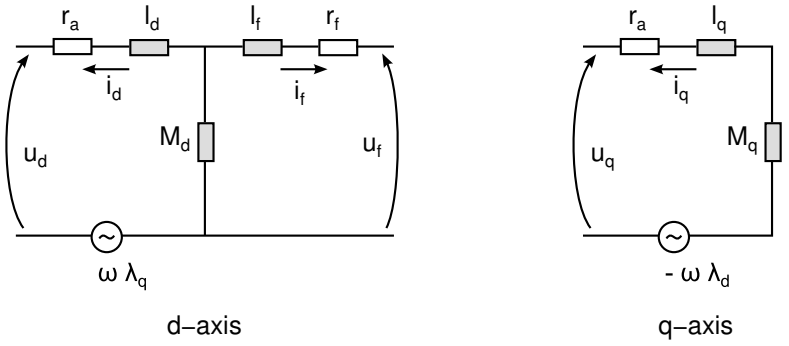

Figure C.1: Equivalent Schematics for Synchronous Generator

The notation used in the model is the following:

r_a	armature resistance
l_d	direct axis stator leakage
M_d	direct axis mutual inductance
l_f, r_f	leakage and resistance of the excitation winding
l_q	stator leakage quadrature axis (taken as equal to l_d)
M_q	quadrature axis mutual inductance

The system of flux equations can be written as

$$\begin{pmatrix} \lambda_d \\ \lambda_f \\ \lambda_q \end{pmatrix} = \begin{pmatrix} M_d + l_d & M_d & 0 \\ M_d & M_d + l_f & 0 \\ 0 & 0 & M_q + l_q \end{pmatrix} \begin{pmatrix} i_d \\ i_f \\ i_q \end{pmatrix} \tag{C.1}$$

From the equivalent circuit of Figure C.1 and the flux equations in (C.1) follow the conventional Park equations:

$$\begin{aligned} u_d &= -r_a i_d + \omega\lambda_d - \dot{\lambda_d} \\ u_f &= r_f i_f + \dot{\lambda}_d \\ u_q &= -r_a i_q + \omega\lambda_d - \dot{\lambda}_q \end{aligned} \tag{C.2}$$

The following are introduced for the common axis fluxes of d and q, allowing i_d and i_f to be eliminated:

$$\begin{aligned} \lambda_{AD} &= M_d\,(i_d + i_f) \\ \lambda_{AQ} &= M_q i_q \end{aligned} \tag{C.3}$$

The following expression converts the excitation signal as output from the voltage regulator to the stator reference:

$$u_f = -\frac{r_f}{M_{dv}} E_{fd} \tag{C.4}$$

where E_{fd} is the output from the voltage regulator and M_{dv} is calculated appropriately according to the base that is chosen for the field voltage.

The generator equations are expressed in terms of a d-q reference system fixed to the rotor. All network equations are expressed on an R-I reference system, so a transformation is needed between the two systems based on the angle difference between them.

$$\begin{pmatrix} E_R \\ E_I \end{pmatrix} = \begin{pmatrix} \sin\theta & \cos\theta \\ -\cos\theta & \sin\theta \end{pmatrix} \begin{pmatrix} E_d \\ E_q \end{pmatrix}$$

Putting all this together and rearranging (see the EuroSTAG manual [64] for details), the final electrical equations are given by the following:

$$-r \cdot \frac{\omega_0 \cdot r_f}{M_{dv}} E_{fd} - \frac{\omega_0 \cdot r_f}{l_f} \cdot \lambda_f + \frac{\omega_0 \cdot r_f}{l_f} \cdot \lambda_{AD} - \frac{d\lambda_f}{dt} = 0 \tag{C.5}$$

$$U_R \cdot \sin\theta - U_I \cdot \cos\theta + r \cdot i_d - \omega \cdot l_q \cdot i_q - \omega \cdot \lambda_{AQ} = 0 \tag{C.6}$$

$$U_R \cdot \cos\theta - U_I \cdot \sin\theta + r \cdot i_q - \omega \cdot l_d \cdot i_d - \omega \cdot \lambda_{AD} = 0 \tag{C.7}$$

$$\frac{M_d}{1 + \frac{M_d}{l_f}} \left(i_d + \frac{\lambda_f}{l_f} \right) - \lambda_{AD} = 0 \tag{C.8}$$

$$M_q \cdot i_q - \lambda_{AQ} = 0 \tag{C.9}$$

To these equations are added the equations for the rotating mass of the rotor. Variation in rotational

speed is given by the following equation:

$$\frac{d\omega}{dt} = \frac{1}{2H}\left(C_m - C_e\right) - \frac{D}{2H}\left(\omega - \omega_{ref}\right) \tag{C.10}$$

where C_m is mechanical torque, C_e is electrical torque, D is a damping coefficient, and H is the inertia constant.

Doing conversion of the base units of C_m to the power base of the numeric calculations $SNREF$ and substituting for the electrical torque with an expression in terms of the variables used in the electrical equations, the final mechanical equation becomes

$$\frac{P_N}{SNREF}C_m + D\left(\omega_{ref} - \omega\right) + \frac{1}{l_f}i_d\lambda_f + \left(\frac{M_d}{1 + \frac{M_d}{l_f}} - M_q\right)i_d i_q - 2H\frac{d\omega}{dt} = 0$$

The angular position is defined in terms of the machine speed and the system reference frequency, which may deviate from nominal frequency and is based on a weighted average of all the machine speeds in the network.

$$\frac{d\theta}{dt} = \left(\omega - \omega_{ref}\right)\omega_0$$

The EuroSTAG model includes the possibility of including the unit step-up transformer in the model as well as saturation of the magnetic circuits, however, these were not used and therefore have not been included in the equations presented.

Model parameters for the synchronous machine may be specified either using the internal quantities, which are exactly the parameters described above, or may be specified according to external parameters:

x_l [p.u.] stator leakage

r_a [p.u.] armature resistance

x_d [p.u.] direct axis reactance

x'_d [p.u.] direct axis transient reactance

T'_{d0} [s] direct axis open-circuit transient time constant

x_q [p.u.] quadrature axis reactance

Appendix D

Induction Machine Model

The full induction machine model is based on the synchronous machine model in which the excitation winding has been short-circuited. For reference, a summary of the derivation of the model is given here, but the full derivation can be found in the EuroSTAG program documentation [64].

Park's equations may be applied, giving the following equivalent circuits, as shown in Figure D.1.

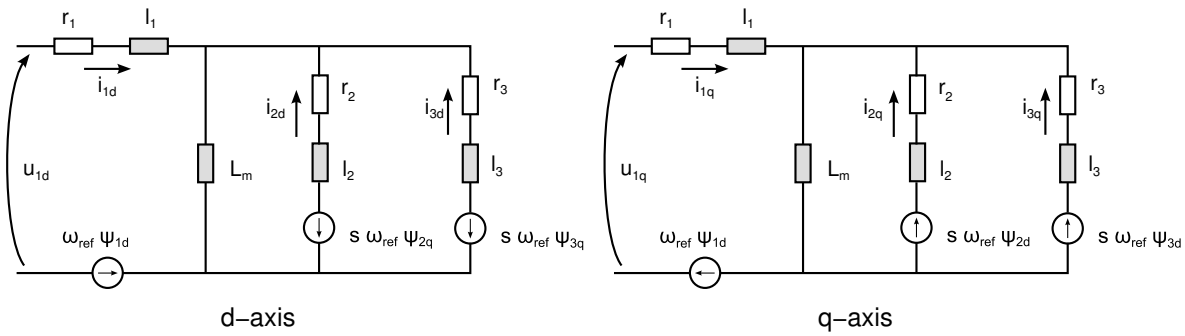

Figure D.1: Equivalent Schematics for Induction Machine

Using the notation of inductances as shown in Figure D.1, the system of magnetic equations can be written as

$$\begin{pmatrix} \psi_{1d} \\ \psi_{2d} \\ \psi_{3d} \\ \psi_{1q} \\ \psi_{2q} \\ \psi_{3q} \end{pmatrix} = \begin{pmatrix} L_m + l_1 & L_m & L_m & 0 & 0 & 0 \\ L_m & L_m + l_2 & L_m & 0 & 0 & 0 \\ L_m & L_m & L_m + l_3 & 0 & 0 & 0 \\ 0 & 0 & 0 & L_m + l_1 & L_m & L_m \\ 0 & 0 & 0 & L_m & L_m + l_2 & L_m \\ 0 & 0 & 0 & L_m & L_m & L_m + l_3 \end{pmatrix} \begin{pmatrix} i_{1d} \\ i_{2d} \\ i_{3d} \\ i_{1q} \\ i_{2q} \\ i_{3q} \end{pmatrix} \tag{D.1}$$

The introduction of some complex variables allows for more concise notation. The following defini-

tions are made:

$$\begin{aligned} U_1 &= u_{1d} + ju_{1q} \\ I_i &= i_{id} + ji_{iq}\ ,\ i = \{1,2,3\} \\ \psi_i &= \psi_{id} + \psi_{iq}\ ,\ i = \{1,2,3\} \end{aligned} \tag{D.2}$$

Using these definitions, Park's equations can be written as

$$U_1 = \dot{\psi_1} + j\omega_{ref}\psi_1 + r_1 I_1 \tag{D.3}$$

$$0 = r_2 I_2 + \dot{\psi_2} + js\omega_{ref}\psi_2 \tag{D.4}$$

$$0 = r_3 I_3 + \dot{\psi_3} + js\omega_{ref}\psi_3 \tag{D.5}$$

with the flux definitions given by

$$\psi_1 = (L_m + l_1)\, I_1 + L_m I_2 + L_m I_3 \tag{D.6}$$

$$\psi_2 = L_m I_1 + (L_m + l_2)\, I_2 + L_m I_3 \tag{D.7}$$

$$\psi_3 = L_m I_1 + L_m I_2 + (L_m + l_3)\, I_3 \tag{D.8}$$

and slip s defined as

$$s = \frac{\omega_{ref} - \omega_R}{\omega_{ref}} \tag{D.9}$$

where ω_{ref} is the system reference frequency and ω_R is the machine rotor speed.

From the above expressions, ψ_1 is neglected and I_2 and I_3 are eliminated algebraicly. In this elimination it is useful to make the following substitutions to reduce the resulting expressions:

$$\begin{aligned} A &= l_2 l_3 + l_2 L_m + l_3 L_m \\ B &= \frac{L_m l_2 l_3}{A} \end{aligned}$$

Using subscripts R and I to indicate the real and imaginary parts of the complex variables, the final electrical equations for the full induction machine model can be written as follows:

$$U_{1R} = r_1 I_{1R} - \omega_{ref}\,(l_1 + B)\, I_{1I} - \omega_{ref}\frac{L_m l_3}{A}\psi_{2I} - \omega_{ref}\frac{L_m i_2}{A}\psi_{3I} \tag{D.10}$$

$$U_{1I} = \omega_{ref}\,(I_1 + B)\, I_{1R} + r_1 I_{1I} + \omega_{ref}\frac{L_m l_3}{A}\psi_{2R} - \omega_{ref}\frac{L_m I_2}{A}\psi_{3R} \tag{D.11}$$

$$\frac{1}{\omega_0}\dot{\psi_{2R}} = \frac{r_2}{l_2}BI_{1R} - \frac{r_2\,(L_m + l_3)}{A}\psi 2R + (\omega_{ref} - \omega R)\,\psi_{2I} + \frac{r_2}{l_2 l_3}B\psi_{3R} \tag{D.12}$$

$$\frac{1}{\omega_0}\dot{\psi_{2I}} = \frac{r_2}{l_2}BI_{1I} - (\omega_{ref} - \omega R)\,\psi_{2R} - \frac{r_2\,(L_m + l_3)}{A}\psi_{2I} + \frac{r_2}{l_2 l_3}B\psi 3I \tag{D.13}$$

$$\frac{1}{\omega_0}\dot{\psi_{3R}} = \frac{r_3}{l_3}BI_{1R} + \frac{r_3}{l_2 l_3}B\psi_{2R} - \frac{r_3\left(L_m + l_2\right)}{A}\psi_{3R} + \left(\omega_{ref} - \omega R\right)\psi_{3I} \tag{D.14}$$

$$\frac{1}{\omega_0}\dot{\psi_{3I}} = \frac{r_3}{l_3}BI_{1I} + \frac{r_3}{l_2 l_3}B\psi_{2I} - \left(\omega_{ref} - \omega R\right)\psi_{3R} - \frac{r_3\left(L_m + l_2\right)}{A}\psi_{3I} \tag{D.15}$$

Electrical torque is given by

$$C_e = \frac{L_m l_3}{A}\left(\psi_{2R}I_{1I} - \psi_{2I}I_{1R}\right) + \frac{L_m l_2}{A}\left(\psi_{3R}I_{1I} - \psi_{3I}I_{1R}\right) \tag{D.16}$$

The mechanical equation relates the change in rotation speed to the difference between electrical and mechanical torque. Note that the torque is expressed in the formulation here as a positive value for loading (i.e. positive slip). The EuroSTAG model implementation includes an option for the induction machine to be used as a generator; in this case the sign convention for torque and output active power is reversed, and these quantities take positive values for generating (i.e. negative slip).

$$\frac{d\omega_R}{dt} = -\frac{C_m\omega_R}{2H} + \frac{L_m l_3}{A}\left(\psi_{2R}I_{1I} - \psi_{2I}I_{1R}\right) + \frac{L_m l_2}{A}\left(\psi_{3R}I_{1I} - \psi_{3I}I_{1R}\right) \tag{D.17}$$

Including both the electrical and mechanical equations, this is a fifth-order model.

Appendix E

Scenario Details

The scenarios for dynamic simulation are characterized by the unit commitment and dispatch that is used. This includes the diesel generating sets, hydro units, wind parks, and pumped storage station. The total load is 81 MW for all scenarios. As discussed in Section 3.4, three scenarios are to be created:

- Dispatch according to the old spinning reserve criteria only; no pumped storage considered
- Dispatch according to modified spinning reserve criteria; no pumped storage included
- Dispatch according to modified spinning reserve criteria; include pumped storage units

All scenarios are considered to have wet and windy conditions that allow the use of as much power from renewable sources as the security criteria and diesel unit technical minimums will allow. Preference has been given to hydro units, which are here dispatched at 0.7 per-unit. Wind parks have generally been connected with an output of 50% of their rated capacity, with curtailment being done by disconnecting parks and only in on park reducing the output of the park to be able to meet the security criteria.

This appendix presents the unit commitment and dispatch that has been created for these three scenarios. The generation values of all production nodes are given in Tables E.1 to E.3. A '*' in the reactive power generation column indicates a PV node in the power flow and a '**' indicates the reference or slack node.

Table E.1: Scenario: Old Spinning Reserve, no pumped storage

Node Name	P_g	Q_g
LOGAN	1.05	*
OGDEN	1.68	*
GOLDEN	2.38	*
GOLDENB	0.	0.
BOWMAR	0.84	*
ENGLE	5.11	*
CHERRYH	11.2	*
CASTLEW	0.50	*
SULLIV	0.	0.
SOUTHGL	0.11	*
GREENW	1.19	0.
AURORA	7.0	*
MANGR1&2	0.	0.
MANGR3	0.	0.
MANGR4T6	0.	0.
MANGR710	0.	0.
MANG1115	0.	0.
MANGR16	9.0	*
MANGR16A	0.	0.
MANGR17	0.	0.
MANGR18	11.4	*
MANGR19	11.4	**
HAVANA	3.25	*
BRIGHTA1	0.	0.
BRIGHTA2	0.	0.
BRIGHTA3	0.	0.
BRIGHTA4	0.	0.
BRIGHTA5	0.	0.
BRIGHTB1	0.	−0.126
BRIGHTB2	0.	−0.126
BRIGHTB3	0.	−0.126
BRIGHTB4	0.	−0.126
BRIGHTB5	0.	−0.126
BRIGHTB6	0.	−0.126
BRIGHTC1	0.	−0.126
BRIGHTC2	0.	−0.126
BRIGHTC3	0.	−0.126
BRIGHTC4	0.	−0.126
LITTLET1	0.	−0.126
LITTLET2	0.	−0.126
BRIGHTD	0.	0.
OGDENA	3.96	2.
ARAPA	3.3	1.
THORNT	3.3	0.5
WELBY	1.65	0.
MORRISA	0.	0.
WESTERNA	4.5	0.
LINCOLNA	0.	0.

Table E.2: Scenario: New Spinning Reserve, no pumped storage

Node Name	P_g	Q_g
LOGAN	1.05	*
OGDEN	1.68	*
GOLDEN	2.38	*
GOLDENB	0.	0.
BOWMAR	0.84	*
ENGLE	5.11	*
CHERRYH	11.2	*
CASTLEW	0.50	*
SULLIV	1.19	0.
SOUTHGL	0.11	*
GREENW	1.19	0.
AURORA	7.0	*
MANGR1&2	0.	0.
MANGR3	0.	0.
MANGR4T6	0.	0.
MANGR710	0.	0.
MANG1115	0.	0.
MANGR16	8.9	*
MANGR16A	2.7	*
MANGR17	11.3	*
MANGR18	11.3	*
MANGR19	11.3	**
HAVANA	3.25	*
BRIGHTA1	0.	0.
BRIGHTA2	0.	0.
BRIGHTA3	0.	0.
BRIGHTA4	0.	0.
BRIGHTA5	0.	0.
BRIGHTB1	0.	−0.126
BRIGHTB2	0.	−0.126
BRIGHTB3	0.	−0.126
BRIGHTB4	0.	−0.126
BRIGHTB5	0.	−0.126
BRIGHTB6	0.	−0.126
BRIGHTC1	0.	−0.126
BRIGHTC2	0.	−0.126
BRIGHTC3	0.	−0.126
BRIGHTC4	0.	−0.126
LITTLET1	0.	−0.126
LITTLET2	0.	−0.126
BRIGHTD	0.	0.
OGDENA	1.6	0.
ARAPA	0.	0.
THORNT	0.	0.
WELBY	0.	0.
MORRISA	0.	0.
WESTERNA	0.	0.
LINCOLNA	0.	0.

Table E.3: Scenario: New Spinning Reserve, 5.0 MW pumped storage

Node Name	P_g	Q_g
LOGAN	1.05	*
OGDEN	1.68	*
GOLDEN	2.03	*
GOLDENB	−5.0	0.
BOWMAR	0.84	*
ENGLE	5.11	*
CHERRYH	11.2	*
CASTLEW	0.50	*
SULLIV	0.	0.
SOUTHGL	0.11	*
GREENW	1.19	0.
AURORA	7.0	*
MANGR1&2	0.	0.
MANGR3	0.	0.
MANGR4T6	0.	0.
MANGR710	0.	0.
MANG1115	0.	0.
MANGR16	9.0	*
MANGR16A	0.	0.
MANGR17	0.	0.
MANGR18	11.4	*
MANGR19	11.4	**
HAVANA	3.25	*
BRIGHTA1	0.	0.
BRIGHTA2	0.	0.
BRIGHTA3	0.	0.
BRIGHTA4	0.	0.
BRIGHTA5	0.	0.
BRIGHTB1	0.	−0.126
BRIGHTB2	0.	−0.126
BRIGHTB3	0.	−0.126
BRIGHTB4	0.	−0.126
BRIGHTB5	0.	−0.126
BRIGHTB6	0.	−0.126
BRIGHTC1	0.	−0.126
BRIGHTC2	0.	−0.126
BRIGHTC3	0.	−0.126
BRIGHTC4	0.	−0.126
LITTLET1	0.	−0.126
LITTLET2	0.	−0.126
BRIGHTD	0.	0.
OGDENA	3.96	2.
ARAPA	3.30	1.
THORNT	3.30	0.
WELBY	1.65	0.
MORRISA	0.	0.
WESTERNA	4.5	2.
LINCOLNA	5.0	0.